MODELLING AND MAPPING ABOVEGROUND BIOMASS AND CARBON STOCK USING ALOS-2 PALSAR-2 DATA IN AYER HITAM TROPICAL RAINFOREST RESERVE IN MALAYSIA

AGNES MONE SUMAREKE
FEBRUARY, 2016

SUPERVISORS:
Dr. A. Y. Hussin
Ir. L.van Leeuwen

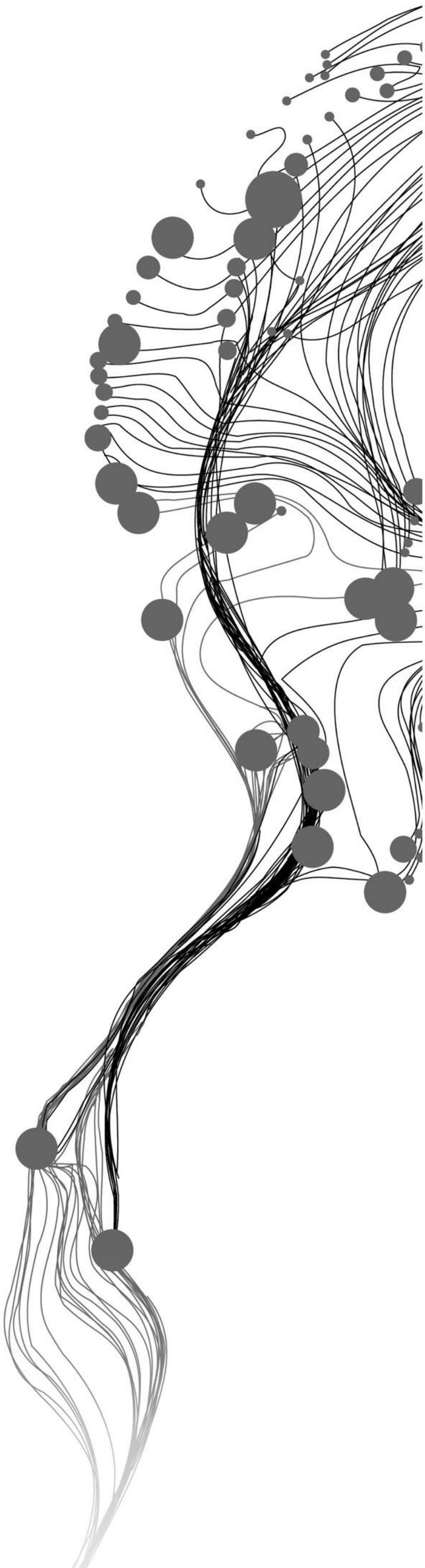

MODELLING AND MAPPING ABOVEGROUND BIOMASS AND CARBON STOCK USING ALOS-2 PALSAR-2 DATA IN AYER HITAM TROPICAL RAINFOREST RESERVE IN MALAYSIA

AGNES MONE SUMAREKE
Enschede, The Netherlands, February, 2016

Thesis submitted to the Faculty of Geo-Information Science and Earth Observation of the University of Twente in partial fulfilment of the requirements for the degree of Master of Science in Geo-information Science and Earth Observation.
Specialization: Natural Resource Management

SUPERVISORS:
Dr. A. Y. Hussin
Ir. L.van Leeuwen

THESIS ASSESSMENT BOARD:
Professor .A. Nelson (Chairman)]
Professor. Madya Dr, M.I. Hasmadi, (External Examiner, Faculty of Forestry, University of Putra, Malaysia)

ABSTRACT

Forest ecosystems constitute large amount of biomass and thus it plays a major and important role in carbon sequestration and global climate regulation. Tropical rainforests are known for their complex structure, rich biodiversity, and high density of biomass and carbon content. Therefore, UNFCC under the REDD+ has recommended the sound measurement, reporting and verification (MRV) methods to estimate AGB and carbon stock to address the climate change and carbon emission issues in tropical countries.

Application of SAR radar backscatter coefficient is one of the MRV methods recommended to estimate AGB and carbon stocks in tropical forests. SAR remote sensing has become very useful in tropical countries for AGB and carbon estimation. SAR is an active sensor and operates, in any weather condition and during day and night and can penetrate through cloud, fog and haze. In this study, ALOS-2 PALSA-2, HH and HV polarization image data, which was acquired in August 26 2015 was used to predict AGB and carbon stock of Ayer Hitam Forest Reserve (AHFR).

The aim of this study was to model and map AGB and carbon stock of Ayer Hitam Rainforest Reserve. Data from 27 plots were assessed. Out of these data, 17 plots were used for developing the model and other 10 plots were retained for model validation. AGB was obtained based on plot level using the improve allometric equation developed by (Chave et al., 2015). Meanwhile, backscatter coefficient from HH and HV polarization were retrieved and converted to sigma nought. Besides, total stand BA, average DBH and height were also obtained.

Correlation and simple linear regression analysis was done separately between observed AGB and backscatter coefficient of ALOS-2 PALSAR-2, HH and HV polarization. Results of the analysis showed a positive and strong relationship (R^2=0.817) between AGB and HV polarized backscatter. About 82% of the variability in AGB was explained by the HV backscatter coefficient. The 10 independent data were used to validate the model. The predicted AGB were plotted against the observed AGB. A strong correlation was identified with R^2 of 0.796. The correlation was significant at 99% and 95% confidence level. AGB of the study area was estimated using the simple linear regression developed with HV backscatter and AGB. The AGB and carbon stock map of the Ayer Hitam Forest Reserve was produced. Carbon stock values were calculated using 0.5 conversion factor.

The observed amount of AGB of AHFR obtained from the measured data using the allometric equation ranges from 60.17 – 367.07 while the estimated AGB using the simple linear model with HV polarized data ranges from 20 – 576.42 ton ha^{-1}. Average AGB for observed and estimated was 208.79 ton ha^{-1} and 257.98 ton ha^{-1} respectively. The total estimated AGB of the whole study area of AHFR derived from HV backscatter is. 321,966.28 ton while the total AGB observed is 260,574.27 tons. Average estimated carbon stock of AHFR is 128.99 ton ha^{-1} and the total estimated carbon stock is 160,983.14 ton.

Present study found that the average value of AGB per ha^{-1} obtained in AHFR agrees with several similar studies which were carried out in tropical countries as well in Malaysia using ALOS PALSAR. This indicate that, ALOS-2 PALSAR-2 is able to estimate AGB accurately in tropical countries. Further study is needed to be undertaken in saturation sensitivity analysis of ALOS-2 PALS-2 in tropical forest with high density of biomass.

Key-words: HH and HV Polarization; radar backscatter; ALOS-2 PALSAR-2, REDD+; Above Ground Biomass (AGB); carbon stock; tropical forest, regression, allometric equation, correlation, linear regression, estimation, mapping.

ACKNOWLEDGEMENTS

First and for most I would like to thank the Almighty God for blessing me with this lifetime opportunity to travel all the way from my home Papua New Guinea to The Netherlands. Glory and Honour to Him.

Next, I would like to take this opportunity to extend my sincere appreciation to Joint Japan World Bank Graduate Scholarship Program granting me the scholarship. Without your support, I would not come this far to undertake this Masters course and achieve my goal. I highly acknowledge your assistance.

To International Institute for Geo-information Science and Earth Observation (ITC), University of Twente, Natural Resource Management Domain, I would like to express my sincere gratitude to you for accepting me to undertake this MSc Program in ITC. It was a challenging path but it all finally came to pass. Firstly, I am grateful for the knowledge, skills and technique in RS and GIS. I acknowledge the hospitality, technical assistance, the learning material and financial assistance for my MSc field work to Malaysia. I learned to teach myself, to work hard and work smart. I have learned and experienced a lot. Thank you.

I am humbled and please to extend my sincere gratitude to my first supervisor Dr. Yousif Ali Hussin. I thank you for your tireless effort and priceless supervision you rendered me during my research. I am grateful for your technical advice, constructive feedbacks, and encouragement throughout the thesis period until the end. To my second supervisor, Ir. Louise van Leeuwen, I extend my heartfelt gratitude to you. I very much appreciate your supervision, expert advice and encouragement, especially during the proposal stage. I would like to thank Mr. Kloosterman for his supervision in the field during the field trip. I very much appreciate your tireless effort in assisting and organizing the team in the field until we return to ITC.

I am very grateful to Dr. Hasmadi and his team from University Putra Malaysia during our field campaign in AHFR. Thank you for the hospitality at UPM and for engaging the amazing team of rangers with us to accomplish our task in the field. Field work was tough, however, the effortless assistance from the rangers was incredible. My sincere thank you to the rangers on site, Mr. Naeem, Ranger Siti Zurina and the team.

Finally but not the least, I would like to express my heartfelt thank you to my LiDAR and Radar group mates, Ms. Tasiyiwa Madhibah, Miss Cora Lawas, Miss Phanintra Soonthornharuethai, Mr. Sadadi Ojoatre and Mr. Zemeron Mehari. Though it was a tough and challenging journey, we made it through. Thank you for those unforgettable moments in Ayer Hitam Forest Reserve.

To the NRM MSc-2014 -2016 colleagues, it was a privilege meeting and working with you all. You are awesome, smart and hardworking students. Thank you for the encouragement, sharing ideas, working together, and sharing the fun times. I wish you all, all the best in your future endeavors.

Lastly, I would like to take this time to thank my family, especially my Papa, Kevin and Mama, Margret for always keeping me in your prayers. My son Joshua and daughter Leah for managing to live without me for 18 months. I owe it to you. I am also grateful to my siblings, my immediate relatives, and friends for the prayers and encouragement. My last word of gratitude to my SH, Martina Kua for your prayer, motivation, and encouragement from the beginning to the end!

Agnes Mone Sumareke
Enschede, The Netherland
February, 2016

……….Dedicated to my Family…….

Specially in Memory of my..

"Belated Beloved Awa Mungili, Bata JACKOZ .Jackson Kopera PIRUWE."

TABLE OF CONTENTS

LIST OF FIGURES

LIST OF TABLES

LIST OF APPENDIX

LIST OF EQUATIONS

LIST OF ACRONYMS

RADAR	**R**adio **D**etection **A**nd **R**anging
ALOS	Advanced Land Observation Satellite
PALSAR	Phased Array Synthetic Looking Aperture Radar
SAR	Synthetic Aperture Radar
SLAR	Side Looking Aperture Radar
HH	Horizontal send, Horizontal receive
HV	Horizontal send, Vertical receive
VV	Vertical send, Vertical receive
VH	Vertical send, Horizontal receive
NRCS	Normalized Radar Cross Section
RS	Remote Sensing
VHR	Very High Resolution
LiDAR	**Li**ght **D**etection **A**nd **R**anging
PRISM	Panchromatic Remote Sensing Instrument for Stereo Mapping
AVNIR-2	Advanced Visible and Near-Infrared Radiometer type2
ABG	Above Ground Biomass
BGB	Below Ground Biomass
DBH	Diameter at Breast Height
BA	Basal Area
UNFCCC	United Nation Framework Conversion on Climate Change
IPCC	International Panel on Climate Change
REDD	Reduce Emission from Deforestation and Degradation
MRV	Measurement, Reporting and Verification
COP	Conference of the Parties
GHG	Greenhouse Gas
FAO	Food and Agriculture Organisation
UN-REDD	United Nation- Reduce Emission from Deforestation and Degradation
UNDP	United Nations Development Program
ESA	European Space Agency
GIS	Geographical Information Systems
AHFR	Ayer Hitam Forest Reserve
PollnSAR	Polarimetric Aperture Radar Interferometry
DN	Digital Number
JAXA	Japan Aerospace Exploration Agency
ITC	Faculty of Geo-information Science and Earth Observation
UT	University of Twente
SPOT	Satellite Pour l'Observation de la Terre
SNAP	Sentinels Application Platform 2
UTM	Universal Transverse Mercator
WV	World View

1. INTRODUCTION

1.1. Background

The topic of climate change had become a paramount concern and received a lot of attention from the international communities over the recent years. The United Nations Framework Conversion on Climate Change (UNFCCC) stated that, change of climate is due to direct or indirect alteration of the global structure by anthropogenic activities. Eventually, the consequences in variability in natural climate have been observed over a long period of time (IPCC, 2001). At present time, climate change is associated with forest and it is dealt with as policy issues at the policy level (Buizer et al., 2014). In a climate change synthesis report, 70% increase in global greenhouse gas (GHG) emission was recorded between the years 1970 and 2004 (Bernstein et al., 2008). Carbon dioxide as the principal anthropogenic GHG increased by 80% annually between the said years.

Forests act as the sink and reservoir of carbon dioxide and regulate the global climate. Apparently, tropical forests are the primary carbon sink ecosystem. They are very complex in structure and cover approximately fifteen percent (15%) of earth's surface (FAO, 2009). Mature tropical forests consist of several layers which make them rich in biomass. Tropical forests store approximately 56% of carbon in biomass and 32 % in forest soil (Pan et al., 2011). Recently biomass and carbon stock estimation in the tropical forest have gained much interest because carbon plays an important role in earth's carbon cycle (Basuki et al., 2013).

Regardless of its ability to sequester a large amount of carbon, these forests are vulnerable to deforestation and degradation. Deforestation in tropical countries add one-fifth of the total human-induced carbon dioxide emissions to the atmosphere (Gibbs et al., 2007). Besides, total land use change accounts for about 20% of the total greenhouse gas emission annually (Angelsen, 2008; Corbera and Schroeder, 2011). It is recorded as the second biggest emission source after fossil fuel (Hirata et al., 2012). Consequently, this has triggered a threat on the global climate and thus has attracted attention from the scientists and policy makers across the globe to develop a potential strategy to address the rate of deforestation and degradation in developing tropical countries.

Accordingly, the UN-REDD Programme, which is the United Nations collaborative initiative on Reducing Emissions from Deforestation and Forest Degradation (REDD) in developing countries was initiated. Its main purpose was to reduce emissions from loss of forests to combat climate change (Næsset et al., 2011). REDD contributes significantly to address mitigation and adaptation to climate change. It substantially aids in the sustainable development and forest management in developing countries (Cosslett, 2014). Eventually, Conference of the Parties (COP) of UNFCCC at its 16th meeting in Cancun in 2010 expended REDD to REDD – Plus (REDD+). The name was adopted because it included other factors such as sustainable forest management, enhancement of forest stand stocks, biodiversity and conservation (Sukhdev., 2012). REDD+ is mainly focused on paying incentives to the forest owners and countries that are concerned about conserving their forests to reduce emissions from forest destructions (Angelsen, 2008). REDD+ is also perceived as a potential approach to generate extensive benefit apart from reducing GHG emissions.

In order to monitor and implement REDD+ activities in the tropical forests, it is crucial to establish a monitoring scheme. Monitoring the changes in forest cover over time and making an accurate measurement in forest biomass and carbon stock is important in both national and international level. Therefore, UNFCCC requested for an appropriate, transparent and robust method to be developed and applied in developing countries to boost the national monitoring system (Hirata et al., 2012). Subsequently, the industrialized countries are required to pay for emitting the GHG through REDD+ program. Therefore, the concept of Measurement, Reporting and Verification (MRV) was initiated at COP 13 in Bali in 2007.

With the aim of estimating more accurate and stable measurements of forest biomass, carbon stock, greenhouse gasses (GHG) and forest cover change; it is essential to incorporated remote sensing with ground-based monitoring systems (Kiyono et al., 2011). Hence, it is crucial to make sure that MRV is accurate, transparent and reliable because credits for REDD+ will be delivered based on this measurement outcome.

The fundamental concern for implementing MRV for the REDD+ activities is to achieve the highest accuracy in forest biomass and carbon stock estimation in tropical forests. Consequently, radar backscattering using Synthetic Aperture Radar (SAR) is one of the methods recommended for estimating carbon stock before REDD+ becomes operational in 2020. Kiyono et al., (2011) recommended Advanced Land Observation Satellite Phased Array L-band Synthetic Aperture Radar (ALOS PALSAR) data because it has an upper hand over other remote sensing (RS) systems including Very High Resolution (VHR) and Lidar systems. Radar is a microwave sensor system and has very high potential to acquire data under any weather conditions and during day and night (Kiyono et al., 2011).

Radar penetrates into clouds to obtain data thus allowing regular monitoring in tropical rainforests. Most importantly, there is a direct relation between radar backscatter and forest Above Ground Biomass (AGB) (Mitchard et al., 2012). This is because the radar energy, which is transmitted as pulse of microwave in the direction of the land cover, penetrates through vegetation and will have a multiple or volume scattering, especially in the cross polarization energy. Later it will be scattered back to the radar antenna as a function of the amount of biomass/carbon stock (Mitchard et al., 2012). In addition, use of spaceborne radar data is gradually becoming essential in assessing biomass and carbon stock in tropical forests on a larger scale (Thapa et al., 2015; Hamdan et al., 2015).

1.2. Problem statement and justification

Tropical rainforest has multiple tree layers and complex structure. Starting from the top or emergent layer to the canopy layer, understory, and down to the forest floor. The composition and diversity of tree species, density of trees and the irregular shapes and sizes of the tree crowns affect the canopy structure (Song et al., 1997). In addition, the higher and lower layers of the forest structure change considerably due to tree species composition. They are exceedingly heterogeneous and intact in biomass, hence, it is challenging to obtain high accuracy of forest AGB. Therefore, it is important to understand and take into consideration complexity of the forest structure to accurately assess and estimate forest AGB (Hamdan et al., 2014).

Goh et al., (2013); Morel et al., (2011); Le Toan et al., (2004); Sinha et al., (2015) indicated that radar backscatter saturates and remain constant when the level of biomass increases to a certain point. Radar backscatter depends on the amount of biomass and the characteristic of the forest. In a tropical forest, AGB estimation can be limited to the lower saturation level at as low as 30 ton ha^{-1} at C-band, 50 ton ha^{-1} at L-band and 150-200 ton ha^{-1} at P-band (Le Toan et al., 2004).

However, SAR data with a longer wavelength, L-band appears promising because of its ability to penetrate through the forest canopy and reach the forest floor (Hamdan et al., 2011; Goh et al., 2013; Thapa et al., 2015). SAR backscatter has a reasonable relationship with the forest stand parameters (e.g., DBH, Height, basal area, timber volume, biomass and carbon stock (Sinha, et al., 2015).

Several studies including, Mitchard et al., 2012; Basuki et al., 2013; Goh et., 2013; Kumar et al., 2012 fused radar image with either lidar or optical multispectral image data acquired from another sensor to estimate AGB. In addition, several studies similar to this study were also done in tropical forest, however, they were conducted in the homogeneous and less dense forest. Some more related studies including, Michelakis et al., 2014; Carreiras et.al., 2012; and Carreiras et al., 2013 were also conducted in tropical rain forests. Hamdan et al., (2011) and Morel et al., (2011) carried out similar studies using PALSAR forests in Malaysia, but the forests were not entirely natural. The forests were either partially planted or logged-over secondary forests. Otukei and Emanuel (2015) stated that usage of ALOS PALSAR in complex forest types in tropics for biomass estimation is less known.

A review paper on estimating biomass using radar by Sinha et al., (2015) also revealed that, limited number of studies were conducted in tropical forests. Consequently, this study is conducted in a natural tropical rainforest and at a different geographical location. Additionally, result from the literature search showed that ALOS-2 PALSAR data has not yet been used in any studies to assess the accuracy of the biomass estimation, therefore this is an opportunity to do a study using ALOS-2 PALSAR-2 data with HH and VH polarization to estimate AGB of tropical rainforest with reasonably high accuracy.

Meanwhile, UNFCC under the REDD+ program recommended a monitoring system that combines remote sensing and ground-based inventories for estimating forest biomass, carbon stock and greenhouse gas emission (Hirata et al., 2012). Therefore, MRV methods are very crucial. The methods recommended for estimating carbon stock for per unit area are either directly by establishing permanent sample plots or indirectly using estimation model for predicting stand carbon stock. The indirect method includes, over story height modelling, crown diameter model, community age model and radar backscattering coefficient which is using the SAR backscatter (Hirata et al., 2012).

The first three indirect methods basically use lidar or optical remote sensing technique to estimate AGB. The overstory height model uses tree heights measured from airborne lidar and field-based biomass measurement to develop the relationship between the height and biomass assuming that they are directly proportional. Extrapolation of the result obtained from this model from one area to another is impossible (Hirata et al., 2012). The basal area obtained from the ground measurement can be combined with the digital height measured by the lidar to estimate AGB (Bhattarai et al, 2015). Crown diameter approach is achieved by using an aerial photograph or high to very high-resolution image to delineate tree crown based on individual tree crown diameter to estimate biomass. This method substitutes the crown projection area for the DBH measurement to estimate AGB and carbon stock. Information only for upper canopy trees is yielded for this method (Hirata et al., 2012).

On the other hand, SAR has the advantage over the optical and infrared RS because SAR can operate during the day and night and in all-weather condition. SAR transmits the microwave signals and measures the backscatter signals that is returned back to the sensor from volume scattering in the forest canopy (Pons, 2010). Therefore, it is recognized to be the only sensor which can measure the volume of the vegetation and is suitable for estimating and mapping AGB and other biophysical parameters (Pons, 2010; Sandberg et al., 2011). It can penetrate through clouds and acquire data in large scale with reasonable resolution. Essentially, SAR has been used to retrieve forest AGB and other biophysical parameters (Santoro et al., 2002).

Synthetic Aperture Radar (SAR) backscatter has a correlation with the AGB up to a certain saturation point (Hirata et al., 2012). Correlation between AGB and radar backscatter coefficient is high for L-band. Hence, PALSAR is recognized as a promising methods to accurately measure the parameters of the forest structure, AGB and carbon stock (Sandberg et al., 2011; Santoro et al., 2002). Carbon stock can be measured directly by modelling the relationship between the AGB and the backscatter coefficient. This method is suitable for estimating and mapping AGB and carbon stock over a large area and is suitable for tropical forests (Hirata et al., 2012).

Since SAR is the most recommended remote sensing technique suitable for tropical forest for REDD+ initiatives, it is essential to use ALOS-2 PALSAR in this study. Therefore, the main focus of this study is to assess, estimate, and develop a model and map AGB and carbon stock of tropical rain forest accurately using ALOS-2 PALSAR.-2 ALOS-2 is an improved version of the original ALOS PALSAR with the enhanced specification (Shimada, 2009).

1.3. Research Objectives

This section includes the general objective of the study, the specific objectives, research questions and the research hypothesis.

1.3.1. General Objective

The main objective of this research is to develop a model to estimate and then map AGB and carbon stock using ALOS-2 PALSAR HH and HV polarized radar images in tropical rainforest reserve of Ayer Hitam in Malaysia.

1.3.2. Specific objectives

1. To analyse the relationship between AGB and radar backscatter of ALOS-2 PALSAR-2, HH, and HV polarization using regression analysis.
2. To analyse the relationship between forest stand parameters such as basal area (BA), DBH and height with backscatter of PALSAR -2 HH and HV polarized image data.
3. To model and validate AGB for Ayer Hitam Forest Reserve based on regression model developed using cross polarised (HH, HV) PALSAR image data.
4. To assess biomass and carbon stock estimates per unit area (ha) using field data.
5. To map AGB and carbon stock of Ayer Hitam tropical rainforest reserve.

1.3.3. Research Questions

1. What is the relationship between AGB and radar backscatter of ALOS-2 PALSAR-2, HH, and HV polarization?
2. How can AGB be modelled using PALSAR HH and HV polarizations?
3. What is the accuracy of AGB derived from radar backscatter of ALOS-2 PALSAR, HH, and VH polarization?
4. What is the AGB of tropical rain forest of Ayer Hitam per unit area in ton/ha derived from field data?
5. How can biomass and carbon stock derived from radar backscatter of ALOS-2 PALSAR, HH, and VH polarization be mapped?

1.3.4. Research Hypothesis

1. Ho: There is no strong positive relationship between ABG and radar backscatter PALSAR-2, HV polarization compared to HH polarization.
   Ha: There is a strong positive relationship between AGB and radar backscatter PALSAR-2, HV polarization compared to HH polarization.

2. Ho: The relationship between AGB and radar backscatter cannot be accurately (< 75%) estimated and modelled and mapped at 95% confidence interval.
   Ha: The relationship between AGB and radar backscatter can be accurately (< 75%) estimated, modelled and mapped at 95% confidence interval.

1.4. Concepts of the study

1.4.1. Synopsis of biomass and carbon stock and estimation techniques

Biomass can be defined as the living material including plant and animal that are found above the ground and below the ground. Biomass is usually expressed as dry weight (Sinha et al., 2015). All biomass that is above the soil including vines, lianas, tree stumps, stem, branches, fruits, leaves, flowers and seeds are categorized as above ground biomass (AGB) while the roots and other materials found in the soil are termed as below ground biomass (BGB) (Sinha et al., 2015). Biomass is of paramount importance because it is related to the structure of the vegetation and consequently it has an influence on the biodiversity. The amount of carbon emitted into the atmosphere is determined by the amount of biomass that is burned, decayed or disturbed based on per unit area (Houghton et al., 2009). In addition, biomass is also associated with the management of water, fire and soil (Houghton et al., 2009).

The significant part of the total biomass is found in forest ecosystems. Trees in tropical rainforests contain a large amount of biomass, thus they sequester and store more carbon (Bhattarai et al., 2015). Nevertheless, deforestation and degradation of tropical forest have a direct impact on the main carbon pool that is stored in forest ecosystem (Gibbs et al., 2007). Thapa et al., (2015) further stated that assessing forest AGB is crucial for carbon quantification in any forest type because about 47-50% of the carbon is stored in the forest AGB. Besides, Okuda et al., 2004 specified that, when assessing carbon stocks and carbon sequestration, it is highly significant to estimate forest biomass in the tropical forest. Forest biomass is considered an important key variable in the terrestrial cycle and more information is needed for quantifying it (Hamdan et al., 2011).

Aboveground biomass in tropical forest is the main actor in the climate change issue. In addition, an increasing importance in REDD+ contemplates accurate quantification of AGB and carbon stock on the local, regional and global scale (Boudreau et al., 2008). Monitoring carbon stock is essential among other parameters of REDD+. Therefore, MRV systems for forest carbon changes must consider and very reliable and accurate method. In addition, uncertainties in forest carbon stock can be reduced with improved MRV systems (FAO, 2009).

There are four main techniques used to estimate live AGB and carbon stock. Destructive sampling is one way whereby biomass is measured directly and the most accurate method. But it is applicable only in the small area. It requires a lot of time, efforts, labour and cost to achieve it (Sessa, 2009). The second method is non-destructive sampling by which, parameter of the trees are measured and the allometric equation is used to estimate the biomass. The third method is estimating biomass using remote sensing techniques and the fourth method is developing models whereby, biomass estimates are derived by integrating remote sensing and field measurement. This method can be applied to a larger area because allometric equations are used to extrapolate to larger scale (Sessa, 2009).

Moreover, estimation of carbon stock per unit area of forest is of paramount interest. Forest carbon is assessed either by, one; directly, by the establishment of permanent sample plots (PSP) and two; indirectly, by modelling the stand carbon stock (Hirata et al., 2012) which involves four methods. The first one is over story height model, second, crown diameter model, third, community age model and fourth, radar SAR).backscattering coefficient (

Gibbs et al., (2007); Bhattarai, et al., (2015) have categorized these carbon estimation methods corresponding to the former as a traditional method (PSP), and the latter as optical RS, VHR imagery, lidar and radar. Apart from the other remote sensing sensor systems, radar was preferred for MRV system because of its numerous advantage in acquiring data in tropical forest (Goh et al., 2013; Hamdan et al., 2011; Morel et al., 2011; Gibbs et al., 2007). Figure 1 shows the illustration of the concept of the study.

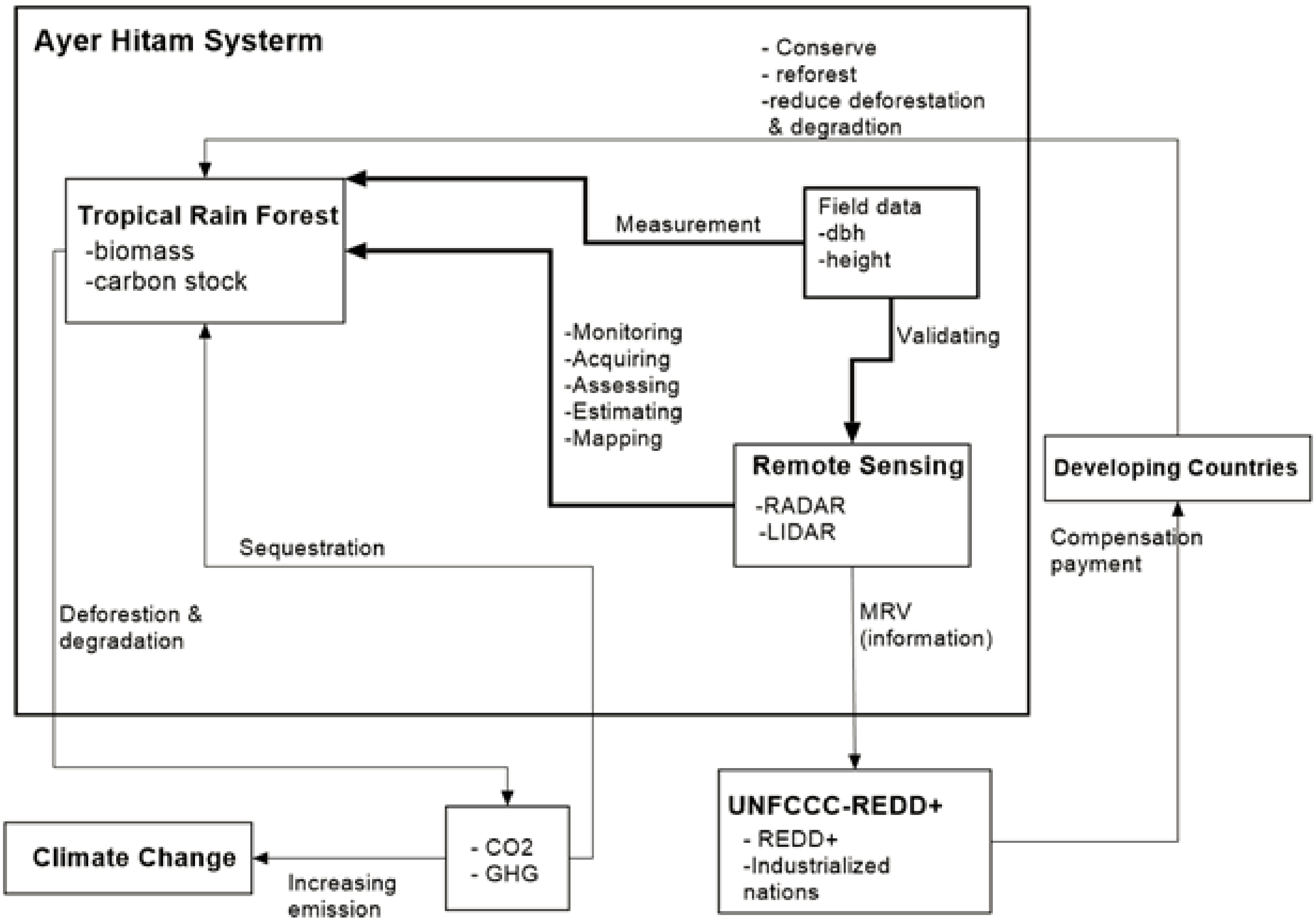

Figure 1: Concept diagram of this study

2. LITERATURE REVIEW

2.1. Mapping Above Ground Biomass and Carbon Stock

Mapping AGB in tropical forest is challenging due to the fact that tropical forests are very complex in structure. They consist of a diversity of species and has a high density of biomass. In addition, frequent cloud cover over tropical forests limits the data acquired from the optical sensors and mountainous and steep topography limits radar sensors (Mitchard et al., 2012). All these lead to a challenge of estimating and mapping AGB and carbon using remote sensing. However, it is vital for the implementation of carbon credit scheme and REDD+(Morel et al., 2011). Despite its challenges, estimation of forest biomass and carbon stock has become increasingly useful in recent years because remote sensing data is available for forest areas that are inaccessible and in larger scale (Goh et al., 2013). Mapping and monitoring biomass and carbon stock in tropical countries attracted scientists around the world. Deforestation and forest degradation accounts for 30% of the carbon emitted by anthropogenic activities (Goetz et al., 2009).

According to Amini and Sumantyo,(2009), remotely sensed data have the advantage over the traditional method of biomass and carbon estimation. This is because data can be collected in the same area repeatedly and are available in digital format. These data can be processed faster to produce biomass and carbon maps. Production of such maps is necessary as it provides essential information on the increase and decrease of forest biomass so as the loss and gain in carbon. This will complement the effort that the global community is exerting in combat climate change through the REDD+ initiatives (Mitchard et al., 2012).

Monitoring change in forest cover and estimation of biomass and carbon can be achieved through satellite remote sensing. Baseline information on the rate of deforestation and degradation can be determined using satellite data as long as an assessment of the forests cover are accurately conducted and validated (Goetz et al., 2009). Optical remote sensing techniques and sensors are employed in acquiring data on forest cover and biomass. However, radar remote sensing has the advantage over the optical satellite sensors because it is the only sensor that can provide information on forest canopy in the tropical regions as it is able to penetrate through clouds and acquire images regardless of any weather conditions (Hamdan et al., 2011). Therefore, radar remote sensing has a significant role to play in continuous observation of tropical forests.

2.2. An Overview on RADAR, SAR and ALOS PALSAR

2.2.1. RADAR

RADAR is an abbreviation derived from **Ra**dio **D**etection **a**nd **R**anging. Radar is simply transmitting pulse to the direction of the distant object and receiving waves that are reflected or scattered back to the sensor. Basically, the pulse of electromagnetic radiation is generated and transmitted by the radar antenna in the direction of the surface object that is far off (Ager, 2011). As soon as the wave hits the object, it can penetrate through the object, scattered from its surface or reflected back to the radar antenna. All these depends on the wavelength, polarization, incidence angle, object geometric and dielectric properties and topography (Ager, 2011). A portion of this pulse is refracted and reflected away while a portion returns back to the sensor as radar backscatter. As the result of the backscatter, the object is detected and its position is determined. In addition, the travel time of this pulse is recorded to define the range or the distance between ground and radar antenna (Ager, 2011).

Radar is an active sensor system that operates in the microwave part of the electromagnetic spectrum. The wavelength ranges from 1 mm to 100 cm. The radar imaging system has about nine bands. However, the most commonly used bands now are: X-band (2.4 – 3.75 cm λ), C band (3.75 – 7.5 cm λ), L band (15 – 30 cm λ) and P band (30 – 100 cm λ) (Henderson, 1998). The full detail on the radar bands and frequency is described in Henderson and Lewis, (1998). In Radar imaging, it is crucial to understand the fundamental issues that determines the radar returns. Table 1 shows the list of the parameter that affects radar returns.

Table 1: Important parameters that influence radar return or radar power return (PR) (Henderson and Lewis 1998).

Fundamental System and Target Parameters that Influence Radar Power Return (PR)	
Systems Parameters	**Target Parameters**
1. wavelength or Frequency	1.Surface Roughness
2. Polarization	2.Complex Dielectric
3. Look Angle	3. Slope Angle and Orientation
4. Look Direction	
5. Resolution	
Direct Interplay of System and Target Parameters	
1.Surface Roughness – defined in terms of system wavelength	
2. Look Angle ($\emptyset$)and Slope Angle(α) – combine to determine Incident Angle(θ)	
3. Look Direction and Slope (or target) Orientation – influence the area and geometry of the target presented to the radar	

The significant characteristic of radar include day and night operation, has a longer wavelength and lower frequency. Hence, it has an advantage to penetrate through the cloud, haze, snow, dust and surficial materials (e.g. sand, vegetation canopy etc.). It can also be operational in all-weather condition. Additional advantages of radar are stated in Ager, (2011). Radar was significantly used in areas where there are frequent snow and clouds such as in the polar and the tropical regions (Smith, 2012; Henderson and Lewis 1998). Besides, it is extensively used in traffic control, navigation of ship and aeroplanes and was applied in numerous scientific fields including geology, agriculture, meteorology, hydrology, forestry and biomass assessment and other more (National Academy of Sciences, 2015; Henderson and Lewis, 1998).

2.2.2. Synthesis Aperture Radar (SAR)

Synthetic Aperture Radar (SAR) came into existence after Side Looking Aperture Radar (SLAR) in the mid-1960s. SAR was introduced to obtain a better resolution of radar by using signal processing. SAR became very useful because it is able to achieve better resolution by using longer wavelength (Chan and Koo, 2008). SAR is beneficial in tropical countries because it can penetrate through clouds, fogs and haze. Therefore, it is used to monitor and detect land cover changes is frequently applied in natural resource and environmental studies (Chan and Koo, 2008). SAR is one of the senor type that operates in the microwave frequency which has been commonly and significantly employed in monitoring forest, forest AGB studies and carbon stock accounting (Sinha, et al., 2015). SAR has its limitations with energy attenuation in high biomass content vegetation, speckle, and shadowing (Sinha et al., 2015). Nevertheless, it can penetrate through clouds to discriminate between different vegetation types(IPCC, 2006) and is able to measure biomass in dense tropical forest, (Thapa et al., 2015; Mermoz, 2014; Goh et al., 2013; Sinha et al., 2015) and derive biomass information (Hamdan, et al., 2011).

The interaction of the pulse transmitted by radar and the vegetation cover is complex. That is because the penetration of the microwave energy into the forest canopy cover depends on the wavelength, polarization and the incidence angle of the radar and the biomass and moisture content of the vegetation (National Academy of Sciences, 2015). When the transmitted pulse interacts with the canopy, it either penetrates and scatters or directly scatters and part of it is returned to the radar antenna as backscatter. The essential features that make SAR unique from optical remote sensing are, dielectric constants, the texture of the surface, different incident angles, like and cross polarisation and ability to penetrate through surficial objects (Sinha et al., 2015).

Biomass estimation using SAR is categorised into two main classes. The first one is by using the backscatter values while the second is by using interferometry technique (Ghasemi et al., 2011). Studies have confirmed that there is a strong and positive relationship existing between biomass/carbon stock and the longer wavelengths (L- and P-band) with cross-polarised radar backscatter (HV and VH) (Ghasemi et al., 2011). The X and C band in the shorter wavelength with like-polarised radar backscatter (HH or VV) have a weak relationship (Dobson et al., 1992; Le Toan et al., 1992). Hussin et al., (1991) also revealed in his study, positive relation between Slash-Pine parameter including biomass with L-band with HV polarisation.

2.2.3. Advanced Land Observation Satellite, Phased Array L-band SAR (ALOS-PALSAR) and ALOS -2 PALSAR-2

The Advanced Land Observation Satellite (ALOS) is a Japanese Satellite launched in January 2006. Unfortunately, it has failed to operate in May 2011. ALOS carried on board the Phased Array L-band Synthetic Aperture Radar (PALSAR), an adjustable resolution polarimetric sensor (PASCO Coperation, n.d.). On board ALOS were two other sensors, the Panchromatic Remote Sensing Instrument for Stereo Mapping (PRISM) and the Advanced Visible and Near-Infrared Radiometer type2 (AVNIR-2) (Hamdan et al., 2011). ALOS was positioned at 691 km in a sun-synchronous orbit that made one full coverage of the Earth or revisit in 46 days (PASCO Coperation, n.d.).

The PALSAR on board ALOS was a stationary instrument. It was faced in the lower direction of the satellite and observed the earth surface in only one position which is towards the direction of the moving satellite. The PALSAR consisted of a High-Resolution mode and a Scan SAR mode and operated in the L-band with a wavelength of 23.6 cm (1270 –MHz) which had a bandwidth frequency between 14 - 28 –MHz (Rosenqvist et al., 2007; PASCO Coperation, n.d.). Besides, it had the highest resolution of 10 m and scanned at a swath width of 250-350 km. Several studies including Goh et al., 2013; Mermoz, 2014; Thapa et al., 2015; Morel et al., 2011; Carreiras, et al., 2012 were conducted using PALSAR to estimate biomass and carbon stock in tropical forests. A similar study to this was carried out using ALOS PALSAR in Malaysia (Hamdan et al., 2011). However, it was done in a different geographical location. Besides, this study used ALOS-2 PALSAR-2 image data.

Advanced Land Observation Satellite-2 (ALOS-2) is a successor Satellite mission of ALOS with improved instruments compared to ALOS. The essential improvement that ALOS has includes high resolution and rapid time of revisit. Visit time is fast and it observes the earth at a higher angle of incident (PASCO Coperation, n.d.). ALOS-2 is also equipped with three sensors, however, it is aimed at SAR instrument. ALOS-2 has an enhanced resolution of 1 m, 3 m and 10 m. It has a dual antenna that observes at wider swath width compared to ALOS with one fixed antenna. It has a faster revisit time of 14 days compared to the 46 days by ALOS (PASCO Coperation, n.d.). ALOS-2 was launched in May 2014, therefore, literature search showed no records of studies relating to forest biomass estimation using image data acquired from ALOS-2. Therefore, there is an opportunity to utilize ALOS-2 PALSAR-2 data for this study.

2.2.4. Polarization and Backscatter

The characteristic of the electromagnetic waves is described by Polarization and is referred to as the direction of the electric field. Synthetic Aperture Radar (SAR) sensor is designed in a way to transmit and receive either horizontal or vertical polarized pulse (Ghasemi et al., 2011). Therefore, if the electric wave is transmitted by the SAR sensor horizontally and received horizontally, the signal is said to be horizontally polarised (HH), and if the wave is transmitted vertically and received by the sensor vertically, the signal is said to be vertically polarised (VV) (Ghasemi et al., 2011; JAXA, n.d.). The electric pulse can also be sent horizontally and received vertically (HV) or can be sent vertically and received horizontally (VH). PALSAR is able to send and receive horizontal and vertical polarised pulses. In addition, the polarized image of PALSAR can reveal the various trend between different polarizations (JAXA, n.d.).

A polarimetric SAR data is used in estimation of forest biomass, basal area and many other studies including mapping of flood and many more. A complete polarimetric SAR data consists of four bands of two like polarization HH and VV and two of cross polarization HV and VH (Maitra et al., 2012). Characteristics of polarization change from one object to another and to different shape and size of an object. Subsequently, the backscatter of the radar signals depends on the polarisation properties of the surface material. The roughness of the surface material determines the pulse that is measured by the sensor. (Maitra et al., 2012).

There are three main scattering mechanisms that contribute to the backscattered energy. The scattering mechanism of incident wave on vegetation is known as volume scattering because the reflection from the vegetation such as forest canopy is diffused or scattered (Joshi et al., 2015). Volume scattering is one of the three main scattering mechanism apart from single bounce which is from a smooth surfaces such as water and double bounce which is from the edges of the building or on grounds and tree trucks of forest (Joshi et al., 2015). Generally, the backscatter depends on the wavelength and the size of the object. Larger the object the bigger the backscatter. Refer to Figure 3 for volume scattering in relation to polarization (JAXA, n.d.).

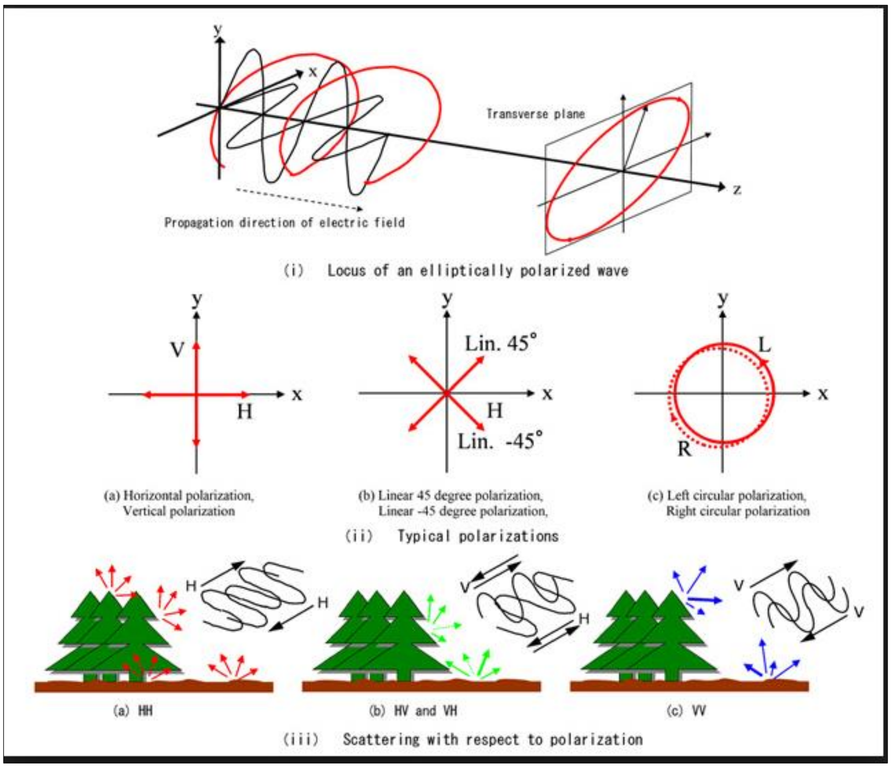

Figure 2: Scattering with respect to polarization (JAXA, n.d.).

2.3. Works related to the present study

There are several ways to collect ground data to estimate aboveground biomass and the carbon. Plot based technique is one of the techniques that is widely used in forest inventory because it is cost-effective and simple to implement. The important parameters measured in a set of sample plots are tree diameter at breast height (DBH), usually at 1.3m from the ground and the tree height. The DBH and the heights are used to calculate the biomass of given forest using an appropriate allometric equation (Bhattaraiet al., 2015). Carbon content in the biomass is approximately 50% of the dry biomass, thus, biomass is multiplied by 0.5 to get the carbon (Houghton, 2003).

Conducting field measurements such as forest inventory can complement the remote sensing techniques as they are essential for validating the accuracy of the satellite data. Several studies including Lu et al., 2012 and Karna et al., 2013 have used circular plots of 0.05 ha for field data collection to complement the study on estimating aboveground biomass and carbon by integrating lidar and other optical remote sensing. Other studies including, Otukei and Emanuel, 2015; Goh et al., 2013; Carreiras et al., 2013 used ALOS PALSA data to estimate the above ground biomass and carbon. A circular plot design was used for the field data collection, however, different radius of 15 m, 25 m and 20 m were used respectively. Hamdan et al., (2015) and Hamdan et al., (2014) carried out a similar study using L-band ALOS PALSAR in a Dipterocarp forest in Peninsular Malaysia and Mangrove forest in Malaysia respectively. However the sample size they used for field data collection was a square plot 30 m x 30 m and rectangular size plot of 20 m x 50 m accordingly.

There are two techniques used to retrieve the backscatter values to estimate the biomass using the radar data. This is achieved by using the SAR that is commonly known as SAR backscatter or by Polarimetric Aperture Radar Interferometry or PollnSAR (Otukei and Emanuel, 2015). The most commonly used technique in retrieving backscatter from the radar data particularly ALOS PALSAR data can be accomplished through converting digital number (DN) values or pixel values to backscatter (values) coefficient (Otukei & Emanuel, 2015). The related studies mentioned previously that used ALOS PALSAR data used the former technique to estimate forest biomass and carbon.

This study used data acquired from the recently launched ALOS-2 PALSAR -2 to estimate and map forest biomass and carbon of Ayer Hitam forest in Malaysia. The SAR backscatter technique was used to retrieve the backscatter values for estimating AGB. Circular plot of $500m^2$ with a radius of 12.62 meters was used for this study for field data collection.

3. STUDY AREA, MATERIALS AND METHODS

This chapter describes the study area and the processes applied in this research from field work preparation to executing the field work in Ayer Hitam Forest Reserve (AHFR). It also includes the processes in pre-processing the PALSAR-2 radar data and analysis of both the field data and the PALSAR-2 radar data to obtain accurate results. The materials and equipment used are also listed and described in this chapter.

3.1. Study Area

3.1.1. Geographical Location

This study was conducted in Ayer Hitam tropical rainforest. It is a Forest Reserve located in Puchong, Selangor State of Malaysia. The total area of the forest is 1248 hectares and is surrounded by urban developments. Ayer Hitam is managed by University Putra Malaysia and it is often utilised for education and research purposes (Awang et al., 2007). It was categorised as a research site in 1984 (Ghani et al., 1999). Therefore, it is directly used by researchers and scientists with an interest in studying tropical forest ecosystem.

Geographically, Ayer Hitam is located between latitude of 20 57' N to 03º 04'N, and longitude between 101º 38' E to 101º 38'E (Figure 2). The Malaysian capital city, Kuala Lumpur is located in the Northeast direction from Ayer Hitam forest and is approximately 6 kilometres away from the University of Putra Malaysia (Jusoff and Hasmadi, 2015).

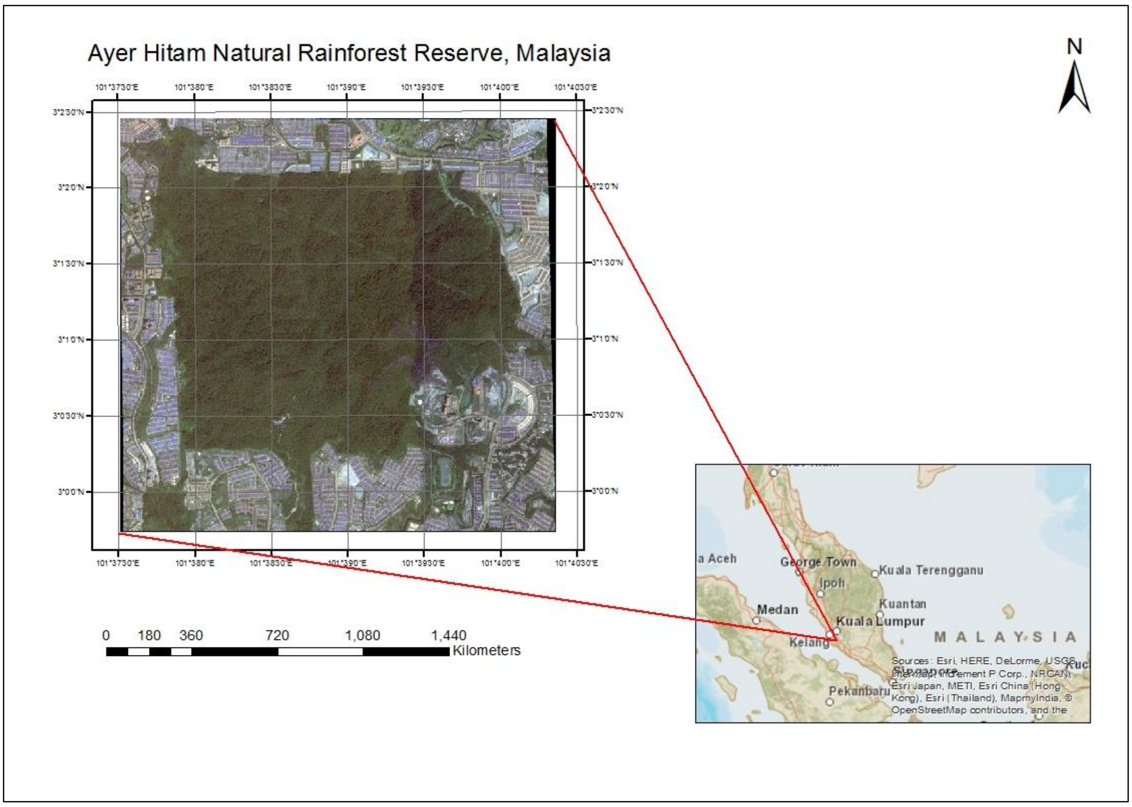

Figure 3: Map showing study area of Ayer Hitam Rainforest Reserve in Malaysia.

3.1.2. Vegetation type and topography

Ayer Hitam forest has a typical tropical rainforest characteristic of undulating topography. It has an average slope of 20% with an elevation ranging from 15 to 157 meters above sea level (Jusoff and Hasmadi, 2015). Generally, AHFR is highly dense with a diversity of unique flora and fauna. The heterogeneous forest structure makes it an interesting site for education and training especially for the Faculty of Forestry in University Putra Malaysia and international researchers and scientists. Ayer Hitam is dominated by Dipterocarp tree species. It is one of the few lowland forest remaining.(Nurul-Shida et al., 2014).

3.1.3. Climate

The monthly temperature of AHFR ranges from 22.6 degree Celsius minimum to maximum of 32.0 degree Celsius. The mean temperature is 28.36 degree Celsius with a mean relative humidity of 87.6%. The annual rainfall of AHFR ranges between 2316.5mm - 4223.4 mm. The highest rainfall is recorded in the month of May while August records the lowest rainfall (Jusoff and Hasmadi 2015).

3.2. Materials

Materials including software, image datasets and field equipment are an important part of any research. Therefore, this section introduces the list of materials used in order to conduct this research.

3.2.1. Satellite data set, ALOS-2 PALSAR-2 radar data

Phase Array L-type Synthetic Aperture Radar (PALSAR) 2, is a SAR sensor on board the Advanced Land Observation Satellite 2 (ALOS-2). The image data of PALSAR-2 used for this study was acquired online from JAXA, the Japan Aerospace Exploration Agency through PASCO cooperation (PASCO Coperation, n.d.). The scene was observed and captured on June 10th 2015 and was processed by JAXA on August 25th, 2015. PALSAR-2 is a Fine Beam Dual Polarization (HH and HV), and a high spatial resolution of 10 m and pixel size of 6.25 m x 6.25 m with 24 cm radar wavelength. The observation mode of PALSAR-2 is Strip Map having observation width of 70 km at an off-nadir angle of 36.6º (PASCO Coperation, n.d.). This data was acquired by ITC-University Twente for this study on August 26th, 2015. Specification of ALOS-2 and other PALSAR products can be seen on this website (http://en.alos-pasco.com/). Table 2 list the specification of PALSAR-2 sensor data.

Table 2: Detailed specification of PALSAR-2 data used in this study.

PALSAR-2 Specifications	
Observation Mode	Strip Map / High resolution
Calibration Factor	-83
Spatial Resolution	10 m
Pixel Spacing	6.25 m (2 looks)
Observation width -	70 km
Product Processed Level	1.5
Range Resolution	9.1 m
Azimuth Resolution	5.3 m
Polarization	HH, HV (Fine Beam Dual Polarization)
Wavelength	0.242 m (24 cm)
Off Nadir angle	36.6º
Incident angle at centre scene	40.55º

3.2.2. Software

Several software were used in this research. One of them was SNAP, which is an abbreviation for Sentinels Application Platform 2, a Sentinel1 Toolbox. It is an open source software that was developed for European Space Agency (ESA). It consists of several processing tools that can assist in analysing data from ESA SAR and also SAR data from ALOS PALSAR (European Space Agency, n.d.). PALSAR-2 data was obtained in the RUD format and was able to open in SNAP. ArcGIS, ArcMap 10.3 was used for all the GIS analysis as well as retrieval of the radar backscatter. Statistical analysis was done using both Microsoft Excel and RStudio software. Finally, Microsoft Word, PowerPoint and Excel were used for writing and presentation. Table 3 list all software use in this study.

Table 3: Software and their uses

Software	Use
Sentinels Application Platform 2 (SNAP)	- Calibration of PALSAR-2 data - Conversion of DN values to radar backscatter - D-speckling of PALSAR-2 data
ArcGIS- ArcMap 10.3	- Geo-correction and rectification - Geo-referencing & re-projecting - Extracting subset of study area from the whole image - Retrieving radar backscatter - Producing AGB and Carbon Map
R –RStudio and SPSS	- Correlation analysis - Linear regression analysis - Modelling and validating - Accuracy check
Microsoft Excel	- Manual preliminary analysis of biometric data
Microsoft Word	- Proposal and Thesis write up
Microsoft PowerPoint	- Proposal and Thesis presentation

3.2.3. Field Equipment

Apart from the satellite datasets and the software used, field equipment was also considered important for conducting this research. The field equipment that were used in this study to collect field data in Ayer Hitam Forest are listed in Table 4.

Table 4: Equipment/materials used for field work, data collection

Equipment	Use
Diameter Tape (5m)	Measuring diameter (dbh) of trees
Leica Disto, Laser	Measuring tree heights
Densitometer	Measuring the canopy % cover
IPad/GPS	Navigation in the forest and for recording GPS location
Distance meter tape (30m)	Measuring the plot radius/area
Sunnto Clinometer	Measuring the slope
Field sheets/pencils	Recording field data
Hard copy of Google and Topo Map	Assist with locating next site for sampling
World View 3 Image	Digitizing study area boundary
ArcGIS Base Map	Geo-referencing
Radar Footprint on Google Map	Confirming the coordinates of radar image data for georeferencing

3.3. Research Methods

Research methods are the crucial part of any research. It indicates the study approaches used to collect, pre-process and analyse data to achieve a suitable result. In this study, the research methods consisted of four different processes. These processes refer to field data collection, processing of biometrics data and PALSAR data, statistical analysis of the data including correlation and regression analysis, and finally modelling and producing the aboveground biomass and carbon map of AHFR. Figure 3 is the flow chat of the main processes done in this study.

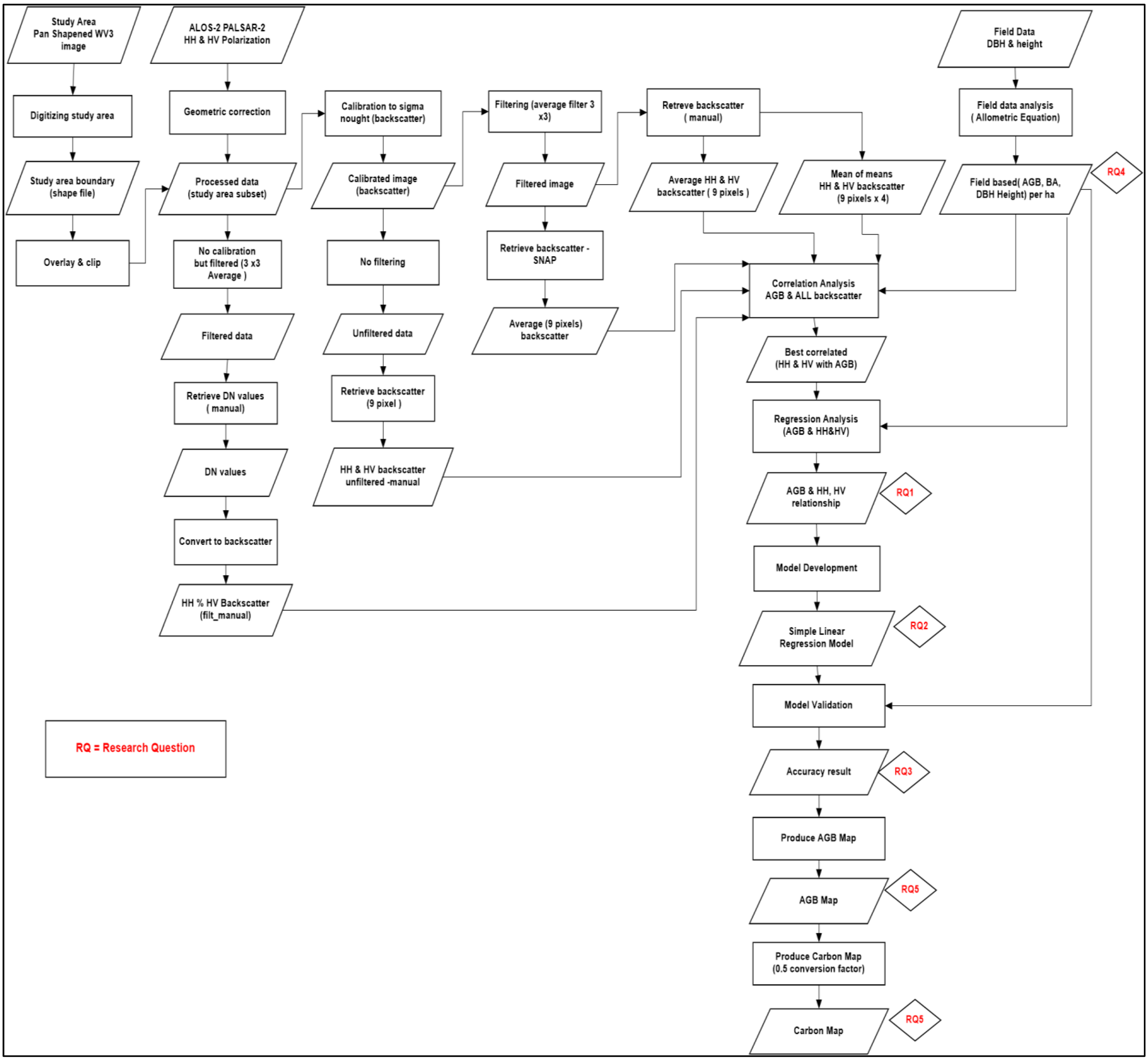

Figure 4: Flow Chart of the study

3.3.1. Field Work

This section includes the field sampling design, determination of plot size and data collection. Field data analysis for AGB and stand basal area (BA) were done and discussed in this section.

3.3.1.1. Field Sampling Design

Sampling is very important in obtaining data or information that is representative of a population and is a vital part especially in forest richness and biodiversity studies (You, 2011)(You, 2011). The purpose of sampling is to obtain reliable and quantitative information about a population to make an inference. In remote sensing, accuracy assessment and model validation are performed based on ground data that are collected from sample plots (Stehman, 1999). Thus, in order to obtain reliable data, appropriate sampling designs are required based on the research objectives. For example, in forest research, direct and accurate data is acquired from establishing sampling plots (van Laar, and Akça, 2007) because it is important to make inference with confidence about a study on a forest population.

According to (Nurul-Shida et al., 2014), AHFR is a logged-over forest in which the three layers of the forest is conspicuous and can be clearly differentiated. However, based on Very High Resolution (VHR) World View (WV) 3 Satellite Image of AHFR that was acquired by ITC for this study, the forest appeared to be generally homogenous. This WV3 image was pan-sharpen before it was used. Thus, the forest could not be differentiated using satellite image. Consequently, prior to the field work, systematic sampling was preferred. Therefore, grids were marked on the WV 3 image and sample plots were generated inside the grids systematically.

However, based on the situation on the ground including the accessibility of the forest, finally, a purposive sampling design was applied. It was more appropriate to apply purposive sampling because of the undulating topography and inaccessibility of most of the forest area. In addition the weight of the Terrestrial Lidar Scanner (TLS) and the accessories was also taken into consideration as they weigh over 25 kilograms. Sites for establishing the sample plots were subjective at a location assuming that, it is representative of the forest population and the plots were sampled at a distance of >50 m apart from each other. Plots for TLS scanning was chosen based on density of the forest undergrowth because clearance needed to be done to avoid occlusion.

To have a representation of the population, the stratification that was used by UPM in their management plan of this forest was adopted. The forest was divided into three strata: 1) undisturbed forest with trees highly dense, 2) burned and degraded forest and 3) high elevation forest with highly dense trees. Six (6) plots were sampled in undisturbed forest, five (5) in burned and disturbed forest area and (21) plots were sampled in forest areas at elevation of 25 meters or greater. Twenty six (26) plots were sampled for TLS while other 6 plots were sampled for collecting only the biometric data. Total of thirty-two (32) plots were sampled.

3.3.1.2. Determining plot size

Determining shape and size of the plot depend on the objective and the purpose of the research. Sampling plots can be of any size and shape. It can be either square, circle or rectangle. However, circular plots are commonly used in forest inventory (Wenger, 1984). Circular plots are easy to establish because only one point, the centre of the plot is defined and the radius of the plot is measured from the centre and the parameter is determined. However, in a rectangle or square plots, four corner points are defined and this can lead to high chances of error.

In this study, a circular plot of 500 m² with a radius of 12.62 m from the centre of the plot was established. Inventory of the forest parameters especially measuring the diameter at breast height (DBH) and height of all trees were done within the plot. Figure 5 is an example of a circular plot.

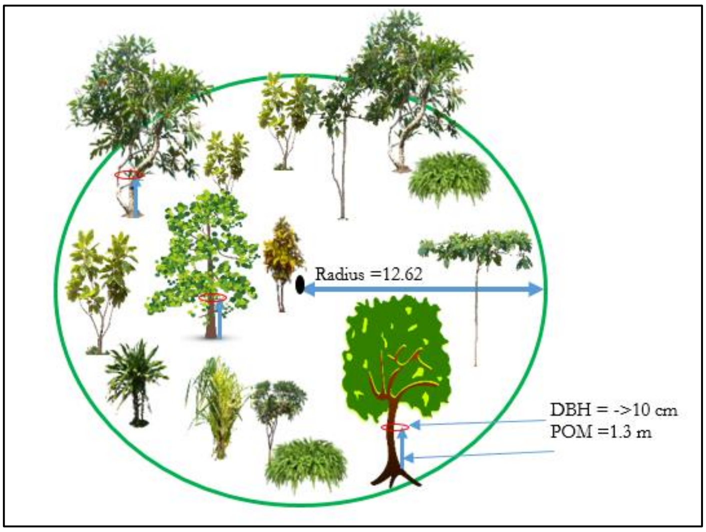

Figure 5: Circular plot of 500 m²

3.3.1.3. Field Data Collection

Data required for estimating aboveground biomass and carbon of a forest is no difference to that of volume estimation from forest inventories. Height and DBH measurements have been the key parameters in forest inventory over the years in forestry and it is useful as well in AGB estimation (Brown, 1997).

The procedure of data collection is crucial in the field. Consequently, measurement of DBH, height and species identification of all trees crown cover percentage and sample centre coordinates were recorded in every sample plots. Prior to plot establishment, a general observation of the area was made to cater for slope correction. In a generally flat forest area, the radius of 12.62 m² was measured from the centre of the plot. However, in an undulating area, slopes were measured using Suunto Clinometer before establishing a radius. Then slope correction was applied to correct the slope to adjust from elliptical to the horizontal shape. This is done because, when the plot is established on a slope, it is more an ellipse than a circle, therefore, slope correction is needed (van Laar, and Akça, 2007). A slope correction table (Appendix 5) was used to adjust the radius of the plot.

The coordinates of the centre of the plots were recorded using the GPS. Following that, all the tree species with a diameter at breast height (DBH) of 10 cm and above that were found within the plot boundary and their heights were measured. The diameter was measured at 1.3 m height from the base of the tree. A standard size stick of 1.3 m was used to minimise variation in DBH measurement and to be consistent with the point of measurement. For trees standing on slopes and higher ground, DBH was measured from the higher ground. Dead litters and debris under the tree were cleared before measuring the DBH. The densiometer was used to measure the crown cover percentage. Five crown cover readings were taken. One taken in the centre of the plot and four in the different directions (N, S, E & W). The final reading was calculated from the average of the five measurements to get a precise and representative canopy cover. Leica Disto Laser height measuring instrument was used to measure the tree heights. All these data were recorded in the field sheet (Appendix 6) and entered in the in Microsoft Excel for analysis.

3.3.1.4. Field Data Analysis of AGB and Basal Area (BA)

To estimate aboveground biomass, wood density is required. Therefore, an FAO default wood density value of 0.57 tons m^3 was used for all the species. This value is applicable for the tree species in a tropical forest in Asia (Hirata et al., 2012). Unfortunately, wood density from Global Wood Density database (Mitchard et al., 2012) was not used because not all trees were identified to species or genera level in order to use species-specific wood density to calculate the biomass.

The allometric equation is the main approach used to estimate above ground biomass. There are many allometric equations available for estimating aboveground biomass for all kinds of forests and many studies. Basuki et al., (2009) used equation specifically for Dipterocarp tropical forest in Indonesia while Tanase et al., 2014 used the allometric equation for Cypress Pine dominated forest in Australia. For this study, a revised and improved Allometric Equations adopted from Chave et al., 2015 specifically for tropical forest trees was used to estimate aboveground biomass and carbon in Ayer Hitam Forest Reserve. Refer to Equation 1 (Chave et al., 2015).

Equation 1: Allometric Equation

$$AGB_{est} = 0.0673 * (\rho\, D^2 H)^{0.976}$$

Where: AGB_{est} is aboveground biomass estimate in kilogram
D is diameter at breast height in centimetre
H is height in meter
ρ is wood density in gcm^3
0.0673 and 0.976 are constants

Total above ground biomass for individual plots was computed using Equation 1 and then converted to tons per hectare (ton $^{-1}$ha). Subsequently, carbon was calculated from the aboveground biomass using the conversion factor of 0.5. Carbon was calculated using Equation 2. Approximately 50 % of the biomass is stored as carbon (Hirata et al., 2012).

Equation 2: Carbon Equation

$$C= B * CF$$

Where: C is the carbon stock in ton C
B is the dry biomass
CF is the carbon fraction (0.5)

Basic statistics such as average height and DBH per plot was computed. Total basal area per hectare (BA/ha) were also calculated using Equation 3 (Missourie education., n.d.).The basal area was calculated to analyse the correlation between the radar backscatter coefficients of HH and HV polarization. Basal area is the area of the cross section of the stem at breast height. Basal area per hectare considered as a measure of stocking or density of forest stand.

Equation 3: Basal Area

$$BA = 0.00007854 * DBH^2$$

Where: 0.00007854 is the constant of π which 3.14
BA is the basal area per square meter (m^2)
DBH is diameter at breast height in centimetres

3.3.2. PALSAR-2 Data Pre-processing

Processing of data is another vital component of research. In this study, PALSAR data was pre-processed before the backscatter coefficient (dB) was retrieved to estimate the biomass of the study area.

Pre-processing is normally done to correct for distortion or degradation in the image to produce a more meaningful data that represents the scene of which the image is captured. In addition pre-processed images are more appropriate to work with (Frulla et al., 1998). Before applying further analysis and processes to the data, it is essential to perform geometric and radiometric calibration to radar images (Frulla et al., 1998). Geometric correction is applied to the SAR to determine its pixel position by allocating its geodetic coordinates in latitude and longitude (Shimada et al., 2009). Conversion of slant range to ground range and multi-look and azimuth compression are part of the geometric correction process. On the other hand, radiometric correction refers to distortion associated with the sensor. In radar remote sensing, especially when dealing with SAR radar image, this process is associated with the conversion of the DN values to NRCS or backscatter coefficient (Shimada et al., 2009).

3.3.2.1. Data Pre-processing - Calibration and Filtering

The PALSAR-2 radar data used for this study was obtained in as Process Level 1.5 data. At this level, most of the radiometric calibration and geometric correction processes were applied prior to acquiring the data. Besides, the map is georeferenced or geocoded (Shimada et al., 2009). Backscatter conversion is possible with data at this level ((Joshi et al., 2015; Kim, 2012).

PALSAR-2 data came in BEAM-DIMAP format and was not possible to open in either ArcGIS or ERDAS, however, it was possible to be opened in SNAP software. In SNAP, backscatter calibration and filtering processes were applied. Backscatter calibration is a process where the PALSAR-2 radar data is calibrated using the Sigma Nought calibration to backscatter coefficient ($\sigma°$) (Sun et al., 2011). This process was applied to HH and HV polarized data. The digital number (DN) values of the data were automatically converted to radar backscatter coefficient also known as Normalized Radar Cross Section (NRCS) (Sun et al., 2011). Calibration was done to correct the HH and HV polarized data so that the DN values represent true radar backscatter of the reflecting surface object (Sun et al., 2011).

Speckle filtering was also applied to the image data after calibrating the image. Speckle filtering is applied to the image to remove the salt and pepper like appearance on the image that is caused by high frequency energy waves caused by reflection of objects on the ground (Joshi et al., 2015). Speckles is one of the common radiometric distortion that randomly appear on all SAR images. The relationship between the surface object and the received backscatter interactions can be influenced by the speckles (Joshi et al., 2015).

Filtering is essential because it reduces speckles in the image and improves the texture of the image (Amini and Sumantyo, 2011) In this study, Mean Filter of 3 x 3 pixel size was applied to both like polarised and crossed polarised images. This method was used to retain the original information of the data. Here, the average of the DN values of the 9 pixels is calculated (Amini and Sumantyo, 2011). The new average value replaces the original centre pixel value. Apart from mean or average filtering method, there are other filters such as median, Lee, Frost, and Gamma available to process SAR images (Babu, 2013) depending on the objective of the study.

3.3.2.2. Data processing- Geo-referencing and Re-projecting.

The pre-processed image was saved in GEOTIFF format and exported to ArcGIS for further processing. The image was georeferenced and re-projected to the universal transverse Mercator (UTM) coordinate system in ArcGIS. Geo-referencing was applied to HH and HV polarized data to convert the coordinate of the image file to a specific map coordinate system and datum. The upper-left, upper right, lower right and lower left coordinates from the footprint of the PALSAR -2 data in the Google Earth Map was used to georeference the data. An ArcGIS online base map was also used as a reference map for geo-referencing the PALSAR-2 image.

Once, the four points on the reference coordinates were assigned to the image file, it was rectified and a new image with map coordinates in degree decimals was produced. The geo-referencing process was updated and the image was displayed with new map coordinates (Zhu et al., 2007). In this case, the image was spatially georeferenced to the geographical coordinate system using the World Geodetic System 84 (WGS_1984) in decimal degree. Subsequently, the map was re-projected to Universal Transverse Mercator (UTM) coordinate system with the appropriate zone. The final image map has the following spatial reference information WGS_1984_UTM_Zone_47N.

Meanwhile, the WV 3 image of the study area with the same spatial reference was digitised and the boundary of the study area was clipped. The study area boundary was overlaid on the PALSAR-2 image map and the subset of the study area, (AHFR) was extracted from the whole image.

3.3.3. Retrieval of radar backscatter coefficient

Radar backscatter coefficient from the HH and HV polarized images were retrieved using two approaches. The first was achieved in SNAP when applying calibration process where DN values were automatically converted to backscatter coefficient. The second approach was manually done in ArcGIS by extracting the DN values and converting them to backscatter coefficient using Equation 4. The DN values do not represent radar backscatter of the surface object, therefore, they were converted to backscatter. Equation 4 is used specifically for ALOS PALSAR for extracting radar backscatter coefficient for a product level 1.5 (Shimada et al., 2009).

Equation 4: Backscatter coefficient conversion

$$NRCS\ (dB) = 10 * \ log_{10}(DN^2) + CF$$

Where: NRCS = Normalized Radar Cross Section
DN = Digital Number value
CF = Calibration Factor of -83

Retrieval of backscatter took into consideration field sample size the pixel size of the image. The HH and HV polarized image have a pixel size of 7 m x 7 m and the field sample plot was a circular plot of 500 m² with a standardized radius of 12.62 m. The plot size could approximately fit in the 9 pixels with the dimension of 3 x 3-pixel window. Since the radius of the plot was 12.62, the diameter of the whole plot was approximately 25 m (i.e.: 12.62 +12.62m) which can approximately fit with 9 pixels (i.e.; of 3 pixels * 7 m =21 m). Moreover, taking an average of 9 pixels gives more representation of the backscatter values (Figure 6). A similar approach was applied in a biomass estimation study (Hamdan et al., 2011). However, a plot size of 50 m x 50 m was sampled and 16 pixels of 4x4 pixels were used to retrieve the DN values then convert to backscatter value.

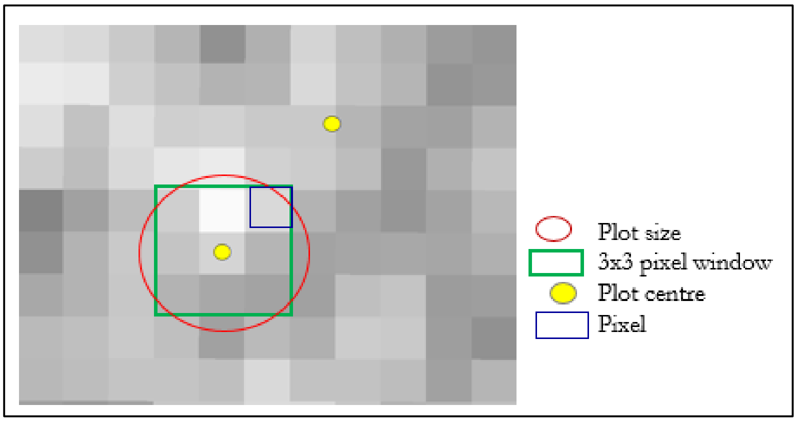

Figure 6: Graphical representation of fitting sample plot with the 9 pixels

Apparently, not all GPS coordinates recorded in the centre of the sample plots perfectly fitted in the centre of the pixel. There were some centre points that were at the edge of two pixels or between two pixels (Figure 7). This has created a problem in identifying the true pixel to consider as the centre pixel to establish the 3x3 pixel window. To address this problem, a different approach was taken.

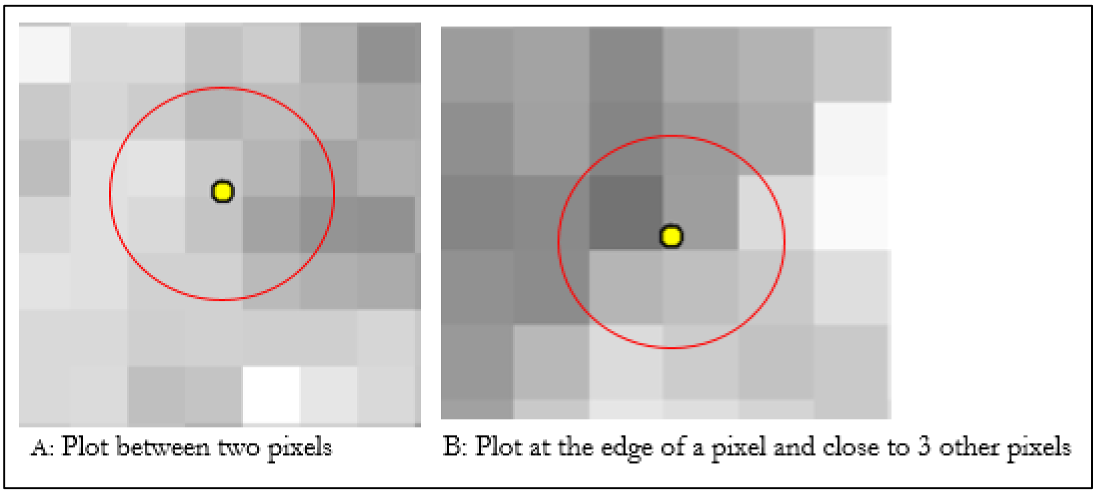

Figure 7: Two different situation in the location of centre points of the plots

Basically, an average of four, 3 x 3-pixel windows was obtained to determine the final pixel value in a plot. First a pseudo point was placed in the centre of the pixel where the original point was located. Next a pixel window of 3 x 3 was established and the average backscatter of the first 9 pixels was calculated. The same was done by placing pseudo points in the centre of 3 other pixels and again an average of the 9 pixels was calculated. Average of the four averages was calculated to use as the final backscatter value to run the model. This process is illustrated in Figure 8. The average backscatter obtained from 9 pixels and average were compared by running the regression model with the AGB to accept the approach that gives the strong R^2 to estimate the AGB and carbon stock of the whole study area.

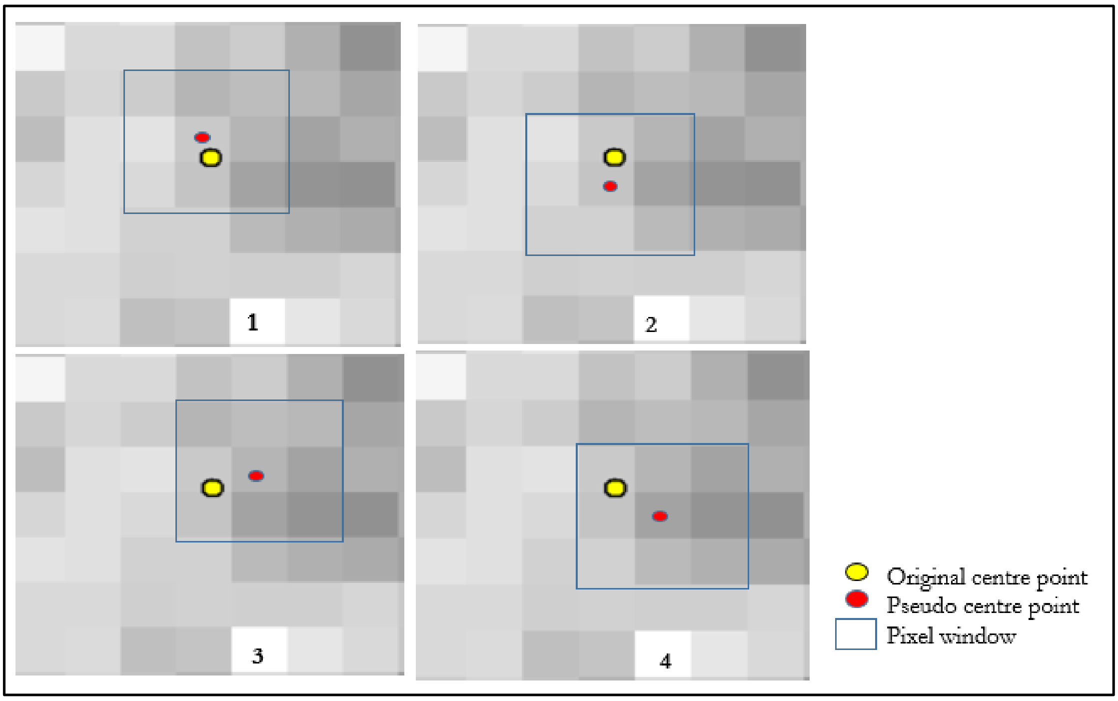

Figure 8: Illustration to determine centre pixel

3.3.4. Correlation analysis

Correlation analysis is an important process in any research because it expresses something about the relationship between two or more variables. In addition, correlation analysis allows one to understand the strength of the relationship between the variables, whether the relationship is weak, strong negative or positive. The correlation coefficient values range between -1 and +1 (Stein, 2002). The value -1 indicates that there is a very strong negative relationship between two variables, and +1 indicates that there is a very strong relationship between the variables. A value of 0 indicates that there is no relationship between the variables (Stein, 2002).

In this study, correlation analysis was carried out between the forest parameters and the radar backscatter coefficient of HH and HV polarized image data. The main focus was to observe the relationship between the AGB and the radar backscatter coefficient. Therefore, initially, a scatter graph was plotted between the variables. Afterwards, Pearson's product – moment correlation coefficient was used to determine the relationship between radar backscatter and AGB and stand basal area (BA). Similarly, a relationship between the field measured AGB and predicted AGB was also assessed to see the variability in the variables. This was executed after the model was developed and validated.

3.3.5. Regression Analysis

A relationship between one dependent variable and one or more independent variables can be identified using regression analysis. The two commonly used regression models are, simple linear and multiple linear regression models (Quinn & Keough, 2002). Researchers widely use linear regression model because the model describes the linear relationship between the independent (x) and dependent (y) variables. It defines the variation in y with a change in x and a new y value can be predicted from a new value of x (Quinn & Keough, 2002). Multiple linear regression is used to assess the relationship between a single dependent variable and more than one independent variable.

Regression models including linear models are some of the main techniques used to predict AGB apart from K nearest neighbourhood and neural network (Lu 2006). Both simple linear and multiple linear regression was performed to assess the relationship between radar backscatter coefficient of HH and HV polarized backscatter coefficient with the AGB. In linear regression analysis, AGB was used as the dependent variable and HV was used as the independent variable to determine the change in the AGB as HV changes. A strong coefficient of determination (R^2) was obtained from this relationship. On the other hand, a multiple linear regression was performed considering AGB as a dependent variable and HH and HV as independent variables. Again, a strong correlation and R^2 was obtained. Simple linear regression between the HH and HV backscatter and other forest parameters including DBH, height and stand BA were also performed.

3.3.6. Model Development and Validation

A total of 27 plots observed in the field were used for model development and validation. These plots were randomly distributed into two sets. 17 plots (60%) was used for developing the model while 10 plots (40%) were retained to validate the model. The backscatter of HV polarized image was correlated with the calculated AGB using linear regression. HV was considered as the independent variable and AGB as the dependent variable. The empirical model produced from this process was used to estimate the AGB and carbon stock of the whole study area. The relationship between the HV backscatter and the AGB is expressed as a linear regression function (Equation 5).

Equation 5: Linear regression function

$$\boldsymbol{Y = \beta_0 + \beta_1 X}$$

Where: Y is the predicted biomass

β_0 and β_1 are model coefficients

X is the HV backscatter value

A validity check is performed to measure the prediction accuracy (Snee, 1977). Thus, validation process is essential before any model can be used. In this study, 40% (10 plots) of the data, which is independent of the model development data was used to validate the linear regression model. The predicted AGB obtained from the model was correlated with the calculated AGB to observe the coefficient of determination (R^2) of model validation. Furthermore, the Root Mean Square Error (RMSE) was calculated using Equation 6 (Deng et al., 2014).

Equation 6: Root Mean Square Error calculation

$$\text{RMSE} = \sqrt{\frac{\sum_{i=1}^{n}(\hat{Y} - Y)^2}{n}}$$

Where: RMSE is Root Mean Square Error

Y is biomass observed or calculated using allometric equation

$\hat{Y}$ is biomass predicted or derived from the radar backscatter using the model

n is the number of validating plots

3.3.7. Mapping aboveground biomass (AGB) and carbon stock

The simple linear regression model developed from HV backscatter and AGB was accepted to estimate the AGB and carbon stock for the study area. The model was chosen after validating its accuracy and the AGB map of the whole study area was produced in ArcGIS. The HV polarized raster map was used to map AGB

Raster calculator is a tool in the spatial analyst toolbox in ArcGIS software that was applied to process the AGB map. In raster calculator, the HV raster map was selected in algebra map expression, and the model equation (Equation 8) was applied. The raster calculator takes every pixel value that is the HV backscatter value in the raster map and converts it to the biomass accordingly. The backscatter values are converted to AGB values and estimation is based on pixel basis (Hamdan et al., 2015). Negative values were assigned to those areas without AGB. Consequently, values were arranged logically in the category (eg, 0 - 80, 80 - 160 etc.) and colours were assigned to the values that represented biomass values. After quantification of the biomass, carbon stock was calculated using equation 2. Consequently, a map showing the distribution of AGB and carbon stock for AHFR was produced.

4. RESULTS

4.1. Descriptive analysis of field data

Forest parameters measured in the field were tree height, diameter at breast height (DBH) and crown cover percentage. Species identification was also done in the field. The mean AGB and stand basal area (BA) per ha is 208.79 ton ha^{-1} and 29.47 m^3 ha^{-1} respectively. Table 5 presents the descriptive statistic for the overall plots (27 plots). About 193 tree species were enumerated. AGB and carbon stock based on per plot and per hectare were calculated and presented in Appendix 1, Table A. Summary statistics of other forest parameters were also assessed and summarized in the same table.

Table 5 Descriptive statistic of forest parameters.

	N	Minimum	Maximum	Sum	Mean		Std. Deviation
	Statistic	Statistic	Statistic	Statistic	Statistic	Std. Error	Statistic
AGB(ton)	27	60.17	367.07	5637.41	208.79	15.29	79.44
BA (m^3)	27	9.92	42.93	795.76	29.47	1.61	8.38
DBH (cm)	27	17	28	-	22.49	0.55	2.85
Height (m)	27	10.76	18.65	-	14.37	0.40	2.08
Tot Tree /plot	27	17	45	778	28.81	1.32	6.85
Crown Cover%	27	70	95	-	86.67	1.10	5.72

Variation in biomass estimation is also influenced by the tree diameter size. Therefore, trees measured in the field were classified according to their diameter class. Table 6 shows the total number of trees, basal areas and above ground biomass recorded per diameter class. Average height and DBH per diameter class were also calculated. Trees in the diameter class of 30-39 cm DBH constitutes more than 1200 tons of AGB based on the 27 plots inventoried. Nevertheless, more trees were found in diameter class 10-19 cm as expected in a natural forest with the least AGB of 649.86 tons (Figure 9).

Table 6: Summary per diameter class

DBH class	**10-19**	**20-29**	**30-39**	**40-49**	**50-59**	**>60**
No. of trees	429.00	179.00	96.00	35.00	25.00	14.00
Total BA (m^3 ha^{-1})	6.72	8.18	8.87	5.68	5.60	4.45
Total AGB ($ton^{-1}ha$)	649.86	1062.06	1232.87	928.35	914.38	789.61
Mean height (m)	11.55	16.04	17.60	16.81	21.97	22.70
Mean DBH (cm)	13.87	23.88	32.61	45.09	53.88	66.45

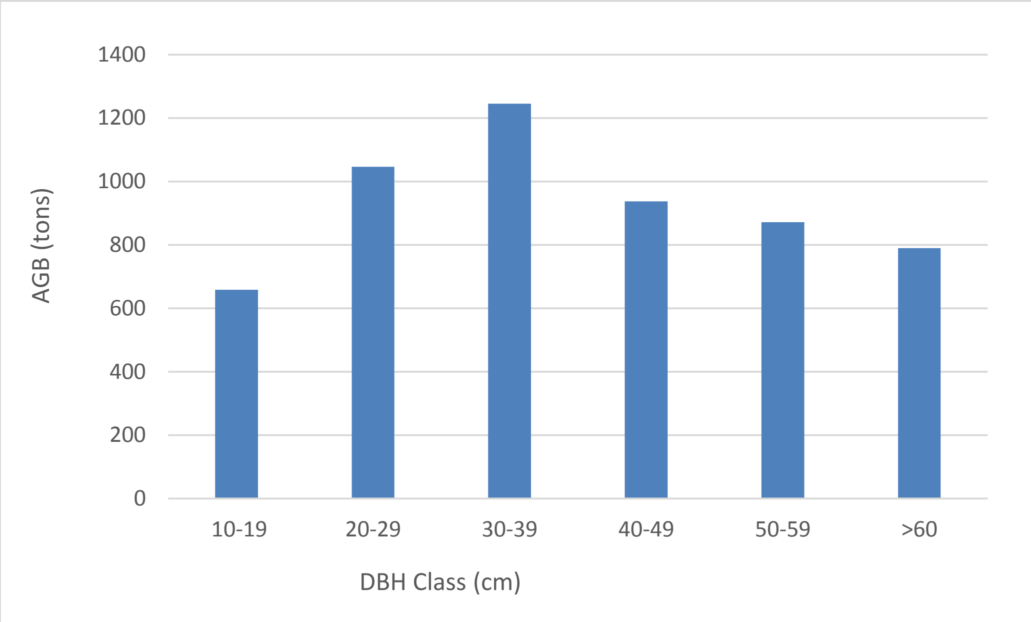

Figure 9: Total amount of biomass per diameter class

4.1.1. Common tree species in Ayer Hitam Forest Reserve

Species identification and enumeration were also carried out in the field. A total of 778 individual trees were recorded. About 768 species from 717 families were identified. The most occurring species and families are presented in Table 7 and Figure 9 respectively. Dipterocarpaceae is the dominant tree family in AHFR. Three frequently occurring species *Hopea sulcata, Shorea macroptera and Dipterocarpus costulata* are from Dipterocarpaceae family.

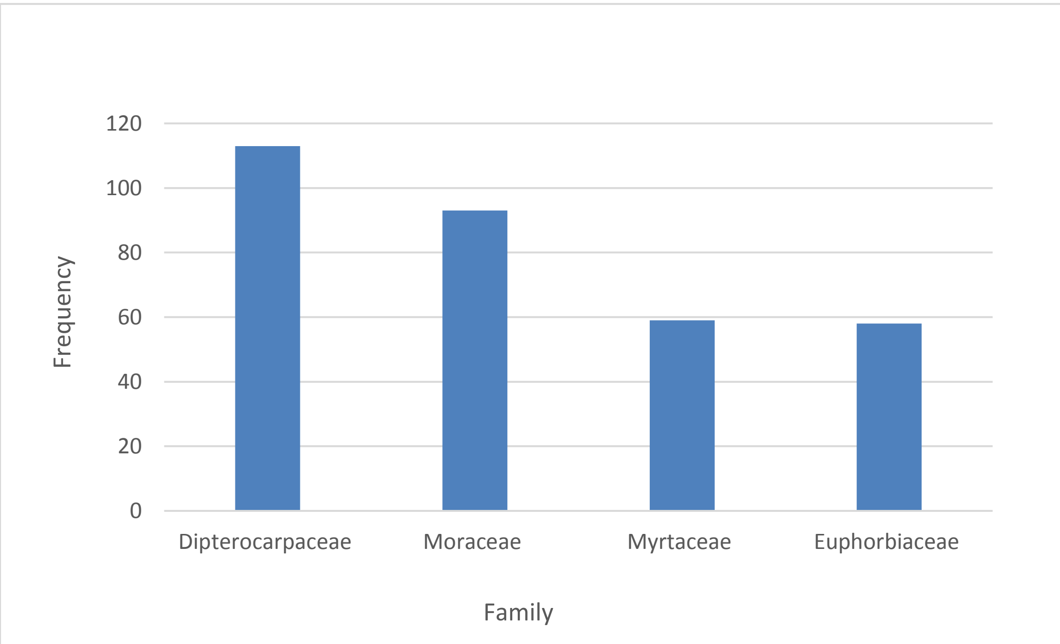

Figure 10: Four dominant tree family in AHFR

Table 7: Most occurring species at AHTF sampled sites

Species	Family	Occurrence
Streblus elongatus	Moraceae	50
Syzygium spp	Myrtaceae	39
Hopea sulcata	Dipterocarpaceae	32
Endospermum diadenum	Euphorbiaceae	30
Shorea macroptera	Dipterocarpaceae	21
Dipterocarpus costulatus	Dipterocarpaceae	20

4.2. Descriptive analysis of the PALSAR-2 backscatter

Prior to any pre-processing of the radar data, it is essential to visually analyse the data. The PALSAR HV and HH polarized data can be distinctively differentiated based on the backscatter. That is, HV appears brighter than HH data. In this case, the forest appears light grey in HV and dark grey in HH polarized image. Figure 11 shows the appearance of the HH and HV image data before and after pre-processing in SNAP. Even after applying calibration and filtering, there is a district difference between the two polarizations. The raw image data of the whole image in appended in Appendix 4, images A and B.

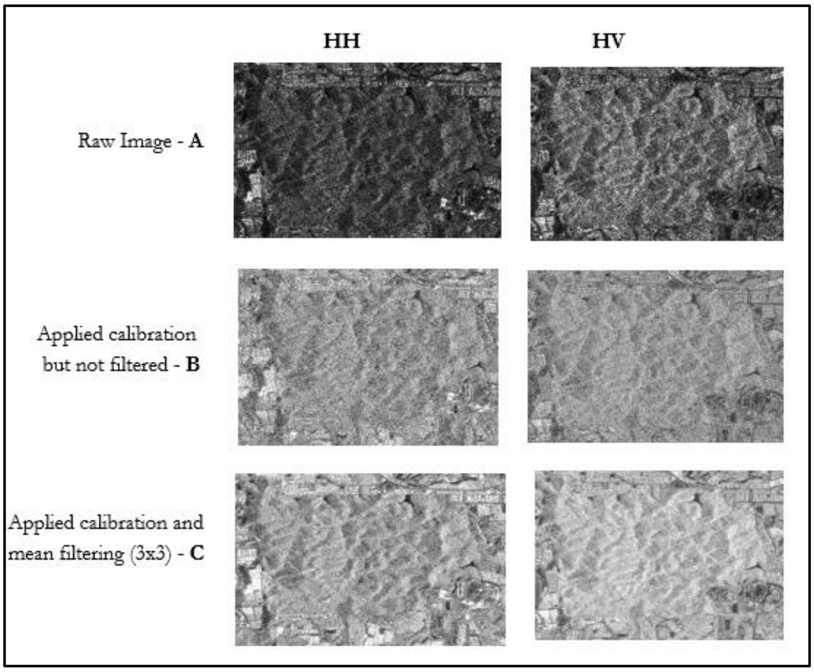

Figure 11: Appearance of PALSAR-2 HH, HV polarised image data before and after retrieving the backscatter values

4.2.1. Correlation of AGB and HH and HV polarized backscatter

Calibration of radar backscatter from digital number (DN) values to backscatter coefficient or sigma noughts was achieved in SNAP software. It was automatically converted from DN values to backscatter coefficient for the HH and HV polarized image. The backscatter were extracted using the 3 x 3 pixel window and the average backscatter was calculated automatically based on the coordinates of the plots. On the other hand, the calibrated image was exported to ArcGIS and backscatter was extracted manually using 3 x 3 pixel window and 4 of 3 x 3 pixel window to obtain the average and average of average pixel values (Figure 6, 7 and 8). HV and HH backscatter retrieved using these different ways were correlated with AGB. The correlation analysis is shown in Table 8.

Table 8: Correlation between AGB and backscatter

		AGB ton ha^{-1}	HV Mean of Means	HH Mean of Means	HV_ Mean	HH_ Mean	HV_SNAP Mean	HH_SNAP Mean
Pearson Correlation	AGB ton ha^{-1}	1	0.904**	0.652**	0.870**	0.660**	0.71	0.142
Sig. (2-tailed)			6.526E-07	0.005	5.757E-06	0.004	0.787	0.587
N		17	17	17	17	17	17	17

Correlation analysis result showed that the backscatter retrieved from the HV polarised image using the average of average (i.e. mean of means) approach correlated well with AGB, having r of 0.904 and a R^2 of 0.81. Therefore, backscatter retrieved from this approach was used to develop the model to estimate the AGB and carbon stock. The backscatter coefficient retrieved using these approaches are appended in Appendix 2, Table A and B.

4.3. Correlation Analysis of HH and HV polarized backscatter and forest parameters

The Pearson's product moment correlation was used to observe the correlation between HH and HV polarized radar backscatter and AGB separately. HH and HV backscatters were also correlated with other forest parameters. There was a strong correlation between HV and AGB at R = 0.90 and HV and basal area at R = 0.82 at 95 % confidence level (Table 9). HH polarization also correlates to AGB and stand BA at 0.65 and 0.68 respectively. Height has the weakest correlation with both HV and HH polarized backscatter. Correlation analysis between AGB and all other forest parameters are appended in Appendix 1, Table C.

Table 9: Correlation between the HH and HV Polarization with basal area, DBH and height

Stand Parameters/	Backscatters	HV	HH
AGB(ton/ha)	Pearson Correlation	**0.904****	**0.652****
	Sig. (2-tailed)	6.5261E-07	0.005
BA(m^3/ha)	Pearson Correlation	**0.819****	**0.670****
	Sig. (2-tailed)	5.687E-05	0.003
Mean DBH	Pearson Correlation	0.321	0.313
	Sig. (2-tailed)	0.209	0.221
Mean height	Pearson Correlation	0.463	0.231
	Sig. (2-tailed)	0.061	0.372

**. Correlation is significant at the 0.01 level (2-tailed).

*. Correlation is significant at the 0.05 level (2-tailed).

The relationship between HH and HV backscatter coefficient and stand BA was also assessed. A positive and moderate correlation was seen with HV backscatter with R^2 of 0.672 (Figure 12). There was a weak relationship observed between HH backscatter and stand BA (Figure 13). The regression statistics of HV polarized backscatter and stand BA is found in Table 10. At 95% confidence level, HV backscatter can explain about 67% of stand BA. Only 45% of the stand BA is described by HH backscatter.

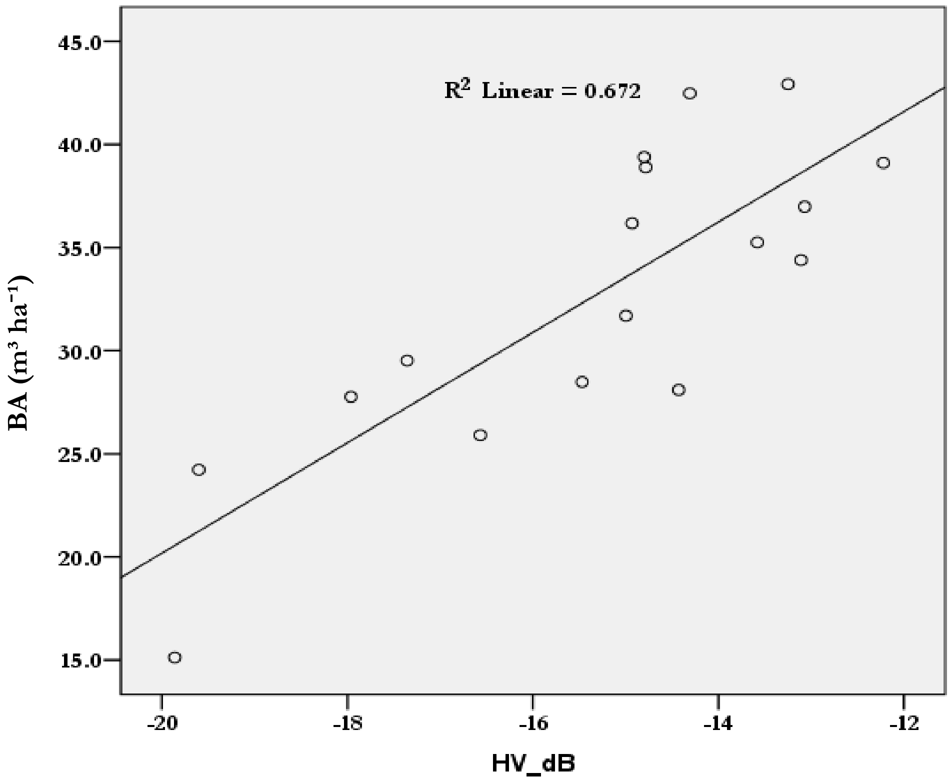

Figure 12: Relationship between basal area (BA) and HV backscatter coefficient

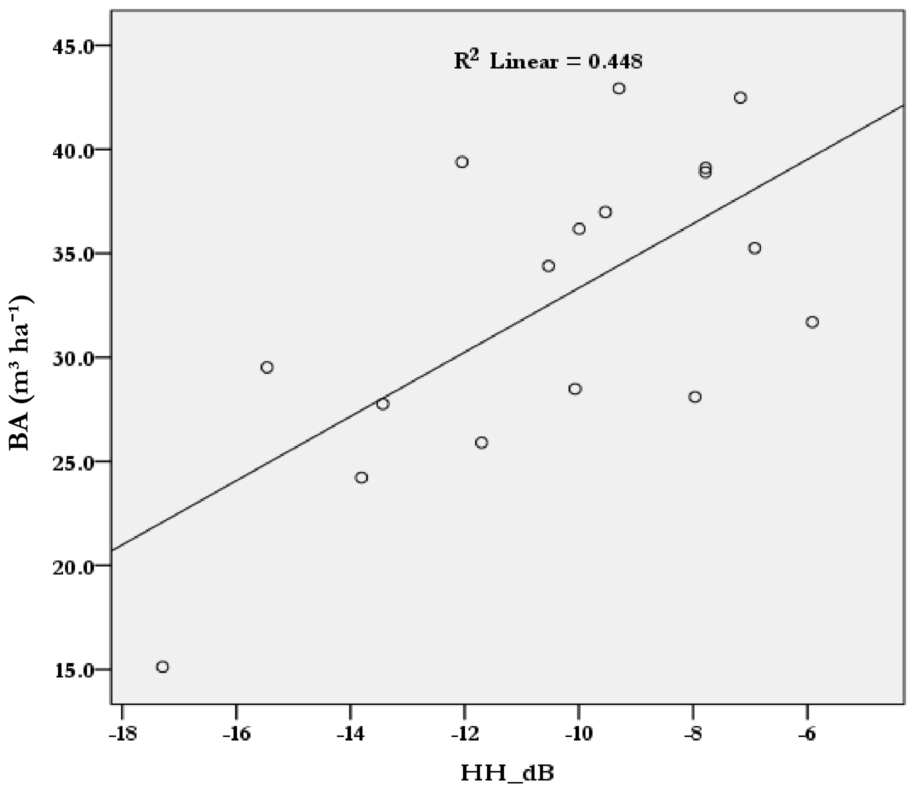

Figure 13: Relationship between basal area (BA) and HH backscatter coefficient

Table 10: Regression analysis of HV and stand BA

Regression Statistics					
Multiple R	0.819				
R Square	0.672				
Adjusted R Square	0.649				
Standard Error	4.353				
Observations	17				
	Coefficients	*P-value*			
Intercept	73.698	6E-08			
HV	2.676	5.69E-05			
ANOVA					
	df	*SS*	*MS*	*F*	*Significance F*
Regression	1	581.205	581.205	30.668	5.6873E-05
Residual	15	284.269	18.951		
Total	16	865.474			

AGB has a positive relationship with stand BA, DBH and height (Table 11). A strong relationship was noticed between AGB and stand BA, and height, but correlates weakly with DBH. The relationship of AGB and stand BA was plotted on the scatter graph (Figure 14). About 71% of AGB can be explained by the stand BA. The summary output of the regression analysis of HH and AGB, HH and BA and AGB and BA are attached in Appendix 3, Tables A, B and C.

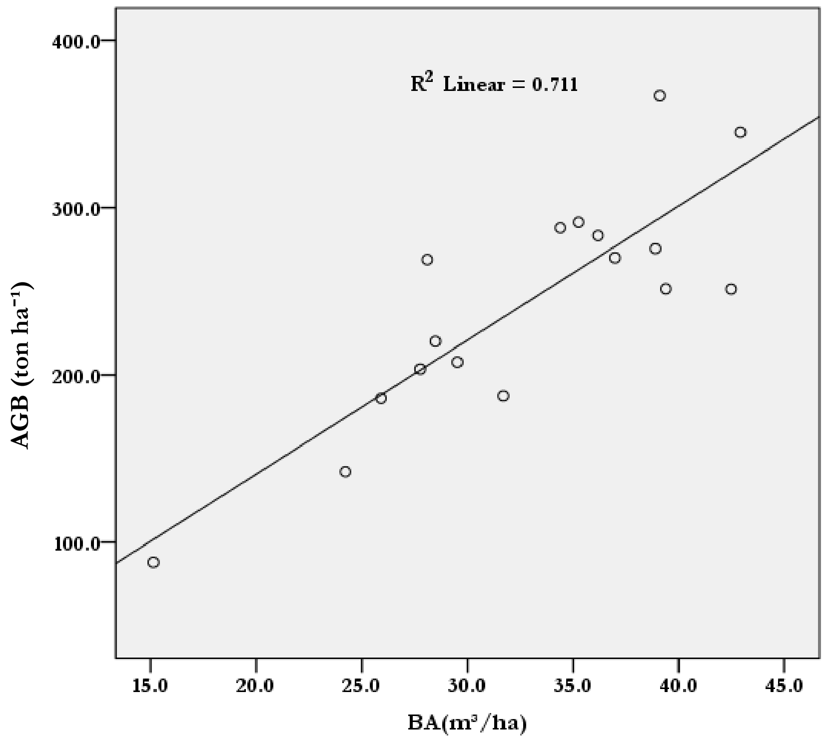

Figure 14: Correlation between AGB and basal area (BA)

Table 11: Correlation between AGB and other forest stand parameters

		Mean DBH (cm)	Mean height(m)	Basal Area (m^3 ha^{-1})
AGB (ton ha^{-1})	Pearson Correlation	0.495*	0.666**	0.843**
	Sig. (2-tailed)	0.044	0.004	2.12138E-05

**. Correlation is significant at the 0.01 level (2-tailed).

*. Correlation is significant at the 0.05 level (2-tailed).

4.4. Regression Analysis of AGB and Palsar-2 backscatter – HH and HV Polarization

Regression analysis was applied to observe the relationship between the HV and HH polarized PALSAR backscatter with aboveground biomass and basal area. Simple linear regression and multi-linear regression was employed.

4.4.1. Developing Regression Model

Linear regression model was used to estimate the AGB with HV polarised backscatter. The summary output of the regression is presented in Table 12 and the graphical representation of the result is shown in Figure 15. The regression result showed a very high R^2 of 0.817 with a standard error of 30.902 tons ha^{-1} of AGB using data from 17 plots. Approximately 82% of the AGB was explained by HV backscatter.

Table 12: Statistics of linear regression of AGB and HV polarized backscatter

Regression Statistics	
Multiple R	0.9038
R Square	0.8169
Adjusted R Square	0.8047
Standard Error	30.9017
Observations	17

	Coefficients	*P-value*
Intercept	672.3961	2.03682E-09
HV	28.0593	6.52608E-07

ANOVA

	df	*SS*	*MS*	*F*	*Significance F*
Regression	1	63917.6536	63917.654	66.935321	6.526E-07
Residual	15	14323.75	954.91667		
Total	16	78241.4037			

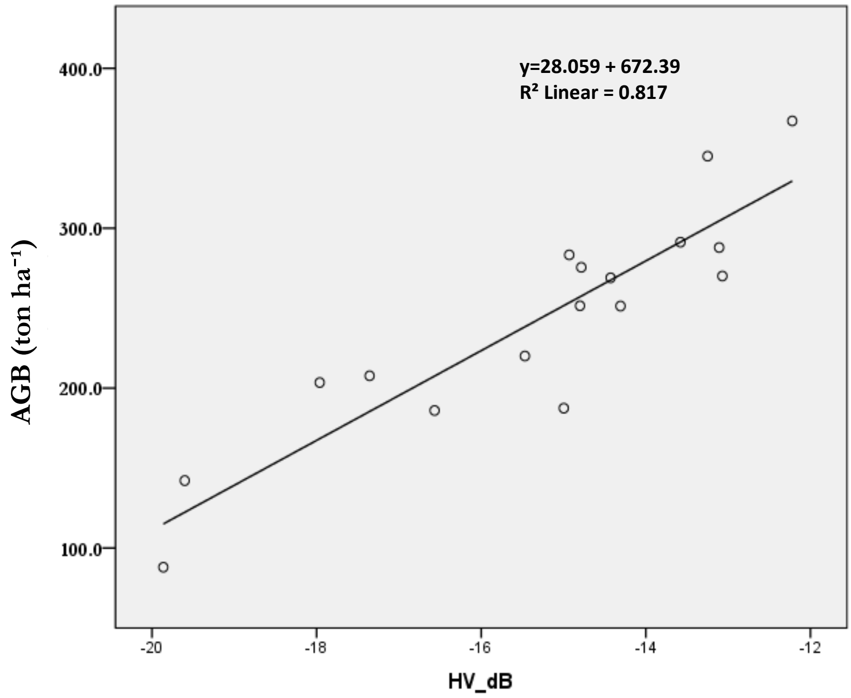

Figure 15: Relationship between AGB and HV backscatter coefficient

A linear regression model was also performed with the HH polarized PALSAR backscatter and the AGB. Nonetheless, the outcome was very weak with R^2 of 0.425 (Figure 16). Ultimately, the model was developed using backscatter retrieved from HV polarization and field measured AGB to model and estimate the AGB of Ayer Hitam Forest Reserve.

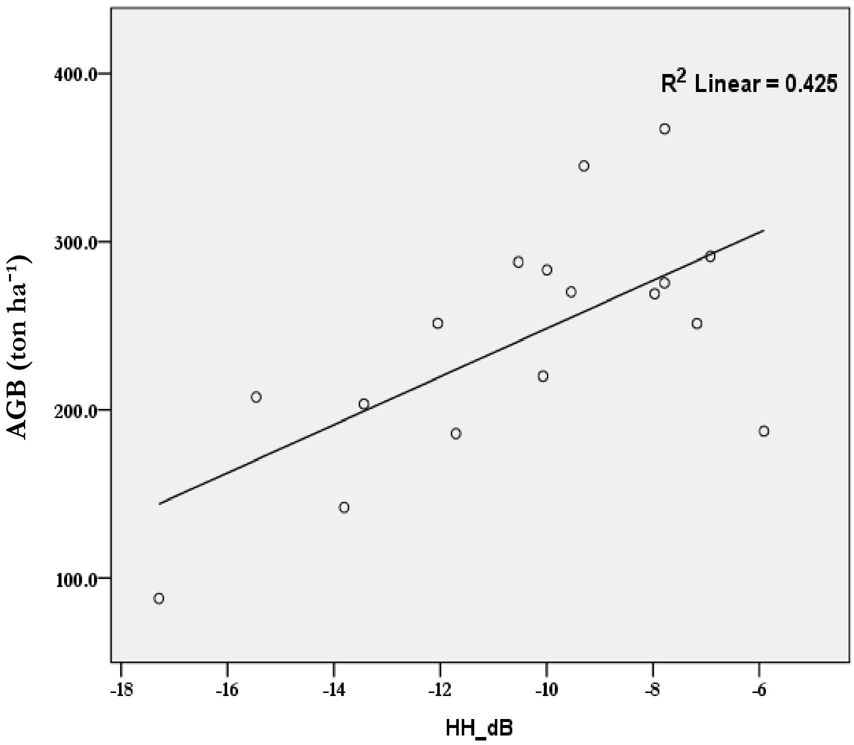

Figure 16: Relationship between AGB and HH backscatter coefficient

4.5. Validating the Model and Accuracy Assessment

4.5.1. Validation data

The 40% of the dataset (10 plots) was used for model validation to measure the predictive accuracy. The validation dataset was independent of the 60% of the dataset (17 plots) used for developing the model. The data for model development and validation are appended in Appendix 1, Table B and C.

4.5.2. Model validation and accuracy assessment

Simple linear regression model was developed from the 60% of the data (17 plots). The correlation between the estimated and observed AGB gave a strong coefficient of determination, R^2 of 0.796. The scatter graph of the estimated and observed AGB is presented in Figure 18. The regression analysis results of model validation are shown in Table 13. Approximately 80% of the observed AGB was explained by the estimated AGB according to this model (Figure 17).

Equation 7: Model Equation

$$Y = \beta_0 + \beta_1 X \Longrightarrow Y = 672.40 + 28.06X$$

Where: Y is the predicted biomass

β_0 is the y intercept which is 672.40

β_1 Is the slope which is 28.06

X is the HV backscatter value

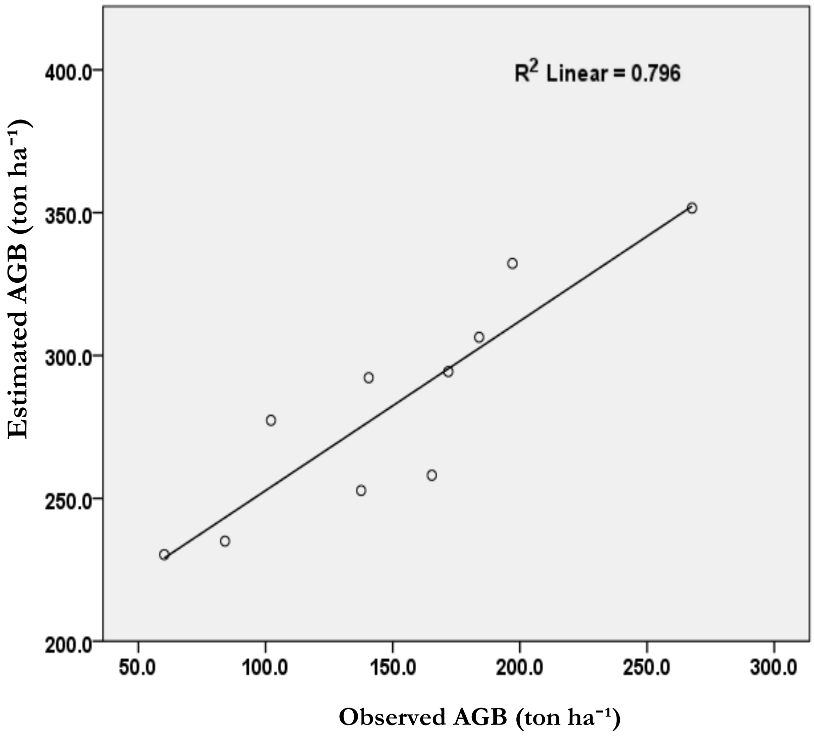

Figure 17: Predicted AGB is plotted against the observed AGB to check model validity

Table 13: Regression analysis of model validation using 10 plots

Regression Statistics					
Multiple R	0.892				
R Square	0.796				
Adjusted R Square	0.771				
Standard Error	19.238				
Observations	10				
	Coefficients	*P-value*			
Intercept	193.394	3.42616E-06			
AGB ton ha⁻¹	0.593	0.000514			
ANOVA					
	df	*SS*	*MS*	*F*	*Significance F*
Regression	1	11578.285	11578.285	31.284	0.000514
Residual	8	2960.866	370.108		
Total	9	14539.151			

The root mean square error (RMSE) was calculated based on the validation data (n=10). The result of the RMSE was very with the value of 135.136. Nevertheless, the simple linear model gave a strong R^2 of 0.82. Such high RMSE is also obtained by Goh et al., 2013 by combining ALOS PALSAR and SPOT 5 images to estimate AGB. He also used 10 plots to validate the regression model. He obtained an RMSE of 150 and 152 ton ha^{-1} and R^2 of 0.46 and 0.47 respectively. Table of RMSE calculation is attached in Appendix 1, Table D.

4.6. Proving the Model with other regression analysis

Besides, multi-linear regression analysis was also performed to test the model. The combination of HH and HV polarized backscatter was used with the observed AGB and the result is presented in Table 14. The regression result shows a R^2 of 0.83 and a standard error of 30.902 ton ha^{-1} at a confidence level of 95%. The regression line plotted against estimated and observed AGB using this model is shown in Figure 18.

Table 14: Result of the multi-linear regression of AGB with combination of HH and HV polarization

Regression Statistics					
Multiple R	0.9106				
R Square	0.8291				
Adjusted R Square	0.8047				
Standard Error	30.9023				
Observations	17				
	Coefficients	*Standard Error*	*t Stat*	*P-value*	
Intercept	699.8140	59.7163	11.7190	1.27E-08	
HV	32.5630	5.6619	5.7512	5.01E-05	
HH	-3.9959	3.9971	-0.9997	0.3344	
ANOVA					
	df	*SS*	*MS*	*F*	*Significance F*
Regression	2	64872.069	32436.035	33.966	4.25316E-06
Residual	14	13369.334	954.952		
Total	16	78241.404			

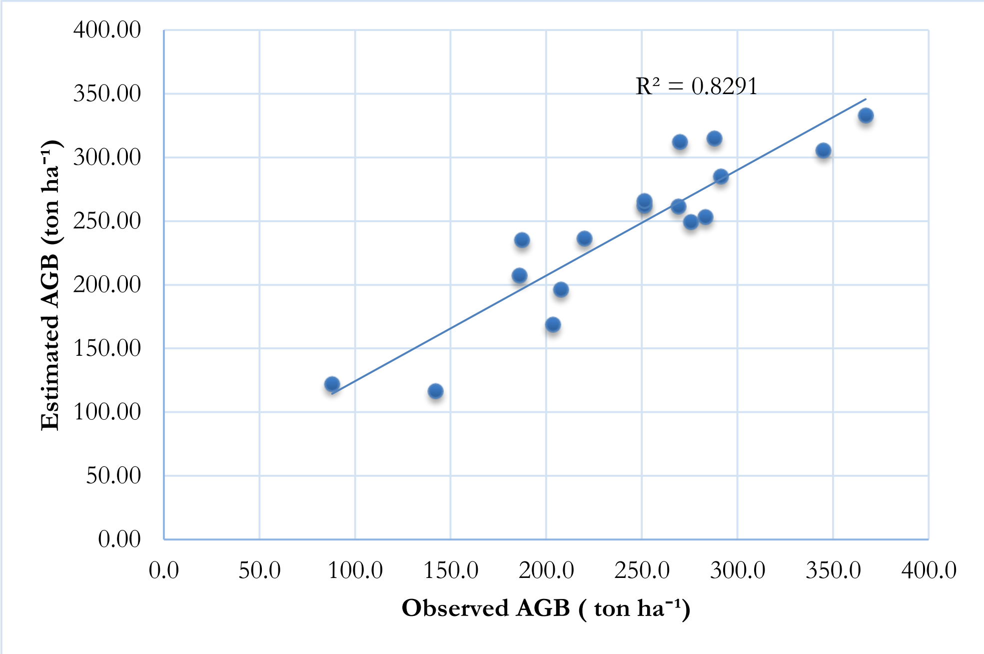

Figure 18: Estimated AGB plotted against observed AGB. Estimated AGB derived from multi-linear regression model developed using AGB and combination of HH and HV.

A regression analysis was formulated by combining stand BA and height with HV. The regression result showed a strong R of 0.863 and R^2 of 0.745 at a significant level of 95% (Table 15). A strong R^2 is obtained in this multi-regression analysis because both BA and height are a function of radar backscatters. Hussin et al., (1991) stated, systems of equations in which these forest stand parameters including AGB can be estimated from radar backscatter directly. This regression analysis supports the validity of the linear regression model used for estimating the AGB of the study area.

Table 15: Multiple regression of HV backscatter coefficient and stand BA and Height

Regression Statistics					
Multiple R	0.8633				
R Square	0.7452				
Adjusted R Square	0.7088				
Standard Error	1.2765				
Observations	17				
	Coefficients	*Standard Error*	*t Stat*	*P-value*	
Intercept	-28.3711	2.4809	-11.4360	1.731E-08	
Mean Height	0.3534	0.1549	2.2816	0.0386778	
BA m^3ha^{-1}	0.2361	0.0446	5.2983	0.0001125	
ANOVA					
	df	*SS*	*MS*	*F*	*Significance F*
Regression	2	66.7180	33.3590	20.473328	6.9712E-05
Residual	14	22.8114	1.6294		
Total	16	89.5294			

Further correlation and regression analysis was done between combination of stand BA and the height, with AGB. Multi-linear regression was performed using these forest parameters. The outcome of the regression result showed a very strong R^2 of 0.974 and the relationship between these forest parameter were very strong (Table 16). AGB correlates very well with BA and height because, AGB is a function of BA and height (Hussin et al., 1991).

Table 16: Regression analysis of AGB and stand BA and height

Regression Statistics					
Multiple R	0.9738				
R Square	0.9482				
Adjusted R Square	0.9409				
Standard Error	17.0071				
Observations	17				
	Coefficients	*Standard Error*	*t Stat*	*P-value*	
Intercept	-234.2207	33.0538	-7.0861	5.45515E-06	
BA m^3ha^{-1}	6.9294	0.5938	11.6691	1.33802E-08	
Mean Height	16.5305	2.0635	8.0111	1.34755E-06	
ANOVA					
	df	*SS*	*MS*	*F*	*Significance F*
Regression	2	74191.988	37095.994	128.253	9.9463E-10
Residual	14	4049.376	289.241		
Total	16	78241.364			

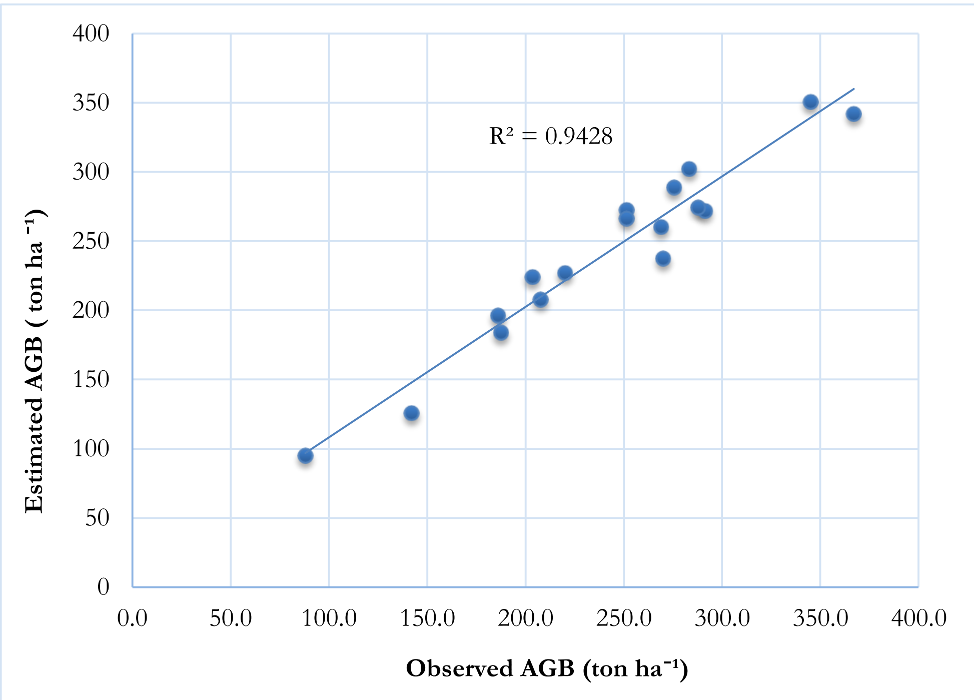

Figure 19: Estimated AGB plotted against observed AGB. Estimated AGB derived from multi-linear regression model developed using AGB and combination of stand BA and height.

.

4.7. Mapping Aboveground biomass and Carbon stock of Ayer Hitam Forest Reserve

Estimation of aboveground biomass for the whole study area was done using Equation 4. An AGB and a carbon stock maps were produced and shown in Figure 20 and 21 respectively. Carbon stock of the study area was calculated based on the conversion factor of 0.5 because about 50% of the forest biomass is stored as carbon (Watson, 2009; Hirata et al., 2012)

Based on the result of the AGB estimation shown on the map. It can be seen that the amount of AGB ranges mostly from 240 tons ha^{-1} to greater than 320 ton ha^{-1}. Areas with AGB less than 80 ton ha^{-1} are those areas close to the boundaries of urban areas. The areas with undulating topography had higher AGB because it is not easily accessible. In addition, biomass is higher in the undulating terrain because of double bounce scattering which is contributed by the tree trunks and branches especially in forests with high biomass that is over 200 ton ha^{-2} (Le Toan et al., 2012). This is true for the present study because according to the AGB estimation map, the estimated biomass in the hilly terrain is 200 ton ha^{-1} and greater as well as in primary forests and undisturbed forests.

Subsequently, the carbon stock map follows a similar pattern of the AGB map because the total amount of forest AGB was dived by 2 (50% of the AGB) to produce it. Consequently, there is a high content of carbon in areas where the amount of AGB is high.

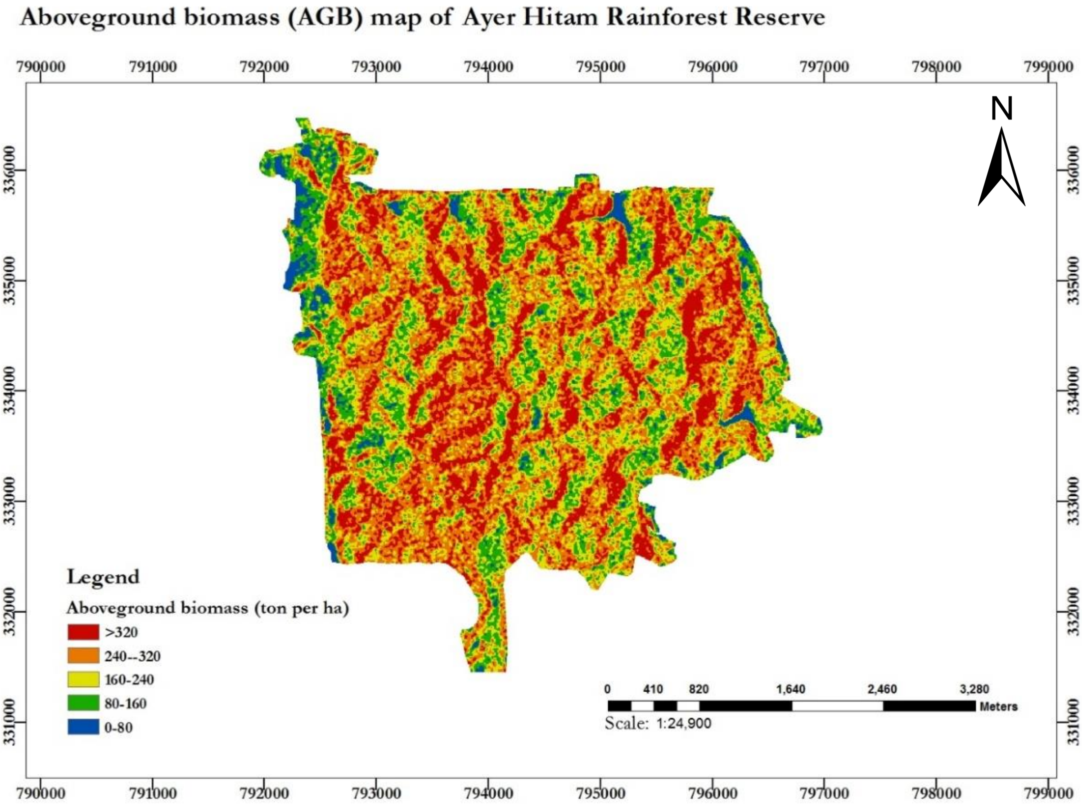

Figure 20: Map of estimated AGB in the study area, AHFR

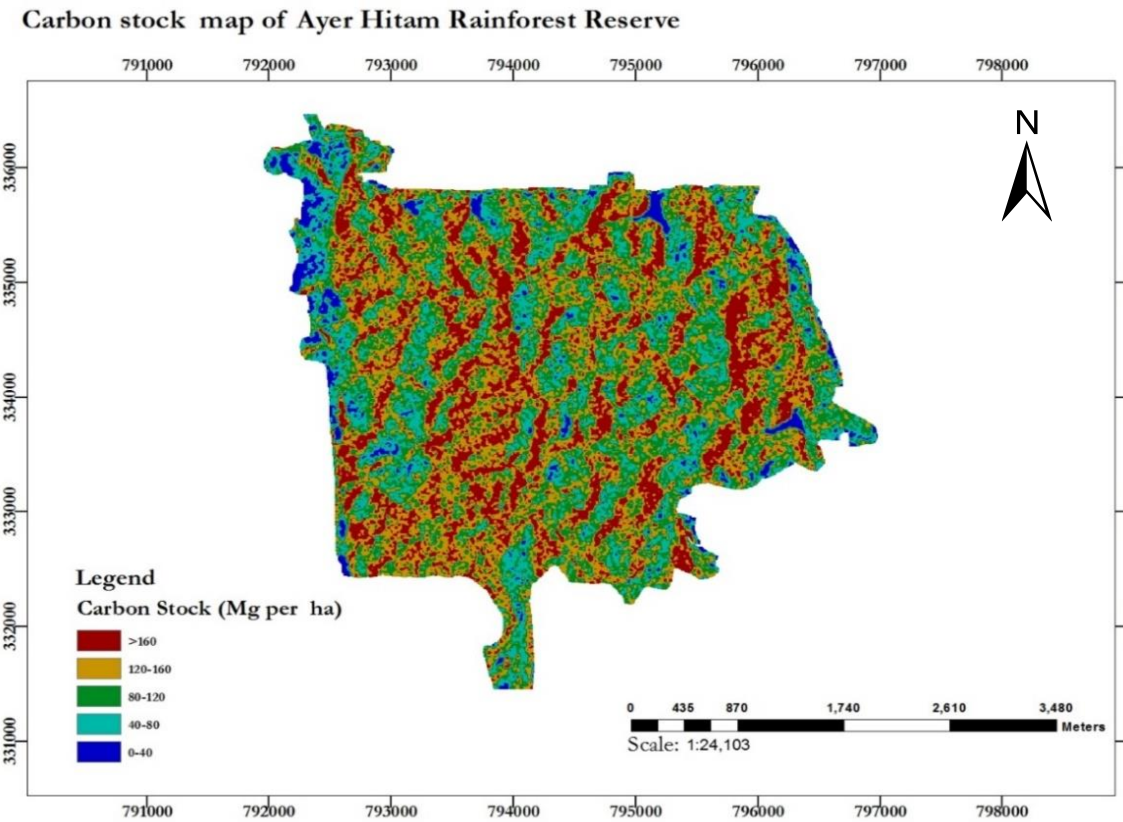

Figure 21: Carbon stock map of Ayer Hitam Forest Reserve

5. DISCUSSION

5.1. Data for Aboveground biomass estimation

It is essential to have reliable AGB values in order to effectively estimate and map AGB and carbon stock of a forest area. Taking into consideration, the calculation of AGB of individual tree, the choice of wood density and also the allometric equation is also important. Appropriate allometric equation suitable for a particular forest type should be used. For example, the Asian tropical forest types are characterised with tall trees and therefore allometric equation developed for tropical forests in other tropical region such as Americas cannot best describe the AGB in Asian forest (Morel et al., 2011). Therefore, an appropriate allometric equation suitable for this forest type (AHFR) is needed to calculate AGB.

The data for estimating AGB were collected from 27 sampled plots in AHFR in October 2015. Diameter at breast height, height, forest canopy cover in percentage and tree species were recorded. AGB was calculated based on improved allometric equation for tropical forests (Chave et al, 2015). This equation is appropriate for application for estimating AGB in tropical forest in Asia including Malaysia. This allometric equation (Equation 1) requires the use of wood density, therefore, default wood density value for Asia (Hirata et al., 2012) was used to calculate the AGB. The default value was used because, all the tree species that were recorded in the field were not identified to the species or genera level. Some of the trees were identified by the common name in Malay and some were identified only to the family level. About 21% of the trees were not identified, therefore, the default wood density was preferred over specific wood density. Since, DBH and height were measured and the wood density was decided with an appropriate allometric equation, the AGB was calculated to be correlated with PALSAR-2, HH and HV polarized backscatter coefficient.

On the other hand, the PALSAR-2, HH and HV polarized data were pre-processed and analysed to retrieve the backscatter coefficient in sigma nought (σ^0). Two approaches were applied to retrieve the backscatters, which is (1) automatically using SNAP software and (2) manually in ArcGIS. Average backscatter coefficient from 9 pixels and mean of means of (4) 9 pixels were calculated. The average values were used to correlate with the AGB and other forest stand parameters. The mean of means backscatter value exhibited a strong correlation with the AGB and it was accepted for further relationship assessment (Table 8).

Consequently, the observed AGB was then related to the HH and HV polarized backscatter coefficient. This correlation is further discussed in section 5.3. AGB was correlated with other forest stand parameters including stand BA, height and DBH. A strong correlation was observed between AGB and the stand BA compared to height and DBH. However, a very strong correlation was observed in a multi-linear correlation between AGB and combination of stand BA and height. Relationship between AGB and other forest stand parameters is discussed in section 5.2.

5.2. Correlation between AGB and Forest Parameters

Aboveground biomass (AGB) of a forest is a function of several forest stand parameters including height, DBH, stand BA and wood density. AGB also relates directly to stand volume (Hussin, 1990). To know AGB of an area, an allometric equation suitable for that particular area must be used. Therefore, in the present study Equation 1 was used. Average height and DBH and total BA per hectare was also calculate to assess their relationship with the AGB.

Pearson's product-moment correlation was used to assess the relationship of AGB with the other forest parameters (Table 11). Correlation of AGB with BA was significant at 99% and 95% confidence level with a very high R^2 of 0.84 and followed by average height with R^2 of 0.66. However, relationship of DBH was weak with R^2 of 0.495 but significant at 95% confidence level. Furthermore, a simple linear regression analysis was formulated to relate AGB to BA (Figure 14). A strong R^2 of 0.71 was observed. In other words, AGB ton ha^{-1} can be described by 71 percent of BA m^3ha^{-1}. Stand BA correlated well to the AGB because BA is known to be the better estimator of AGB (Le Toan et al., 1992).

To further assess the relationship of AGB with height and BA, multi-linear regression analysis was formulated. Combination of height and BA were tested with AGB. The regression showed a very strong R^2 of 0.948 and an r of 0.97 and standard error of 17 ton ha^{-1}. Almost 95 percent of the AGB is explained by height and stand BA. This is not a surprise because AGB correlates strongly with these two parameters individually. Besides, AGB is a function of stand BA and the height (Hussin et al., 1991).

5.3. Correlation between AGB and PALSAR-2 HH and HV polarized backscatter

Field data of 27 plots were used in this study. Seventeen (17) plots were used for developing the model while the other ten (10) plots were used to validate the model. Observed AGB was used to assess its relationship with the PALSAR-2, HH and HV polarised backscatter coefficient separately. Pearson product-moment correlation was used for correlation analysis.

Meanwhile, backscatter from an average of 3 x 3 pixels and mean of mean backscatter (backscatter calculated from 4 of 3 x 3 pixels) were assessed to consider the backscatter value that correlates well with the AGB to run the model. Besides, backscatters retrieved from unfiltered HH and HV polarized data and the backscatter retrieved automatically using SNAP software were also assessed. The mean of mean backscatter coefficient showed a strong correlation with AGB. A very strong relationship was observed between AGB and HV polarized backscatter with an r of 0.904. The relationship was significant at 99% and 95% confidence level. AGB in relation to HH polarized backscatter was moderate with the r of 0.652 at both 99% and 95% confidence level.

Consequently, regression analysis was done to further assess the relationship between the AGB and HH and HV separately. In addition, AGB was also plotted against the HH and HV separately. According to the regression analysis and the scatter plot, HV appeared to have a strong relationship with AGB. HV polarized backscatter had a R^2 of 0.817. This indicates that approximately 82% of the AGB is explained by the HV backscatter. Alternatively, HH backscatter had a weak R^2 of 0.425. Approximately, 43% of AGB was explained by HH backscatter. Several studies including Carreiras et al., 2012; Le Toan et al., 2011 also revealed positive and strong relationship between AGB and HV polarization . A study carried out by Hussin et al., 1991 on estimating biomass of slash pine using the L-band HV polarized data obtained from an aircraft also reported a positive and very strong relationship between HV polarized backscatter and biomass and other forest stand parameters. Mitchard et al., (2009) found stronger relationship exists between AGB and HV backscatter in his study in four different landscapes in Africa.

The strong association between HV polarized backscatter and AGB is because of multiple volume scattering. The forest is characterized by highly dense woody vegetation especially trees and diversity of tree species with a multi-layered structure, therefore HV polarization reflects volume scattering. The PALSAR HV polarization, penetrates through the forest canopy, hence, they react well to forest stand volume and biomass (Basuki et al., 2013). Le Toan et al., (2011) stated that HV is strongly related to AGB because HV backscatter is dominated by volume scattering in the forest canopy. HH polarization is weak because radar signal becomes weak as it penetrates through the forest canopy.

In addition, HH polarisation is dominated with surface scattering and interacts strongly with trunk and stems and the backscatter return to the sensor is low (Le Toan et al., 2011). This results in weak relation with the forest biomass. Furthermore, a weak relationship between the HH polarised radar backscatter and AGB is also due to the complexity and the density of the forest (Carreiras et al., 2012). The HH polarization has been proven to be a poor estimator of AGB (Morel et al., 2011). Morel et al., (2011) further stated that depolarization of the radar signal on the forest canopy results in the reflection of HV backscatter, therefore, HV backscatter is strongly correlates with AGB than HH. Scattering in the forest is generally illustrated in Figure 22.

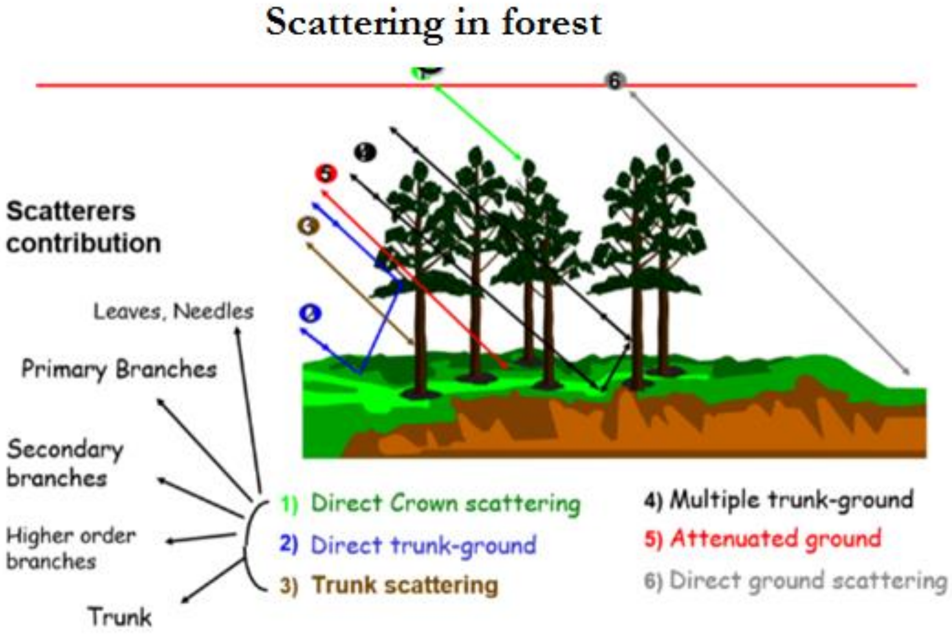

Figure 22: Different types of scattering in the forest. Source: (LeToan, 2005)

On the other hand, combination of HH and HV backscatter and AGB was assessed using multi-linear regression analysis. The analysis showed a promising result with a strong coefficient of determination (R^2) of 0.829. This indicates that, about 82% of the variation of AGB can be described by the regression model developed. The standard error of the multi-linear regression is 30.902 ton ha^{-1}. This standard error (SE) value gives an idea on how much, observed AGB differs from the estimated AGB. However, the ideal equation for modelling was a simple linear regression (Equation 7) because it has a lower RMSE compared to the multi-linear regression. RMSE is further discussed in section 5.6.

5.4. Correlation between PALSAR-2 HV polarized backscatter and forest parameter (DBH, BA, height)

In order to determine the correlation between the PALSAR HH and HV polarisation and the forest stand parameters, data collected from the 17 plots were used. Average DBH, height and total stand basal area (BA) per hectare was correlated with HH and HV polarized backscatter.

The Pearson product –moment correlation was performed between the liked-polarised (HH) and the cross-polarised (HV), and the forest stand parameters. Correlation results indicated that generally the HV polarization had a higher correlation with the forest stand parameter compared to HH polarization.

A positive but very weak relationship between HV polarization and DBH and height measurement was recorded with r of 0.321 and 0.463 respectively (Table 9). There is a weak correlation between DBH and HV polarization because the correlation is made based on unit area, which is on per ha basis. The relationship was not based on DBH of a single tree and HV backscatter, it was based on the average DBH of the forest stand and HV polarized backscatter. Therefore the weak result was obtained. The same can be explained for the relationship between average height and the HV polarized backscatter.

This is confirmed by Zhang et al., 2014, where he also revealed very weak relation between SAR backscatter and forest parameters at stand level. His study was on forest on correlation analysis between ALOS PALSAR and forest parameters based on stand level. He found that correlation of mean height and DBH with HV was very weak with lowest R^2 of 0.0.304 and 0.0.254 respectively. In addition, Iizuka and Tateishi, 2014 correlated average DBH and the average height of *Cryptomeria japonica* (Sugi) with L-band HV backscatter and a low relationship of R^2 of 0.177 for DBH and R^2 of 0.214 for height was observed . Main parameters that contribute to AGB is height and BA, therefore, average stand height alone does not correlate well with HV backscatter but the AGB relates well with HV backscatter.

The weak correlation between HV polarized backscatter and DBH and height is also due to volume scattering because of the dense canopy cover of the forest. The mean canopy cover percentage is approximately 90% in the study area. Due to very high percentage of crown cover, the penetration of the radar L-band signal attenuates to interact with individual trees (Hussin et al., 1992). Figure 23 shows the illustration.

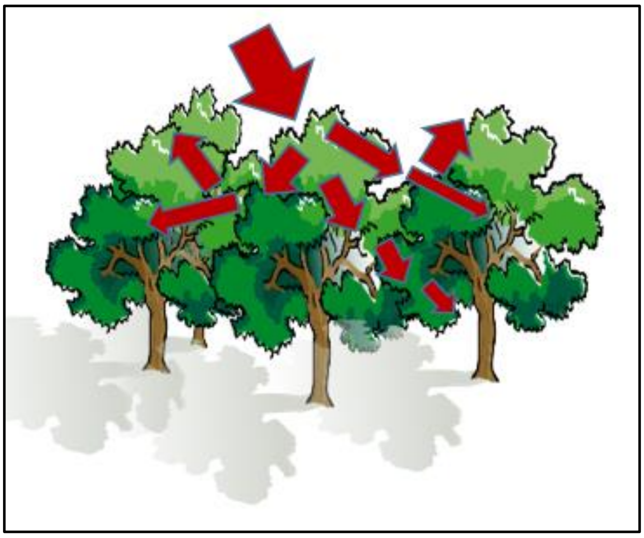

Figure 23: Volume scattering in the dense forest canopy. Backscatter is scattered and absorbed and attenuates in the crown canopy as it penetrates into the canopy to react with other parameters.

The stand basal area (BA) correlated strongly with HV polarization, having r of 0.891 at the confidence level of 95% (Table 9). According to Le Toan et al., (1991), stand BA correlated well with L-band HV polarization having R^2 of 0.91. This indicates that HV associates very well with the basal area rather than DBH and height. HV polarized backscatter relates well with stand BA because BA is the cross section of trees in a stand which is measured at breast height and expressed as per unit area of land (per hectare basis). Moreover, correlation is strong because stand BA is based on per unit area and not on individual tree basis. The simple linear regression (Table 14) analysis was performed between HV and stand BA and a R^2 of 0.671 was obtained. This result shows the close association between BA and HV and is supported by (Hussin et al., 1991).

A study conducted by Le Toan, (1991) showed very strong R^2 of 0.91 from correlating stand BA and L-band HV polarization by relating forest parameter to SAR data, This is because the woody vegetation especially, the branches, stems and the truck of the forest trees contribute mainly to the backscatter. Hussin et al., (1991) observed a strong and positive correlation between L-band HV polarized backscatter and forest stand parameters per ha including, biomass, height, and BA. Besides, radar backscatter can describe the basal area and height using systems of equations that can be used to estimate the forest parameters namely, height, basal area and biomass from the radar backscatter (Figure 23) (Hussin et al., 1992).

Model 1

$$\widehat{BA} = f(RB)$$
$$\hat{H} = f(RB)$$
$$\hat{B} = f(\widehat{BA}, \hat{H}). \qquad \text{[Eq 2]}$$

Figure 24: Basal area (BA) and height (H) as a function of radar backscatter (RB) and biomass (B) as a function of basal area and height (Hussin et al., 1992)

Hussin et al., (1992) revealed strong positive relationship exists with L-band HV radar backscatter and stand parameter including DBH and height according to their study on assessing the effect of polarization on radar backscatter to slash pine stand. Nga, (2010) also observed correlation between the HV and DBH with r of 0.69 in the natural forest of Afram Headwater Forest Reserve in Ghana. She also observed a strong R^2 using multi-linear regression model to test AGB against a combination of HH and HV. Figure 25 shows the regression line of estimated AGB plotted against the observed AGB.

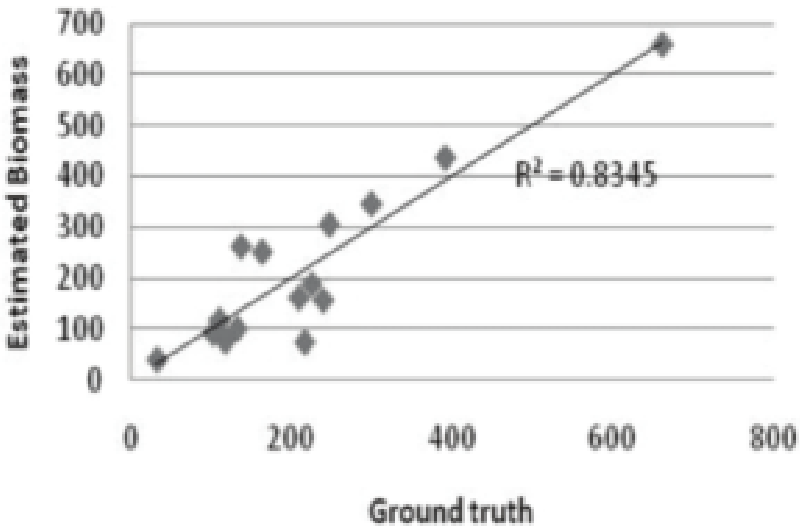

Figure 25: Model adjustment result adopted from (Nga, 2010)

5.5. Regression and Estimation of AGB

Having reliable AGB values is important to effectively produce an AGB and carbon map. Therefore, it is essential to have reliable field data and the appropriate allometric equation for calculating AGB (Morel et al., 2011). The AGB values derived from the measured forest parameters can be used to develop several models to estimate AGB and carbon stock of the study area.

Regression models are often used to describe the relationship between one or more independent (x) variable and a dependent (y) variable. The regression models are normally linear (Equation 9). Non-liner models are also developed and applied in many studies (Snee, 1977). Linear regression model was used in several studies including Goh et al., 2013a; Nizalapur, et al., 2010; Deng et al., 2014; Nga 2010; Morel et al., 2011; Hussin, et al., 1990 to estimate AGB using PALSAR image data. Le Toan et al., (1992) used both linear and non-linear regression in her study.

Equation 8: Multi-linear regression equation

$$E(y) = \beta_0 + \beta_1 X_1 + \beta_2 X_2 + \cdots \beta_P X_P$$

Where β is the coefficient which is estimated from the measured data
E(y) is the predicted y value or dependent variable
X is the independent variable

In this study, a simple linear regression model was developed using the HV polarized backscatter as the independent variable and the measured AGB as the dependent value. Linear regression was used to assume that a relationship between HV backscatter and AGB is represented by a straight line. The outcome of the simple linear regression model showed a very strong R^2. At 95% confidence level, the relationship between AGB and HV polarized backscatter was significant in which almost 82% of HV backscatter can describe the AGB observed from the field. Thus, this model was accepted for estimating the AGB.

5.6. Validation and Accuracy Assessment of Linear Regression Model

Model validation and accuracy assessment is essential to know how well a model can perform. Lu, (2006) reported that, many research that were conducted previously failed to validate and assess the accuracy of their models due to lack of field data collection. Assessing the accuracy of the predicted values and evaluating the performance of the developed model is crucial. The two most often used methods to evaluate the performance of the model are; 1) Assessing the R^2 from either simple linear or multi-linear regression analysis and 2) assessing the RMSE. Generally, low RMSE or a high R^2 specifies the reliability of the model with the field measurement data (Lu, 2006).

The regression model was validated using ten (10) plots. R^2 of the model was 0.817 with an RMSE of 135.14 ton ha^{-1}. The high RMSE was due to lack of appropriate number of sample plots or the ground truth for both model development and model validation. This statement is confirmed by Englhart et al. 2011 stating that a large number of sample plots can improve the accuracy of the regression models for estimating biomass. Nevertheless, the correlation between the estimated and observed AGB gave a strong coefficient of determination (R^2) of 0.796 with standard error of 19.23 ton ha^{-1}. Approximately, 80% of the estimated AGB was explained by the observed AGB. This indicates that this model is reasonable to estimate AGB and carbon stock accurately.

To justify the validity of the regression model, several other linear models were developed to observe the relationship of AGB with other parameters. A multi-linear regression model was developed by combining HH and HV polarized backscatter as the independent variable and measured AGB as the dependent variable (Table 14). The model assessment resulted with a R^2 of 0.829. The accuracy assessment of the estimated value resulted in having RMSE of 138.86.

Similarly, a combination of total stand BA and average height were correlated with HV backscatter. A multi-linear regression analysis returned a high R^2 of 0.745 with a reasonably low standard error of 1.276 ton ha^{-1}. Stand BA and height was tested with HV to assess if the model will give a good fit because both BA and height are a function of AGB (Hussin et al., 1992). Additional multi-linear regression analysis between AGB with combination of height and BA was performed to observe the relationship and model showed a very strong R^2 of 0.948 at 95% significance level. Almost 95 % of AGB is described by height. This is not surprising because AGB can be derived directly from BA and height as long as these two parameters are known (Hussin et al., 1992). All three multi-linear regression gave a strong R^2, therefore, they support the validity of the simple linear regression model.

In line with the high RMSE which resulted from this study, Nga, (2010) also obtained an RMSE of 179 ton ha^{-1} for natural forest and a R^2 of 0.65 using multi-linear regression model in a similar study she conducted in Afram Headwaters Forest in Ghana. Goh et al., (2013a) estimated biomass in the humid tropical forest by combining ALOS PALSAR and SPOT 5 images where he obtained RMSE of 150 and 152 ton ha^{-1} with R^2 of 0.46 and 0.47 respectively. He used 10 plots for validating two multi-linear regression model that he developed. Morel et al., (2011) produced an AGB map with a model that resulted with an R^2 of 0.35 and an RMSE of 125 Mg ha^{-1}. The study was conducted to estimate AGB in Sabah Malaysia using ALOS PALSAR and the total estimated AGB was greater than 450 Mg ha^{-1}. Comparing, the accuracy result of these studies to the present study, it can be seen that, all these three studies had RMSE of over 100 ton ha^{-1} and weak R^2. The present study has a high R^2 of 0.871 despite the large RMSE of 135.136 ton ha^{-1}. Hence, AGB and carbon stock can be map accurately using the regression model.

5.7. Mapping AGB and Carbon Stock

The extrapolation and estimation of AGB were done in ArcGIS using the raster calculator. The HV polarized backscatter raster map was used for mapping the AGB and the carbon map. The raster map has already been calibrated whereby the DN values were converted to backscatter values representing each pixel (Morel et al., 2011). The regression coefficients which was derived from the linear regression analysis was substituted in the linear regression equation in raster calculator. Since the HV backscatter value is the x variable in the equation, the computer automatically calculates and estimates AGB based on per pixel (backscatter) value (Uidaho.edu/nrgis, n.d.). The output is a pixel with AGB values. Hamdan et al., (2015) applied a similar technique whereby distribution of AGB for the whole study was predicated using the model that was developed. The estimated AGB were based on pixel values which were converted to AGB values.

Raster calculator tool in ArcGIS was also used by Marcus et al., (2012) to map AGB, stand volume and stand BA in a Western Brazilian Amazon forest. He obtained average estimated AGB estimated f of 231.6 Mg ha^{-1}. However, he used airborne scanning lidar to estimate the forest AGB and identify low-intensity logging sites. Andersen et al.,(2014) also used raster calculator to map areas with canopy with different canopy heights in his study. Ultimately the estimated AGB was mapped. Afterwards, carbon stock map was calculated and mapped using the conversion factor of 0.5 (Hirata et al., 2012).

5.7.1. Distribution of AGB in the Study Area

Based on the AGB observed from the 27 sample plot, the highest AGB was recorded in Plot 5 and 19 with total AGB of 367.071 ton ha^{-1} and 345.040 ton ha^{-1} respectively. The lowest AGB, which is below 100 ton ha^{-1} was recorded in plots 27, 10 and 1 with 60.170 ton ha^{-1}, 84.040 ton ha^{-1} and 88.003 ton ha^{-1} respectively. Average AGB measured was about 208.793 ton ha^{-1}. About 44.4% of the 27 plots have AGB ranging from 200-300 ton ha^{-1}. The other 37% of the plots had biomass ranging from 100-199 ton ha^{-1}. Summary of the descriptive statistic of all the other parameters based on plots are appended in Appendix 1. Table 17shows the summary of total AGB ton ha $^{-1}$, BA m³ ha^{-1}, mean DBH and mean heights of these plots.

There were similar studies conducted in tropical forests that recorded AGB around the same value as the AGB value obtained in present study. For example, Mermoz et al., (2014) carried out a study on biomass of dense forest related to L-band radar data in several African tropical forests and found AGB ranging from 150-550 ton ha^{-1}, while Goh et al., 2013 reported approximately 360 ton ha^{-1} of AGB his study conducted in Central Nature Reserve in Singapore. Hamdan et al., (2015) obtained AGB of greater than 200 Mg ha^{-1} in Dipterocarp forest in Peninsular Malaysia. He stated that a strong relationship was observed between AGB and the HV polarization with an average AGB of 342 Mg ha^{-1} and AGB ranging from 21 to 578 Mg ha^{-1}. The observed, AGB for the present study ranges from 60.17 – 367.07 ton ha^{-1}, while estimated AGB ranges from 20 - 576.14 which are in line with these studies done in tropical forest using ALOS PALSAR radar image data.

Table 17: Summary of Highest and lowest AGB based on plots

	AGB ton ha^{-1}	Plot ID	No. of trees	Total BA m³ ha^{-1}	Mean DBH (cm)	Mean height (m)
>300	367.071	5	23	39.103	28.35	18.65
	345.04	19	35	42.925	23.69	17.53
<100	88.003	1	18	15.123	21.23	13.32
	84.04	10	25	17.858	19.8	10.73
	60.17	27	17	9.924	18.35	13.29

Based on Table 17 explanation can be made regarding why these plots are having less or more AGB than the other. DBH and height can influence the AGB enormously. A number of trees in a plot can have little influence because DBH and height determine the overall AGB. Plot 19 has less AGB and more BA than plot 5 because the total number of trees found in plot 19 are higher than plot 5. However, it is limited to the diameter class, as more than 50% of the trees in plot 19 are found between DBH class of 10 -20 cm. In plot 5, about 39% of the trees were found in diameter class between 30 and 60>, 22 % in diameter class 20-30 and 39% of the trees fall in DBH class below 20 cm. More than half of the trees in plot 5 have over 20 cm DBH, therefore, contributes to higher mean DBH compared to plot 19. The plot with the lowest AGB has the least value in the total number of trees, total BA, mean DBH and mean height. Despite having low mean height value, plot 10 has high values in other parameters compared to plot 27.

Table 18: AGB estimation in Malaysia (Majid, 2015)

Table 1.0: Aboveground biomass estimations (t ha^{-1}) in Malaysia from 1969-2012.

Region	Area /Types	Total (t ha^{-1})	Source
Peninsular Malaysia	All types (average)	271	Aman and Parlan, 2009
	Undisturbed mix dipterocarp forest	360	Abu Bakar, 2000
	Disturbed forest	230	
Perlis	Mata Ayer Forest Reserve	402.6	Hikmat, 2005
Kedah	Langkawi (mangrove forest)	115.56	Norhayati and Latiff, 2001
	Mt.Mat Chinchang	527.94	Raffae, 2002
Negeri Sembilan	Pasoh Forest Reserve	475	Kato *et al.*, 1978
	Tanjung Tuan	234.20	Mat Salleh *et al.*, 2003
Selangor	Ayer Hitam Forest Reserve	209-222	Ismariah and Fadli, 2007
		355	Lepun 2002
		278	Lim and Tagat, 1983
		83.7-232.4	Kueh and Lim, 1999
	Bangi Forest Reserve	200.6	Norashidah, 1993
	(Logged over forest)	362.32	Lajuni, 1996
Pahang	Cameron Highlands	288	Kira, 1969
	Tasik Chini Forest Reserve	425.43	Norwahidah, 2005
	Taman Negara (Merapoh)	453.14	Norziana, 2003
	Bukit Rengit (Krau)	574	Fakhrul Hatta, 2003
	Perlok	419	Fakhrul Hatta, 2003
	Lesong Virgin Jungle Reserve	955.61	Suhaili , 2004
	Tersang Forest Reserve	383.05	Mohd Ridza, 2004
	Lepar Forest Reserve	399.01	Mohd Ridza, 2004
	Fraser Hill	306.40	Shamsul, 2002
Terengganu	Bukit Bauk Forest Reserve	551.2	Hikmat, 2005
Johor	Mt. West Janing	305.07	Soepadmoe, 1987
	Ulu Endau	210.10	
	Endau- Rompin	167.49	
	Mt. Pulai	320.6	Hikmat, 2005
Sarawak	Lambir Forest Reserve	502	Yamakura *et al.*, 1986
		497	Chave *et al.*, 2008
	Mt.Mulu	280-330	Proctor *et al.*, 1983
Sabah	Ulu Segama	261	Pinard and Putz, 1996
	Deramakot Forest Reserve: Primary Forest	482-522	Seino *et al.*, 2005
	Old Logged Forest	483-596	
	Malua Forest Reserve	323	Saner *et al.*, 2012
	East Coast Sabah	493	Kira, 1969

Majid (2015) included a table (Table 17) which contained a list of areas and forest types in Malaysia with corresponding AGB for those areas. There were four researchers who carried out studies in Ayer Hitam Forest. According to the AGB estimation table, the researchers estimated different amount of AGB in AHFR in different years. The average AGB values obtained were 209-222 ton ha^{1}, 355 ton ha^{-1}, 278 ton ha^{-1} and 83.7-232.4 ton ha^{-1}. The present study has observed the average AGB per hectare be 208. 79 ton ha-1 and average estimated AGB of 257. 98 ton ha-1 which are within the range of 200 -300 ton ha^{-1}.

5.8. Errors and Uncertainties in Research

In most research, errors and uncertainties exist. Therefore, it is important to take into consideration the factors leading to this issue when conducting a research.

5.8.1. Errors and uncertainties associated with field measurement

One of the important factor to take into consideration is the sample size, especially when the purpose of the field data collection will be related to the SAR backscatter Morel et al., (2011). He further, stated that 1 ha plot size appeared to be the most reliable compared to the other plot size. It has proven to show very strong correlation with PALSAR backscatter. Besides, errors related to parameter measurement are more likely to be less because the measurement is taken in a wider scale.

Taking measurement and recording of field measurement is crucial as well. Especially when measuring the height of the trees. Tree height is important for estimating the AGB. The height of one tree can be mistaken for the other tree when the tree crowns overlap each other. Measurement of tree heights depend on the forest condition and the experience of the person taking the measurement. It is often difficult to take an accurate height measurement of a very tall tree specifically in a dense tropical forest (Hunter et al.,2013).

Height measurement is challenging especially in the natural forest because the understory is densely populated with mixed vegetation and tall and closed dense canopy. Hunter et al., (2013) revealed five uncertainties associated with height measurement; 1) offset in height between measured distance and crown-top position, 2) tree top occlusion 3: ground slope 4) obstacles for distance measurement and 5) instrument operator error. Hunter et al.,(2013) explains in detail about these 5 uncertainties in tree height measurement. Measuring tree heights in a tropical forest are laborious and can have a high error associated with it.

Diameter at breast height (DBH) is often the easiest and direct measurement compared to height and errors associated with it (Magalhães et al., 2015). However, it has errors associated with it. DBH measurement errors can arise from reading taken from the dbh tape, recording the reading in the field sheet, inconsistency in point of measurement (1.3 m) which is easily overlooked, tension on the tape after using it for some time and placing of the tape on the tree at point of measurement when taking the measurement (Elzinga, et al., 2001). To minimize the error associated with the point of measurement, a standard stick of 1.3 m was made to be used by different persons. Trees with buttress are a problem, especially in the primary tropical forest. Most often the trees with buttresses are big trees and extend some meters above the ground which makes it difficult for DBH measurement (West, 2009).

5.8.2. Errors and Uncertainties associated with use of Wood Density Value

Use of wood density can also pose errors. Chave et al., (2005) mentioned that use of specific wood density is important because it leads to improvement in models developed for estimating AGB. In this study, a default value of 0.57 recommended for Asia by Hirata et al., 2012 was used because most trees were not identified to the species or genera level in order to use their specific wood density. Ketterings et al., (2001) used mean wood density estimated from a combination of measured and reported wood density data because specific wood density for the trees he used in his study were not obtained. He further recommended that wood density can also be estimated from published data for the tree species occurring at that particular geographical location.

5.8.3. Errors and Uncertainties associated with Radar data Processing

Processing of the radar data is critical. It is important to make sure that the image data and the field data are well registered prior to estimating AGB. Errors can be introduced when applying the different processes such as geo-referencing, filtering, calibration and geometric corrections. Even errors propagate when importing and exporting data from one software to another. All these errors accumulates and eventually results in high RMSE. Errors are also introduced through the acquisition of the image data, techniques involved in data processing, atmospheric corrections until registration of the image data with the field sample plot (Lu, 2006).

6. CONCLUSION

The ALOS -2 PALSAR-2, dual polarization of HH and HV bands and field data collected from 27 plots were used in this study. A correlation analysis between the AGB derived from the field data and the HH and HV polarized backscatter was employed to assess the strength in their relationship. The analysis showed a strong relationship between AGB and the HV polarization. Therefore, HV backscatter and AGB were used to develop the linear regression model to estimate the AGB and carbon stock of AHFR, Based on the results obtained from this research, conclusions were made to address the research questions.

Research Question 1

What is the relationship between AGB and radar backscatter of ALOS-2 PALSAR-2, HH, and HV polarization?

- The result of correlation assessment proved that there was a strong relationship between AGB and liked polarized (HH) backscatter (r=0.652). However, a very strong correlation was observed between the cross-polarized (HV) backscatter (r=0.904). The correlation was significant at 99% and 95% confidence level.

Research Question 2

How can AGB be modelled using PALSAR HH and HV polarizations?

- A simple linear regression analysis was done for the observed AGB and HH and HV polarized backscatter separately. Regression result showed a weak correlation coefficient of determination (R^2 =0.425) for HH but a strong correlation coefficient of determination (R^2 =0.817) for HV polarized backscatter.
- Therefore, HV was chosen for model development. Simple Linear regression model was developed using the AGB and HV polarized backscatter to estimate the AGB.

Research Question 3

What is the accuracy of AGB derived from radar backscatter of ALOS-2 PALSAR, HH and HV polarization?

- The simple linear regression model was validated with 10 independent data sets. The estimated AGB was plotted against the observed AGB and approximately 82% of the estimated AGB was explained by observed AGB.
- Multi-linear regression analysis between observed AGB and combined HH and HV backscatter gave a R^2 of 0.829. This confirms the strong relationship between the AGB and the radar backscatter and the accuracy of the AGB estimation.
- Since AGB is a function of stand BA and height, a multi-linear regression was employed between these two parameters and observed AGB. A very strong R^2 of 0.942 was obtained.
- The RMSE resulted from estimated AGB was 135.136 ton ha $^{-1}$. Even though the RMSE is big, the R^2 was strong. Besides, such a large RMSE is obtained in similar other studies explained in section 5.6.

Research Question 4

What is the AGB of tropical rain forest of Ayer Hitam per unit area in ton/ha derived from field data?

- The minimum and maximum total AGB derived from the field data was 60.17 ton ha^{-1} and 367.07 ton ha^{-1} respectively
- The total AGB for the whole study area of AHFR is 260,574.27tons.and the average AGB derived from the field data was 208.79 ton ha^{-1}. Total carbon stock is 130,287.08 ton and average carbon stock is 104.39 tons ha^{-1}.

Research Question 5

How can biomass and carbon stock derived from radar backscatter of ALOS-2 PALSAR, HH, and VH polarization be mapped?

- Since the R^2 value obtained from the simple linear model was higher, the coefficients obtained from this model was used to estimate the AGB. Carbon stock was calculated from the AGB. Both AGB and carbon stock were mapped using ArcGIS.
- The maps were produced from AGB derived from HV backscatter because HV gave a strong R^2 compared to HH backscatter.
- The total AGB of AHFR derived from HV is 321,966.28 tons and total carbon stock is 160,983.14 tons
- Average AGB derived from HV is 257.98 ton ha^{-1} and average carbon stock is 128.99 ton ha^{-1}.

In conclusion, ALOS-2 PALSAR-2 HH and HV polarization had a positive correlation with AGB, however, HV polarized backscatter had a stronger relationship with AGB compared to HH. The AGB obtained from this study is in line with results from several similar studies conducted in tropical forests. Finally, the AGB and carbon stock can be estimated and accurately mapped for Ayer Hitam Forest Reserve.

7. LIST OF REFERENCES

Ager, T. P. (2011). An introduction to synthetic aperture radar (SAR) imaging. Special issue on ocean remote sensing with SAR. *Oceanography*, *24*(3), 162–173. http://doi.org/10.5670/oceanog.2011.65

Amini and Sumantyo, .S.T.J. (2009). Employing a method on SAR and optical images for forest biomass estimation. Biomass-detetion, production and useage. *IEEE Transactions on Geoscience and Remote Sensing*, *47*(12), 4020–4026. http://doi.org/10.5772/18930

Amini, J., & Sumantyo, J. (2011). SAR and optical images for forest biomass estimation. *Biomass–Detection, Production and Usage*, *47*(12), 4020–4026. http://doi.org/10.5772/18930

Andersen, H., Reutebuch, S. E., Mcgaughey, R. J., Marcus, V. N., & Keller, M. (2014). Monitoring selective logging in Western Amazonia with repeat lidar flights. *Remote Sensing of Environment*, *151*, 157–165. http://doi.org/10.1016/j.rse.2013.08.049

Angelsen, A. (2008). *Moving ahead with REDD. Issues, options and implications* (Vol. 6). Bogor, Indonesia: Center for International Forestry Research. http://doi.org/10.1002/tqem.3310060102

Awang Noor, A., G., Norini, H., Khamurudin, M. N., Ahmad, A., N., &, & Ismariah, A. (2007). Valuing the rain forest: The economic values of selected forest goods and services in Ayer Hitam Forest Reserve, Puchong, Selangor. *Pertanika Journal of Tropical Agricultural Science*, *30*(2), 141–152.

Babu, Y. M. M. (2013). Effect of speckle filtering on SAR high resolution data for image fusion. *International Journal of Engineering and Innovative Technology (IJEIT), ISSN: 2277-3754*, *3*(1).

Basuki, T. M., Skidmore, A. K., Hussin, Y. a., & Van Duren, I. (2013). Estimating tropical forest biomass more accurately by integrating ALOS PALSAR and Landsat-7 ETM+ data. *International Journal of Remote Sensing*, *34*(13), 4871–4888. http://doi.org/10.1080/01431161.2013.777486

Basuki, T. M., van Laake, P. E., Skidmore, A. K., & Hussin, Y. A. (2009). Allometric equations for estimating the above-ground biomass in tropical lowland Dipterocarp forests. *Forest Ecology and Management*, *257*(8), 1684–1694. http://doi.org/10.1016/j.foreco.2009.01.027

Bernstein, L., Bosch, P., Canziani, O., Chen, Z., Christ, R., Davidson, O., Madan, P. (2008). *Climate Change 2007 Synthesis Report . A report of Intergovernmental Panel on Climate Change (IPCC). Intergovernmental Panel on Climate Change*. Geneve, Switzerland. Retrieved from https://www.ipcc.ch/pdf/assessment-report/ar4/syr/ar4_syr_full_report.pdf

Bhattarai, T., Skutsh, M.M., Midmore, D. & Shrestha, H. (2015). Carbon measurement : An overview of forest carbon estimation methods and the role of Geographical Information System and Remote Sensing techniques for REDD + implementation. *Journal of Forest and Livelihood_ResearchGate*, *13*(1). Retrieved from http://www.researchgate.net/publication/280611950

Boudreau, J., Nelson, R., Margolis, H., Beaudoin, A., Guindon, L., & Kimes, D. (2008). Regional aboveground forest biomass using airborne and spaceborne LiDAR in Québec. *Remote Sensing of Environment*, *112*(10), 3876–3890. http://doi.org/10.1016/j.rse.2008.06.003

Brown, S. (1997). *Estimating biomass anb Biomass change of tropical forests : A Primer . (FAO Forestry Paper - 134)*. Illinois, USA: FAO. Retrieved from hhttps://books.google.nl

Buizer, M., Humphreys, D., & de Jong, W. (2014). Climate change and deforestation: The evolution of an intersecting policy domain. *Environmental Science & Policy*, *35*, 1–11. http://doi.org/10.1016/j.envsci.2013.06.001

Carreiras, J. M. B., Melo, J. B., & Vasconcelos, M. J. (2013). Estimating the above-ground biomass in Miombo savanna woodlands (Mozambique, East Africa) using L-band synthetic aperture radar data. *Remote Sensing*, *5*(4), 1524–1548. http://doi.org/10.3390/rs5041524

Carreiras, J.M.B., Vasconcelos, M.J., & Lucas, R. M. (2012). Understanding the relationship between aboveground biomass and ALOS PALSAR data in the forests of Guinea-Bissau (West Africa). *Remote Sensing of Environment*, *121*, 426–442. http://doi.org/10.1016/j.rse.2012.02.012

Chan, Y. K., & Koo, V. C. (2008). An introduction to Synthetic Aperture Radar (SAR). *Progress In Electromagnetics Research B*, *2*, 27–60. http://doi.org/10.2528/PIERB07110101

Chave, J., Andalo, C., Brown, S., Cairns, M. a., Chambers, J. Q., Eamus, D., Yamakura, T. (2005). Tree allometry and improved estimation of carbon stocks and balance in tropical forests. *Oecologia*, *145*(1), 87–99. http://doi.org/10.1007/s00442-005-0100-x

Chave, J. et al, . (2015). Improved allometric models to estimate the aboveground biomass of tropical trees. *Global Change Biology*, *20*, 3177–3190. http://doi.org/10.1111/gcb.12629

Corbera, E., & Schroeder, H. (2011). Governing and implementing REDD+. *Environmental Science and Policy*, *14*(2), 89–99. http://doi.org/10.1016/j.envsci.2010.11.002

Cosslett, C. E. (2014). *On the road to REDD+, The UN-REDD programme's support to REDD+ readiness 2008-2013. UN-REDD Programme,* (Vol. 462). Geneva. Retrieved from http://www.un-redd.org/AboutUN-REDDProgramme/tabid/102613/Default.aspx

Deng, S., Katoh, M., Guan, Q., Yin, N., & Li, M. (2014). Estimating forest aboveground biomass by combining ALOS PALSAR and WorldView-2 data: A case study at Purple Mountain National Park, Nanjing, China. *Remote Sensing*, *6*(9), 7878–7910. http://doi.org/10.3390/rs6097878

Dobson, M. C., Ulaby, F. T., Le Toan, T., Beaudoin, A., Kasischke, E. S., & Christensen, N. (1992). Dependence of radar backscatter on coniferous forest biomass. *IEEE Transactions on Geoscience and Remote Sensing*, *30*(2), 412–415. http://doi.org/10.1109/36.134090

Elzinga, C., Shearer, Raymond., C., & Elzingga, G. (2001). Observer variation in tree diameter. Retrieved from http://www.fs.fed.us/rm/pubs_exp_forests/coram/rmrs_2005_elzinga_c001.pdf

Englhart, S., Keuck, V., & Siegert, F. (2011). Aboveground biomass retrieval in tropical forests — The potential of combined X- and L-band SAR data use. *Remote Sensing of Environment*, *115*(5), 1260–1271. http://doi.org/10.1016/j.rse.2011.01.008

European Space Agency. (n.d.). Sentinel Tool Boxes. Retrieved September 18, 2015, from https://sentinel.esa.int/web/sentinel/toolboxes/sentinel-1

FAO. (2009). The State of the world's forests 2009. *Food and Agriculture Organization of the United Nation*. Rome, Italy: Food and Agriculture Organization. Retrieved from www.fao.org

Frulla, L. a., Milovich, J. a., Karszenbaum, H., & Gagliardini, D. a. (1998). Radiometric corrections and calibration of SAR images. *IEEE Geoscience and Remote Sensing*, *2*(1414), 1147–1149. http://doi.org/10.1109/IGARSS.1998.699700

Ghani, A.N.ABD., Bawon, P., Othman, M.S.HJ., Mohd, R., Mohamed, S., & Hanum, I.F., & Hussin, M. Z. (1999). Direct uses of Ayer Hitam Forest Reserve , Puchong , Selangor. *Tropical Agricultureal Science*, *22*(2), 203–206.

Ghasemi, N., Sahebi, M. R., & Mohammadzadeh, A. (2011). A review on biomass estimation methods using synthetic aperture radar data. *International Journal of Geoinformatics and Geosciences*, *1*(4), 776–788. Retrieved from http://ipublishing.co.in/jggsvol1no12010/EIJGGS2038.pdf

Gibbs, H. K., Brown, S., Niles, J. O., & Foley, J. A. (2007). Monitoring and estimating tropical forest carbon stocks: making REDD a reality. *Environmental Research Letters . IOP Science*, *2*(4), 045023. http://doi.org/10.1088/1748-9326/2/4/045023

Goetz, S. J., Baccini, A., Laporte, N. T., Johns, T., Walker, W., Kellndorfer, J., Sun, M. (2009). Mapping and monitoring carbon stocks with satellite observations: A comparison of methods. *Carbon Balance and Management*, *4*(1), 2. http://doi.org/10.1186/1750-0680-4-2

Goh, J., Miettinen, J., Chia, A., Chew, P., & Liew, S. (2013). Biomass estimation in humid tropical forest using a combination of ALOS PALSAR and Spot 5 satellite imagery. *Asian Journal of Geoinformatics*, *13*.

Hamdan, O., Khali, H. A., & Abd Rahman, K. (2011). Remotely sensed L-band SAR data for tropical forest biomass estimation. *Journal of Tropical Forest Science*, *23*(3), 318–327. Retrieved from <Go to ISI>://WOS:000293812800012

Hamdan, O., Khali, A.H , and Hasmadi, M. I. (2014). L-band ALOS PALSAR for biomass estimation of Matang Mangroves , Malaysia. *Remote Sensing of Environment*. http://doi.org/10.1016/j.rse.2014.04.029

Hamdan, O., Mohd Hasmadi, I., Khali, A.H., Norizah, K., & Zulhaidi, M. H. (2015). L-band saturation level for aboveground biomass of Dipterocarp forests in Peninsular Malaysia. *Journal of Tropical Forest Science*. Retrieved from http://www.researchgate.net/publication/280008588

Hamdan,O.; Mohd, H. I., Khali, A. H. & Helmi, Z. M. S. (2014). Factors affecting L-band ALOS PALSAR backscatter on tropical forest biomass. *Global Journal of Science Frontier Research (D) Agriculture and Verterinary*, *14*(3). Retrieved from http://www.researchgate.net/publication/263337098

Henderson, F. M. and L. A. (1998). *Principles and applications of imaging radar. Manual of remote sensing, Third Edition, Volume 2. American Society fro Photogrammetry and Remote Sensing* (Third, Vol. 2). New York, USA: John Wiley & Sons, Inc. http://doi.org/10.1029/99EO00047

Hirata Y, Takao G, Sato, T., & Toriyama, J. (2012). *REDD+ Cookbook. How to measure and monitor forest carbon*. Tsukuba, Japan: REDD Research and Development Center, Forestry and Forest Products Research Institute Japan 156pp. ISBN 978-4-905304-15-9 A. Retrieved from http://theredddesk.org/resources/redd-plus-cookbook-how-measure-and-monitor-forest-carbon

Houghton, R. a. (2003). Why are estimates of the terrestrial carbon balance so different? *Global Change Biology*, *9*(4), 500–509. http://doi.org/10.1046/j.1365-2486.2003.00620.x

Houghton, R. A., Hall, F. &, & Goetz, S. J. (2009). Importance of biomass in the global carbon cycle. *Journal of Geophysical Research: Biogeosciences*, *114*(3), 1–13. http://doi.org/10.1029/2009JG000935

Hunter, M. O., Keller, M., Victoria, D., & Morton, D. C. (2013). Tree height and tropical forest biomass estimation. *Biogeosciences*, *10*(12), 8385–8399. http://doi.org/10.5194/bg-10-8385-2013

Hussin, Y. A. (1990). The effect of polarization and incidence angle on radar backscatter from forest cover. In *PhD Dissertation*. Colorado State University.

Hussin, Y. A., Reich, R. M. &, & Hoffer, R. M. (1991). Estimating slash pine biomass using radar backscatter. *IEEE Transactions on Geoscience and Remote Sensing*, *29*(3), 427–431. Retrieved from http://ieeexplore.ieee.org/stamp/stamp.jsp?arnumber=79433

Hussin, Y. A., Reich, R. M., & Hoffer, R. M. (1992). Effect of polarization on radar backscatter in relation to Slash Pine stand biomass using aircraft and SIR-B data. *ISPRS Journal of Photogrammetry and Remote Sensing*, *29*, 661–667.

Iizuka, K., & Tateishi, R. (2014). Simple relationship analysis between L-band backscattering intensity and the stand characteristics of Sugi (Cryptomeria japonica) and Hinoki (Chamaecyparis obtusa) Trees. *Advances in Remote Sensing*, (December), 219–234. http://doi.org/http://dx.doi.org/10.4236/ars.2014.34015

IPCC. (2001). Climate change 2001: The scientific basis. *Contributing to working group1 to the third assessment report of Intergovernmental Panel on Climate Change.* New York, USA. Retrieved from http://www.ipcc.ch/

IPCC. (2006). 2006 IPCC Guidelines for national greenhouse gas inventories. Agriculture, forestry and other land use. In *Forestry* (Vol. 4, pp. 1–29). http://doi.org/10.1016/j.phrs.2011.03.002

JAXA. (n.d.). ALOS research and application project; Polametric observation by PALSAR. Retrieved January 14, 2016, from http://www.eorc.jaxa.jp/ALOS/en/img_up/pal_polarization.htm

Joshi, N., Mitchard, E., Schumacher, J., Johannsen, V., Saatchi, S., & Fensholt, R. (2015). L-band SAR backscatter related to forest cover, height and aboveground biomass at multiple spatial scales across Denmark. *Remote Sensing*, *7*(4), 4442–4472. http://doi.org/10.3390/rs70404442

Joshi, N., Mitchard, E. T., Woo, N., Torres, J., Moll-Rocek, J., Ehammer, A., Fensholt, R. (2015). Mapping dynamics of deforestation and forest degradation in tropical forests using radar satellite data. *Environmental Research Letters*, *10*(3), 034014. http://doi.org/10.1088/1748-9326/10/3/034014

Jusoff, K. and Hasmadi, I. . (2015). Ayer Hitam Forest Reserve from space using satellite remote sensing. *Tropical Agricultureal Science*, *22*(2). Retrieved from http://www.researchgate.net/publication/279194668

Karna, Y. K., Hussin, Y. A., Gilani, H., Bronsveld, M. C., Murthy, M., Qamer, F. M., … Bhattarai, T. (2013). Integration of WorldView-2 and airborne LiDAR data for tree species level carbon stock mapping in Khayar Khola watershed, Nepal. *ISPRS Journal of Photogrammetry and Remote Sensing*, *In Review*, 280–291. http://doi.org/10.1016/j.jag.2015.01.011

Ketterings, Q. M., Coe, R., Noordwijk, M. Van, Ambagau, Y., & Palm, C. A. (2001). Reducing uncertainty in the use of allometric biomass equations for predicting above-ground tree biomass in mixed secondary forests. *Forest Ecology and Management*, *146*, 199–209.

Kim, C. (2012). Quantataive analysis of relationship between Alos Palsar backscatter and forest stand volume. *Journal of Marine Science and Technology*, *20*(6), 624–628. http://doi.org/10.6119/JMST-012-0402-1

Kiyono, Y., Saito, S., Takahashi, T., Toriyama, J., Awaya, Y., Asai, H., Matsumoto, M. (2011). Practicalities of non-destructive methodologies in monitoring anthropogenic greenhouse gas emissions from tropical forests under the influence of human intervention. *Japan Agricultural Research Quarterly*, *45*(2), 233–242. http://doi.org/10.6090/jarq.45.233

Kumar, S., Pandey, U., Kushwaha, S. P., Chatterjee, R. S., & Bijker, W. (2012). Aboveground biomass estimation of tropical forest from Envisat advanced Synthetic Aperture Radar data using modeling approach. *Journal of Applied Remote Sensing*, *6*(1), 063588. http://doi.org/10.1117/1.JRS.6.063588

Le Toan, T., Beaudoin, A., Riom, J., & Guyon, D. (1992). Relating forest parameters to SAR data. *IEEE Geoscience and Remote Sensing*, *30*(2), 403–411. http://doi.org/10.1109/IGARSS.1991.579979

Le Toan, T., Quegan, S., Davidson, M. W. J., Balzter, H., Paillou, P., Papathanassiou, K., Ulander, L. (2011). The biomass mission: Mapping global forest biomass to better understand the terrestrial carbon cycle. *Remote Sensing of Environment*, *115*(11), 2850–2860. http://doi.org/10.1016/j.rse.2011.03.020

Le Toan, T., Quegan, S., Woodward, I., Lomas, M., Delbart, N., & Picard, G. (2004). Relating radar remote sensing of biomass to modelling of forest carbon budgets. *Climatic Change*, *67*(2-3), 379–402. http://doi.org/10.1007/s10584-004-3155-5

Le Toan, T., Villard, L., Lasne, Y., Mermoz, S., & Koleck, T. (2012). Assessment of tropical forest biomass: A challenging objective for the biomass mission. *International Geoscience and Remote Sensing Symposium (IGARSS)*, 7581–7584. http://doi.org/10.1109/IGARSS.2012.6351873

LeToan, T. Le. (2005). SAR image information content Scattering physics Active system : day and night operations. Retrieved January 21, 2016, from (http://earth.eo.esa.int/dragon/LeToan1_SAR_scattering_physics.pdf)

Lu, D. (2006). The potential and challenge of remote sensing-based biomass estimation. *International Journal of Remote Sensing*, *27*(7), 1297–1328. http://doi.org/10.1080/01431160500486732

Lu, D., Chen, Q., Wang, G., Moran, E., Batistella, M., Zhang, M., … Saah, D. (2012). Aboveground forest biomass estimation with Landsat and LiDAR data and uncertainty analysis of the estimates. *International Journal of Forestry Research*, *2012*(1), 1–16. http://doi.org/10.1155/2012/436537

Magalhães, T. M., Seifert, T., Florestal, D. D. E., & Mondlane, U. E. (2015). Estimation of Tree Biomass , Carbon Stocks , and Error Propagation in Mecrusse Woodlands. *Open Journal of Forestry*, (April), 471–488. http://doi.org/http://dx.doi.org/10.4236/ojf.2015.54041

Maitra, S., Gartley, M. G., & Kerekes, J. P. (2012). Relation between degree of polarization and Pauli color coded image to characterize scattering mechanisms. In *SPIE Asia Pacific Remote Sensing* (Vol. 8364, p. 83640F–83640F–9). http://doi.org/10.1117/12.918486

Majid, A. S. and N. A. A. (2015). Aboveground biomass and carbon stock estimation in logged-over lowland tropical forest in Malaysia. *International Journal of Agriculture, Forestry and Plantation*, *1*(1978), 1–14.

Marcus, V. N., Reutebuch, S. E., & Andersen, H. (2012). Estimating forest biomass and identifying low-intensity logging areas using airborne scanning lidar in Antimary State Forest , Acre State , Western Brazilian Amazon. *Remote Sensing of Environment*, *124*, 479–491.

Mermoz, S., Rejou-M'echain2, M., Villard, L., Le Toan, T., Rossi, V., Gourlet-Fleury, S. (2014). Biomass of dense forests related to L-band SAR backscatter. *IEEE Geoscience and Remote Sensing*, (May). http://doi.org/10.1109/IGARSS.2014.6946605

Michelakis, D., Stuart, N., Lopez, G., Linares, V., & Woodhouse, I. (2014). Local-scale mapping of biomass in tropical lowland Pine savannas using ALOS PALSAR. *Forests*, *5*(9), 2377–2399. http://doi.org/10.3390/f5092377

Missourie education. (n.d.). Natural Resources Biometric -Basal Area. Retrieved January 6, 2016, from http://oak.snr.missouri.edu/nr3110/topics/basalarea.php

Mitchard, E. T. a, Saatchi, S. S., Woodhouse, I. H., Nangendo, G., Ribeiro, N. S., Williams, M., … Meir, P. (2009). Using satellite radar backscatter to predict above-ground woody biomass: A consistent relationship across four different African landscapes. *Geophysical Research Letters*, *36*(23), 1–6. http://doi.org/10.1029/2009GL040692

Mitchard, E. T. A., Saatchi, S. S., White, L. J. T., Abernethy, K. A., Jeffery, K. J., Lewis, S. L., … Meir, P. (2012). Mapping tropical forest biomass with radar and spaceborne lidar in Lopé National Park, Gabon: Overcoming problems of high biomass and persistent cloud. *Biogeosciences*, *9*(1), 179–191. http://doi.org/10.5194/bg-9-179-2012

Morel, A. C., Saatchi, S. S., Malhi, Y., Berry, N. J., Banin, L., Burslem, D., … Ong, R. C. (2011). Estimating aboveground biomass in forest and oil palm plantation in Sabah, Malaysian Borneo using ALOS PALSAR data. *Forest Ecology and Management*, *262*(9), 1786–1798. http://doi.org/10.1016/j.foreco.2011.07.008

Næsset, E., Gobakken, T., Solberg, S., Gregoire, T. G., Nelson, R., Ståhl, G., & Weydahl, D. (2011). Model-assisted regional forest biomass estimation using LiDAR and InSAR as auxiliary data: A case study from a boreal forest area. *Remote Sensing of Environment*, *115*(12), 3599–3614. http://doi.org/10.1016/j.rse.2011.08.021

National Academy of Sciences. (2015). *A strategy for active remote sensing amid increased demand for radio spectrum*. Washington, D.C. Retrieved from http://www.nap.edu/catalog.php?record_id=21729

Nga, T. N. (2010). Estimation and mapping of aboveground bioomass for the assessment and mapping of carbon stocks in tropical forest using SAR data - a case study in Afram Headwaters Forest, Ghana. In *MSc Thesis*. ITC-University of Twente, Enschede, The Netherlands. Retrieved from http://www.itc.nl/library/papers_2010/msc/nrm/nga.pdf

Nizalapur, V., Jha, C. S., & Madugundu, R. (2010). Estimation of above ground biomass in Indian tropical forested area using multi - frequency DLR-ESAR data. *International Journal of Geomatics and Geosciences*, *1*(2), 167–178.

Nurul-Shida, S., Faridah-Hanum, I., Razali, W. W. M., & Kamziha, K. (2014). Community structure of trees in Ayer Hitam forest reserve, Puchong, Selangor,Malaysia. *Malaysian Forester -*, *77*(1). Retrieved from http://www.researchgate.net/publication/270106458

Okuda, T., Suzuki, M., Numata, S., Yoshida, K., Nishimura, S., Adachi, N., Hashim, M. (2004). Estimation of aboveground biomass in logged and primary lowland rainforests using 3-D photogrammetric analysis. *Forest Ecology and Management*, *203*(1-3), 63–75. http://doi.org/10.1016/j.foreco.2004.07.056

Otukei, J. R., & Emanuel, M. (2015). Estimation and mapping of above ground biomass and carbon of Bwindi impenetrable National Park using ALOS PALSAR data. *South African Journal of Geomatics*, *4*(1), 1–13. http://doi.org/: http://dx.doi.org/10.4314/sajg.v4i1.1

Pan, Y. (2011). A Large and persistent carbon sink in the world's forests. *Science AAAS*, *333*(988). http://doi.org/10.1126/science.1201609

PASCO Coperation. (n.d.). ALOS-2,ALOS (Advanced Land Observing Satellite "Daichi") data. Retrieved September 17, 2015, from http://en.alos-phttp//en.alos-pasco.com/. Date Retrieved :17/09/2015

Pons, D. H. (2010). Remote sensing technologies for forest monitoring and carbon stocks estimations. *Aulavirtual.Ig.Conae.Gov.Ar*. Retrieved from http://aulavirtual.ig.conae.gov.ar/moodle/pluginfile.php/513/mod_page/content/38/Diego_Pons.pdf

Quinn, G. P., & Keough, M. J. (2002). *Experimental design and data analysis for Biologists*. New York, USA: Cambridge University Press. http://doi.org/10.1017/CBO9780511806384

Rosenqvist, A., Shimada, M., Ito, N., & Watanabe, M. (2007). ALOS PALSAR: A pathfinder mission for global-scale monitoring of the environment. *IEEE Transactions on Geoscience and Remote Sensing*, *45*(11), 3307–3316. http://doi.org/10.1109/TGRS.2007.901027

Sandberg, G., Ulander, L. M. H., Fransson, J. E. S., Holmgren, J., & Le Toan, T. (2011). L- and P-band backscatter intensity for biomass retrieval in hemiboreal forest. *Remote Sensing of Environment*, *115*(11), 2874–2886. http://doi.org/10.1016/j.rse.2010.03.018

Santoro, M., Askne, J., Smith, G., & Fransson, J. E. S. (2002). Stem volume retrieval in boreal forests from ERS-1 / 2 interferometry. *Remote Sensing of Environment*, *81*, 19–35.

Sessa, R. (2009). Biomass: T12 Assessment of status of the development for the terestrial essential climate variables. *Global Terrestrial Observing System (GTOS) Essential Climate Variable Reports*. Rome, Italy. Retrieved from http://www.fao.org/docrep/012/i1238e/i1238e00.htm

Shimada, M. (2009). Advance Land Observation Satelite (ALOS) and its follow-on satellite,ALOS-2. *Japan Aerospace Exploration Agency*. Retrieved from http://www.researchgate.net/publication/237516352

Shimada, M., Isoguchi, O., Tadono, T., & Isono, K. (2009). PALSAR radiometric and geometric calibration. *IEEE Transactions on Geoscience and Remote Sensing*, *47*(12), 3915–3932. http://doi.org/10.1109/TGRS.2009.2023909

Sinha, S., Jeganathan, C., Sharma, L. K., & Nathawat, M. S. (2015). A review of radar remote sensing for biomass estimation. *International Journal of Environmental Science and Technology*, 1779–1792. http://doi.org/10.1007/s13762-015-0750-0

Smith, R. B. (2012). Interpreting digital radar images. *Introduction to Interpreting Digital Radar Images*. Lincoln,Nebraska: MicroImages,Inc. Retrieved from http://www.microimages.com/documentation/Tutorials/radar.pdf

Snee, R. D. (1977). Validation of regression models: Methods and examples. *Technometrics*, *19*(4), 415–428. http://doi.org/10.2307/1267881

Song, B., Chen, J., Desander, P. V., Reed, D. D., Bradshaw, G. A., & Franklin, J. F. (1997). Modeling canopy structure and heterogeneity across scales: From crowns to canopy. *Forest Ecology and Management*, *96*(3), 217–229. http://doi.org/10.1016/S0378-1127(97)00021-2

Stehman, S. V. (1999). Basic probability sampling designs for thematic map accuracy assessment. *International Journal of Remote Sensing*, *20*(12), 2423–2441. http://doi.org/10.1080/014311699212100

Stein, A. . F. van M. and B. G. (2002). *Spatial Statistics For Remote Sensing. Remote sensing and digital image processing.* Dordrecht, The Netherlands: Kluwer Academic Publishers. Retrieved from https://books.google.nl

Sukhdev, P., Prabhu, R., Kumar, P., Bassi, A., Patwa-Shah, W., Enters, T., Labbate, G., & Greenwalt, J. (2012). *UN-REDD Programme Policy Brief. REDD+and green economy:Oportunity for a mutually supportive relation.* Geneva, Switzerland. Retrieved from http://theredddesk.org/sites/default/files/resources/pdf/2012/unep_policy_brief.pdf

Sun, G., Ranson, K. J., Guo, Z., Zhang, Z., Montesano, P., & Kimes, D. (2011). Forest biomass mapping from lidar and radar synergies. *Remote Sensing of Environment*, *115*(11), 2906–2916. http://doi.org/10.1016/j.rse.2011.03.021

Tanase, M. a., Panciera, R., Lowell, K., Aponte, C., Hacker, J. M., & Walker, J. P. (2014). Forest biomass estimation at high spatial resolution: Radar versus lidar sensors. *IEEE Geoscience and Remote Sensing Letters*, *11*(3), 711–715. http://doi.org/10.1109/LGRS.2013.2276947

Thapa, R. B., Watanabe, M., Motohka, T., & Shimada, M. (2015). Potential of high-resolution ALOS–PALSAR mosaic texture for aboveground forest carbon tracking in tropical region. *Remote Sensing of Environment*, *160*, 122–133. http://doi.org/10.1016/j.rse.2015.01.007

Uidaho.edu/nrgis. (n.d.). Lesson 7: Raster models in GIS-raster regression models. Retrieved from http://www.webpages.uidaho.edu/nrgis/secure/pdf_slides/lesson7.pdf: Date retrieved: 2015-02-04

van Laar, A. and Akça, A. (2007). *Forest Mensuration*. (M. von Gadow, K., Pukkala, T., & Tomé & Instituto, Eds.)*Managing Forest Ecosystem* (Vol. 13). Dordrect, The Netherlands: Springer. http://doi.org/10.1126/science.24.624.760

Watson, C. (2009). Forest carbon accounting: Overview and principles. CDM capacity development in Eastern and Southern Africa. *UNDP, UNEP, UNEP RISQ Center, Energy , Climate and sustainable development*. UK. Retrieved from http://www.cabdirect.org/abstracts/20103082947.html

Wenger, K. F. (1984). Section 7: Timber inventory. In *Forestry Handbook* (Second). New York: John Wiley & Sons. Retrieved from https://books.google.nl/books?isbn=0471062278; Date retrieved:15/08/2015

West, P. W. (2009). *Tree and Forest Measurement*. *Springer* (3rd ed.). Lismore, Australia: School of Environment, Science and Engineering. http://doi.org/10.1007/978-3-319-14708-6

You, S. (2011). Assessing sampling plot shape and size on measures of tropical forest diversity: A simulation study. California, USA: Berkeley, College of Natural Resources. Retrieved from https://scholar.google.nl/scholar?q=Assessing+sampling+plot+shape+and+size+on+measures+of+tropical+forest+diversity:

Zhang, W., Ieee, D. G. G. F., Richardson, A., Chen, E., & Li, Z. (2014). Forest stand level correlation analysis of ALOS-1 PALSAR Signatures provided by the Xunke Forestry Department . A survey. *IEEE Geoscience and Remote Sensing*, 2332–2335.

Zhu, L., Errving, A., Koistinen, K., Nuikka, M., Junnilainen, H., Heiska, N., & Haggrén, H. (2007). Georeferencing multi-temporal and multi-scale imagery in photogrammetry. *ISPRS - International Archives of the Photogrammetry, Remote Sensing and Spatial Information Sciences*, (July), 225–230. Retrieved from http://www.isprs.org/congresses/beijing2008/proceedings/5_pdf/40.pdf; Date retrieved:12/09/2015

8. APPENDIX

Appendix 1: Results of Data Analysis

Table A: Summary of forest parameters based on per plot

Plot ID	Tot Tree /plot	Mean DBH	Mean height	Total AGB/plot	Total AGB (ton)/ha	Carbon stock Mg C	Total BA/plot	BA(m^3/ha)	Mean CC(%)
1	18	21.23	13.62	4.40	88.00	44.00	0.76	15.13	90
2	33	20.24	14.08	8.59	171.85	85.92	1.36	27.15	95
3	29	24.93	16.72	14.17	283.33	141.67	1.81	36.17	90
4	29	23.93	14.26	9.85	197.06	98.53	1.59	31.83	80
5	23	28.35	18.65	18.35	367.07	183.54	1.96	39.10	85
6	31	20.32	15.26	9.30	186.03	93.01	1.30	25.90	90
7	29	20.59	12.90	7.03	140.56	70.28	1.15	22.98	90
9	31	22.65	11.95	9.37	187.47	93.73	1.58	31.70	90
10	25	19.80	10.76	4.20	84.04	42.02	0.89	17.86	90
11	29	22.52	11.90	8.27	165.38	82.69	1.39	27.83	90
13	25	21.16	11.58	7.11	142.17	71.09	1.21	24.22	90
14	35	19.34	14.86	9.20	183.95	91.97	1.31	26.23	95
17	36	16.86	12.71	5.11	102.12	51.06	0.91	18.12	85
18	37	22.97	12.81	12.57	251.34	125.67	2.12	42.48	90
19	35	23.69	17.51	17.25	345.04	172.52	2.15	42.93	80
20	24	24.04	15.58	11.00	220.08	110.04	1.42	28.48	90
21	45	20.69	13.78	12.57	251.50	125.75	1.97	39.39	85
22	41	21.20	15.93	14.56	291.29	145.64	1.76	35.25	80
23	31	23.16	16.45	14.40	287.91	143.96	1.72	34.39	70
24	26	26.62	15.38	13.78	275.52	137.76	1.94	38.90	85
25	25	23.68	14.42	10.38	207.69	103.84	1.48	29.52	80
26	28	20.25	12.21	6.88	137.56	68.78	1.15	22.91	80
27	17	18.35	13.29	3.01	60.17	30.08	0.50	9.92	90
28	17	28.18	18.32	13.45	269.00	134.50	1.40	28.10	90
29	29	23.48	13.00	13.50	270.10	135.05	1.85	36.98	80
30	30	22.03	13.90	13.38	267.67	133.83	1.73	34.52	90
32	20	26.95	16.20	10.18	203.52	101.76	1.39	27.76	90

Table B: Data used for Model development

Plot ID	HV-Filt (4,3x3) M	AGB (ton $^{-1}$ha)	BA(m^3/ha^{-1})	Mean height	Mean DBH
1	-20	88	15.13	13.62	21.23
3	-15	283.33	36.17	16.72	24.93
5	-12	367.07	39.1	18.65	28.35
6	-17	186.03	25.9	15.26	20.32
9	-15	187.47	31.7	11.95	22.65
13	-20	142.17	24.22	11.58	21.16
18	-14	251.34	42.48	12.81	22.97
19	-13	345.04	42.93	17.51	23.69
20	-15	220.08	28.48	15.58	24.04
21	-15	251.5	39.39	13.78	20.69
22	-14	291.29	35.25	15.93	21.2
23	-13	287.91	34.39	16.45	23.16
24	-15	275.52	38.9	15.38	26.62
25	-17	207.69	29.52	14.42	23.68
28	-14	269	28.1	18.32	28.18
29	-13	270.1	36.98	13	23.48
32	-18	203.52	27.76	16.2	26.95

Table C: Data used for model validation

Plots ID	HV-Filt (4,3x3) M	AGB (ton $^{-1}$ha)	BA(m^3/ha^{-1})	Mean height	Mean DBH
2	-13	171.85	27.15	14.08	20.24
4	-12	197.06	31.83	14.26	23.93
7	-14	140.56	22.98	12.9	20.59
10	-16	84.04	17.86	10.76	19.8
11	-15	165.38	27.83	11.9	22.52
14	-13	183.95	26.23	14.86	19.34
17	-14	102.12	18.12	12.71	16.86
26	-15	137.56	22.91	12.21	20.25
27	-16	60.17	9.92	13.29	18.35
30	-11	267.67	34.52	13.9	22.03

Table C: Correlation of all parameters

Correlations

		HV	HH	AGB (ton ha^{-1})	BA (m^3 ha^{-1})	Mean DBH	Mean height	CC(%)	Tot Tree /plot
HV	Pearson Correlation	1	.796**	.904**	.819**	0.32103	0.46274	-0.42793	0.43469
	Sig. (2-tailed)		0.000134	6.52608E-07	5.68728E-05	0.20897	0.06143	0.08661	0.08121
	N	17	17	17	17	17	17	17	17
HH	Pearson Correlation	.796**	1	.652**	.670**	0.31307	0.23117	-0.08907	0.34563
	Sig. (2-tailed)	0.00013		0.00454	0.00328	0.22112	0.37201	0.73389	0.17419
	N	17	17	17	17	17	17	17	17
AGB(ton ha^{-1})	Pearson Correlation	.904**	.652**	1	.843**	.495*	.666**	-0.31096	0.32612
	Sig. (2-tailed)	6.526E-07	0.004545		2.12138E-05	0.04356	0.00353	0.22442	0.20143
	N	17	17	17	17	17	17	17	17
BA(m^3 ha^{-1})	Pearson Correlation	.819**	.670**	.843**	1	0.22511	0.22763	-0.33221	.625**
	Sig. (2-tailed)	5.687E-05	0.00328	2.12138E-05		0.38501	0.37958	0.19265	0.00733
	N	17	17	17	17	17	17	17	17
Mean DBH	Pearson Correlation	0.3210286	0.3130732	.495*	0.22511	1	.651**	0.16109	-.564*
	Sig. (2-tailed)	0.20897	0.22112	0.04356	0.38501		0.00466	0.53680	0.01826
	N	17	17	17	17	17	17	17	17
Mean height	Pearson Correlation	0.462742	0.231171	.666**	0.22763	.651**	1	0.03093	-0.22204
	Sig. (2-tailed)	0.06143	0.37201	0.00353	0.37958	0.00466		0.90620	0.39172
	N	17	17	17	17	17	17	17	17
CC(%)	Pearson Correlation	-0.4279	-0.0891	-0.3110	-0.3322	0.1611	0.0309	1	-0.37449
	Sig. (2-tailed)	0.0866	0.7339	0.2244	0.1927	0.5368	0.9062		0.13862
	N	17	17	17	17	17	17	17	17
Tot Tree /plot	Pearson Correlation	0.43469	0.34563	0.32612	.625**	-.564*	-0.222035	-0.374485	1
	Sig. (2-tailed)	0.08121	0.17419	0.20143	0.00733	0.01826	0.39172	0.13862	
	N	17	17	17	17	17	17	17	17

*. Correlation is significant at the 0.01 level (2-tailed).

*. Correlation is significant at the 0.05 level (2-tailed).

Appendix 2: Backscatter coefficient retrieved using different approaches per plot. The mean of means (4, 3x3) HV polarized back scatter coefficient retrieved manually was used.

Table A: Backscatter coefficient for 17 plots used for model development.

Plot ID	HH No Filt	HV No Filt	HH-Filt_ SNAP	HV_Filt SNAP	HV-Filt (4,3x3) M	HH_Filt (4,3x3) M	HH-3x3 Manual	HV-3x3 Manual
1	-11	-13	-10	-14	-20	-17	-18	-21
3	-10	-15	-11	-17	-15	-10	-10	-15
5	-11	-14	-10	-13	-12	-8	-8	-13
6	-8	-14	-7	-12	-17	-12	-14	-20
9	-12	-22	-13	-21	-15	-6	-5	-15
13	-10	-16	-11	-16	-20	-14	-14	-20
18	-10	-12	-8	-13	-14	-7	-8	-14
19	-12	-17	-9	-15	-13	-9	-9	-15
20	-15	-19	-9	-16	-15	-10	-10	-16
21	-8	-14	-10	-14	-15	-12	-12	-15
22	-8	-11	-7	-11	-14	-7	-6	-13
23	-12	-17	-13	-17	-13	-11	-10	-13
24	-12	-19	-13	-16	-15	-8	-7	-15
25	-14	-18	-14	-17	-17	-15	-16	-18
28	-9	-14	-6	-13	-14	-8	-8	-15
29	-7	-15	-7	-15	-13	-10	-9	-13
32	-7	-11	-8	-11	-18	-13	-14	-18

Table B: Backscatter coefficients for 10 plots used for model validation

Plots ID	HH No Filt	HV No Filt	HH-Filt_ SNAP	HV_Filt SNAP	HV-Filt (4,3x3) M	HH_Filt (4,3x3) M	HH-3x3 Manual	HV-3x3 Manual
2	-12	-19	-11	-17	-13	-10	-10	-14
4	-9	-15	-10	-14	-12	-8	-8	-12
7	-10	-14	-11	-17	-14	-9	-9	-14
10	-12	-21	-11	-16	-16	-13	-14	-17
11	-7	-13	-10	-16	-15	-11	-10	-16
14	-12	-17	-12	-17	-13	-8	-8	-13
17	-8	-11	-8	-11	-14	-12	-13	-14
26	-12	-15	-12	-16	-15	-8	-8	-15
27	-11	-13	-8	-12	-16	-9	-9	-16
30	-14	-16	-13	-14	-11	-9	-9	-11

Appendix 3: Summary output of regression statistics

Table A: HH backscatter and AGB

Regression Statistics	
Multiple R	0.652
R Square	0.425
Adjusted R Square	0.387
Standard Error	54.745
Observations	17

ANOVA

	df	*SS*	*MS*	*F*	*Significance F*
Regression	1	33285.473	33285.473	11.106	0.004545
Residual	15	44955.930	2997.062		
Total	16	78241.404			

	Coefficients	*Standard Error*	*P-value*
Intercept	391.367	46.525	4.61446E-07
HH	14.295	4.289	0.00454

Table B: HH backscatter and stand BA

Regression Statistics	
Multiple R	0.66953
R Square	0.44827
Adjusted R Square	0.41149
Standard Error	5.64213
Observations	17

ANOVA

	df	*SS*	*MS*	*F*	*Significance F*
Regression	1	387.9686	387.9686	12.1874	0.00328
Residual	15	477.5049	31.8337		
Total	16	865.4735			

	Coefficients	*Standard Error*	*P-value*
Intercept	48.7731	4.7949	3.9915E-08
HH	1.5433	0.4421	0.00328

Table C: AGB and stand BA

Regression Statistics	
Multiple R	0.8432
R Square	0.7110
Adjusted R Square	0.6917
Standard Error	38.8262
Observations	17

ANOVA

	df	*SS*	*MS*	*F*	*Significance F*
Regression	1	55629.220	55629.22	36.902	2.12633E-05
Residual	15	22612.144	1507.4763		
Total	16	78241.364			

	Coefficients	*Standard Error*	*P-value*
Intercept	-19.6271	44.2092	0.6634095
BA m^3ha^{-1}	8.0171	1.3197	2.126E-05

Table D: Calculation of RMSE

Plot ID	AGB_Obsv	AGB_Pred	Obsv-Pred	$(Obsv\text{-}Pred)^2$
2	171.8	294.38	122.5	15013.679
4	197.1	332.21	135.1	18264.797
7	140.6	292.24	151.7	23004.410
10	84.0	235.02	151.0	22793.704
11	165.4	258.08	92.7	8593.979
14	183.9	306.40	122.4	14993.584
17	102.1	277.31	175.2	30689.686
26	137.6	252.75	115.2	13268.633
27	60.2	230.31	170.1	28948.396
30	267.7	351.62	83.9	7047.242
n =10		Sum $(Obsv\text{-}Pred)^2$		182618.109
		Sum $(Obsv\text{-}Pred)^2/n$		18261.811
		Sqrt (Sum $(Obsv\text{-}Pred)^2/n$)		135.1362679
		RMSE		135.136

Appendix 4: Image data (ALOS-2 PALSAR-2) and image footprint from Google Earth

Image A: Raw image data

HH Polarization Image Data

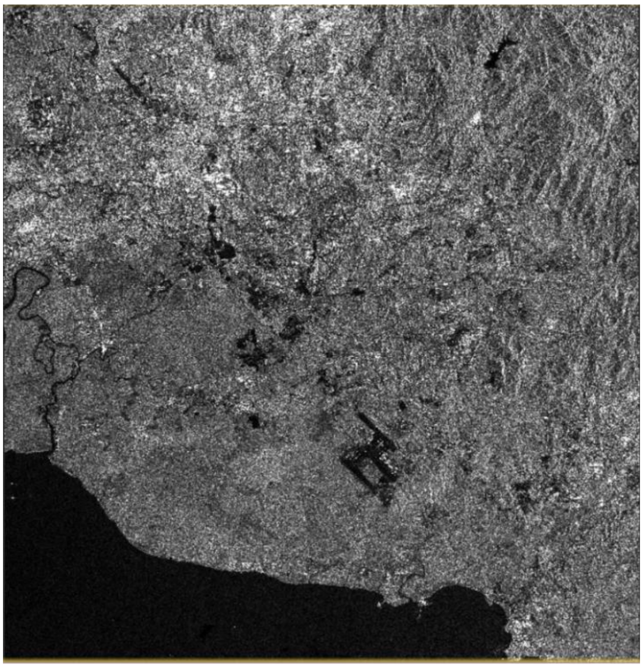

HV Polarization Image Data

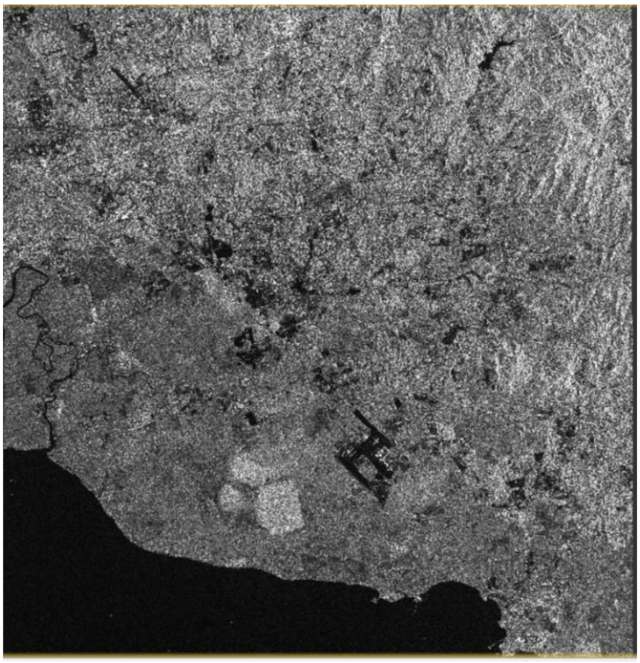

Image B: ALOS-2 PALSAR-2 Image footprint from Google Earth Map

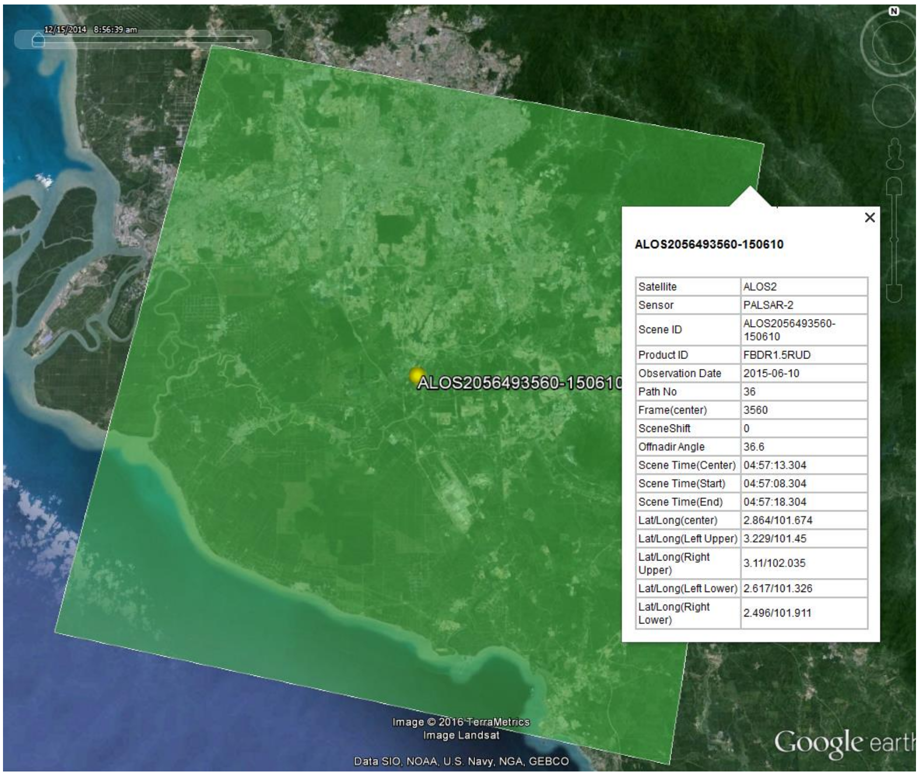

Appendix 5: Slope correction Table

Slope correction table

Plot size 500 m^2

Slope%	Radius(m)	Slope%	Radius(m)	Slope%	Radius(m)
0	12.62				
1	12.62	36	13.01	71	13.97
2	12.62	37	13.03	72	14.00
3	12.62	38	13.05	73	14.04
4	12.62	39	13.07	74	14.07
5	12.62	40	13.09	75	14.10
6	12.63	41	13.12	76	14.14
7	12.63	42	13.14	77	14.17
8	12.64	43	13.16	78	14.21
9	12.64	44	13.19	79	14.24
10	12.65	45	13.21	80	14.28
11	12.65	46	13.24	81	14.31
12	12.66	47	13.26	82	14.35
13	12.67	48	13.29	83	14.38
14	12.68	49	13.31	84	14.42
15	12.69	50	13.34	85	14.45
16	12.70	51	13.37	86	14.49
17	12.71	52	13.39	87	14.52
18	12.72	53	13.42	88	14.56
19	12.73	54	13.45	89	14.60
20	12.74	55	13.48	90	14.63
21	12.75	56	13.51	91	14.67
22	12.77	57	13.53	92	14.71
23	12.78	58	13.56	93	14.74
24	12.79	59	13.59	94	14.78
25	12.81	60	13.62	95	14.82
26	12.82	61	13.65	96	14.85
27	12.84	62	13.68	97	14.89
28	12.86	63	13.72	98	14.93
29	12.87	64	13.75	99	14.97
30	12.89	65	13.78	100	15.00
31	12.91	66	13.81	101	15.04
32	12.93	67	13.84	102	15.08
33	12.95	68	13.87	103	15.12
34	12.97	69	13.91	104	15.15
35	12.99	70	13.94	105	15.19

de Gier – 2000
(Source: Yousif 2015, lecture notes)

Appendix 6: Field Data Sheet

DATA COLLECTION SHEET (AYER HITAM TROPICAL RAIN FOREST RESERVE, MALAYSIA

Name of recorder.. **Date**...

Sample Plot No.		GPS Coordinates	X:	Grid cell No.	Slope (%)	Plot Radius	Undergrowth		Crown Cover (%)
			Y:				Y	N	

Tree No.	Species	DBH (cm)	Hgt 1 (Leica)	Hgt 2 (Haga)	Hgt 3 (TruPulse)	Crown diam.(m)	Tree No.	Species	DBH (cm)	Hgt 1 (Leica)	Hgt 2 (Haga)	Hgt 3 (TruPulse)	Crown diam.(m)
1							36						
2							37						
3							38						
4							39						
5							40						
6							41						
7							42						
8							43						
9							44						
10							45						
11							46						
12							47						
13							48						
14							49						
15							50						
16							51						
17							52						
18							53						
19							54						
20							55						
21							56						
22							57						
23							58						
24							59						
25							60						
26							61						
27							62						
28							63						
29							64						
30							65						
31							66						
32							67						
33							68						
34							69						
35							70						

Appendix 7: Field Pictures